NASA TECHNICAL NOTE

NASA TN D-6898

NASA TN D-6898

FIXED-BASE SIMULATOR STUDY OF AN EXTERNALLY BLOWN FLAP STOL TRANSPORT AIRPLANE DURING APPROACH AND LANDING

by

William D. Grantham, Luat T. Nguyen,
James M. Patton, Jr., Perry L. Deal, Robert A. Champine,
Langley Research Center

and

C. Robert Carter

Langley Directorate,
U.S. Army Air Mobility R&D Laboratory

NATIONAL AERONAUTICS AND SPACE ADMINISTRATION • WASHINGTON, D. C. • OCTOBER 1972

1. Report No.	2. Government Accession No.	3. Recipient's Catalog No.
NASA TN D-6898		

4. Title and Subtitle	5. Report Date
FIXED-BASE SIMULATOR STUDY OF AN EXTERNALLY BLOWN FLAP STOL TRANSPORT AIRPLANE DURING APPROACH AND LANDING	October 1972
	6. Performing Organization Code

7. Author(s)	8. Performing Organization Report No.
William D. Grantham, Luat T. Nguyen, James M. Patton, Jr., Perry L. Deal, Robert A. Champine, Langley Research Center; and C. Robert Carter, Langley Directorate, U.S. Army Air Mobility R&D Laboratory	L-8394
	10. Work Unit No. 760-61-02-01
9. Performing Organization Name and Address NASA Langley Research Center Hampton, Va. 23365	11. Contract or Grant No.
	13. Type of Report and Period Covered Technical Note
12. Sponsoring Agency Name and Address National Aeronautics and Space Administration Washington, D.C. 20546	14. Sponsoring Agency Code

15. Supplementary Notes

16. Abstract

A fixed-base simulator study was conducted to determine the flight characteristics of a representative STOL transport having a high wing and equipped with an external-flow jet flap in combination with four high-bypass-ratio fan-jet engines during the approach and landing. Real-time digital simulation techniques were used. The computer was programed with equations of motion for six degrees of freedom and the aerodynamic inputs were based on measured wind-tunnel data. A visual display of a STOL airport was provided for simulation of the flare and touchdown characteristics. The primary piloting task was an instrument approach to a breakout at a 61-meter (200-ft) ceiling with a visual landing.

17. Key Words (Suggested by Author(s))	18. Distribution Statement
STOL handling qualities Command augmentation systems Engine-out performance STOL flight director Aircraft noise	Unclassified – Unlimited

19. Security Classif. (of this report)	20. Security Classif. (of this page)	21. No. of Pages	22. Price*
Unclassified	Unclassified	97	$3.00

*For sale by the National Technical Information Service, Springfield, Virginia 22151

FIXED-BASE SIMULATOR STUDY OF AN EXTERNALLY BLOWN FLAP STOL TRANSPORT AIRPLANE DURING APPROACH AND LANDING

By William D. Grantham, Luat T. Nguyen, James M. Patton, Jr.,
Perry L. Deal, Robert A. Champine
Langley Research Center

and C. Robert Carter
Langley Directorate, U.S. Army Air Mobility R&D Laboratory

SUMMARY

A fixed-base simulator study was conducted to determine the flight characteristics of a representative STOL transport having a high wing and equipped with an external-flow jet flap in combination with four high-bypass-ratio fan-jet engines during the approach and landing. Real-time digital simulation techniques were used. The computer was programed with equations of motion for six degrees of freedom and the aerodynamic inputs were based on measured wind-tunnel data. A visual display of a STOL airport was provided for simulation of the flare and touchdown characteristics. The primary piloting task was an instrument approach to a breakout at a 61-meter (200-ft) ceiling with a visual landing.

The results of the study indicated that satisfactory handling qualities could be obtained, but considerable augmentation was required. The pilots could easily capture and track the localizer and glideslope for any of the simulated approach angles $\left(4^{\circ}, 6^{\circ}, 7\frac{1}{2}^{\circ}, \text{and } 9^{\circ}\right)$, and the pilot rating for the instrument approach task remained the same for all approach angles. It was concluded, however, that the maximum glideslope from which the airplane should be landed was 6°; and furthermore, in order to have any confidence in making consistently precise landings, a two-segment approach to a glideslope of 4° should be used.

With all the augmentation systems operative, the loss of a critical engine during an instrument approach posed no problems insofar as tracking the localizer and glideslope. However, this engine-out condition did present problems in making a precision landing.

If the subject STOL airplane does not have crosswind gear, a 90° crosswind of approximately 20 knots is the largest that could be handled and maintain adequate rudder control margins.

INTRODUCTION

The requirement for STOL (short take-off and landing) transport airplanes has emphasized the need for high lift to reduce the approach and landing speeds. Lower approach and landing speeds are desirable not only from a standpoint of reducing landing distance but also for reducing airspace requirements, lowering weather minimums, and obtaining greater safety. STOL airplanes may take a variety of forms, and an equal or greater variety of approach and landing techniques may be feasible. One method of increasing the lift coefficients of these airplanes is through the use of powered-lift systems such as the external-flow jet-flap system. In the external-flow jet-flap system, the jet exhaust from pod-mounted engines is deflected through slotted flaps to induce additional lift on the wing.

The present simulation program is a follow-on to the handling-qualities work on jet-flap airplanes, reported in references 1 and 2, to add more realism to the simulation and to investigate additional problems. The study was conducted with a fixed-base cockpit and a visual display of a STOL airport. Real-time digital simulation techniques were used. The computer was programed with equations of motion for six degrees of freedom and the aerodynamic coefficients were based on measured wind-tunnel data (see refs. 3, 4, and 5). The primary piloting task was an instrument approach to a breakout at a 61-meter (200-ft) ceiling, with a visual landing.

The objectives of the study were as follows:

(1) Evaluate the general handling qualities of the unaugmented airplane in level flight in the approach configuration and at the approach speed.

(2) Develop the stability augmentation and flight control systems required to optimize these handling qualities.

(3) Determine the benefits of having a flight director specifically developed for STOL operation.

(4) Evaluate the effects of autospeed, direct lift control (DLC), and approach angle on pilot workload.

(5) Evaluate the effects of various atmospheric conditions, including turbulence, steady winds, and wind shear, on the ability of the pilot to make a satisfactory approach and landing.

(6) Determine the effects of including the changes in aerodynamics due to ground proximity on the pilot's ability to make satisfactory landings.

(7) Develop the best flight control system and piloting technique for compensating for the loss of a critical engine during the landing approach.

(8) Determine the effects of the outboard engine location (0.30 semispan compared with 0.42 semispan) on the stability augmentation system (SAS) required for satisfactory handling qualities, as well as the ability of the pilot to compensate for the loss of power on an outboard engine.

(9) Determine the effects of piloting technique on the noise level perceived at various ground stations.

SYMBOLS AND DEFINITIONS

In order to facilitate international usage of the data presented, dimensional quantities are presented in both the International System of Units (SI) and U.S. Customary Units. The measurements and calculations were made in U.S. Customary Units. Dots over symbols denote differentiation with respect to time.

a_n	normal acceleration, g units
a_y	lateral acceleration, g units
a'_y	compensated lateral acceleration $\left(a_y - Y_{\delta_r}\delta_r\right)$, g units
b	wing span, meters (feet)
C_D	drag coefficient
$C_{D,ge}$	incremental drag coefficient due to ground effect
C_L	lift coefficient
$C_{L,ge}$	incremental lift coefficient due to ground effect
C_l	rolling-moment coefficient
$\Delta C_{l,E1}$	incremental rolling-moment coefficient due to failure of number one engine
C_m	pitching-moment coefficient
$C_{m,ge}$	incremental pitching-moment coefficient due to ground effect
C_n	yawing-moment coefficient

$\Delta C_{n,E1}$	incremental yawing-moment coefficient due to failure of number one engine
C_T	thrust coefficient
C_X	longitudinal-force coefficient
$C_{X,E1}$	longitudinal-force coefficient with only three engines operating
C_Y	side-force coefficient
$\Delta C_{Y,E1}$	incremental side-force coefficient due to failure of number one engine
C_Z	vertical-force coefficient
$C_{Z,E1}$	vertical-force coefficient with only three engines operating
c	local chord, meters (feet)
$\bar{c}$	mean aerodynamic chord, meters (feet)
g	acceleration due to gravity, meters/second^2 (feet/second^2)
h	altitude, meters (feet)
h_{gs}	altitude of glideslope radio beam, meters (feet)
h_{lg}	altitude of airplane landing gear, meters (feet)
I_X, I_Y, I_Z	moments of inertia about X, Y, and Z body axes, respectively, kilogram-meters^2 (slug-feet^2)
I_{XZ}	product of inertia, kilogram-meters^2 (slug-feet^2)
K	gain
m	mass
P	period, seconds
P_{ph}	period of phugoid oscillations, seconds

P_{sp}	period of longitudinal short-period oscillation, seconds
p,q,r	rolling, pitching, and yawing angular velocities, respectively, degrees/second or radians/second
S	wing area, meters^2 (feet^2)
S_{a_n}	static normal acceleration gust sensitivity, g/(m/sec) (g/(ft/sec))
s	Laplace operator
T	thrust, newtons (pounds force)
T_c	thrust commanded, newtons (pounds force)
t	time, seconds
t_{ge}	time spent within ground effects, seconds
$t_{1/2}$	time to damp to one-half amplitude, seconds
t_2	time to double amplitude, seconds
u_g,v_g,w_g	random gust velocity along the X, Y, and Z body axes, respectively, meters/second (feet/second)
V	airspeed, knots (feet/second)
V_a	resultant aerodynamic velocity of airplane, knots (feet/second)
V_c	velocity commanded, knots (feet/second)
W	airplane weight, newtons (pounds force)
X	distance from runway threshold, positive down runway, meters (feet)
X,Y,Z	coordinate axes
Y	lateral displacement from localizer, meters (feet)

$Y_{\delta_r} = \rho V_a^2 S C_{Y_{\delta_r}} / 2m$

α	angle of attack, degrees
α_c	angle of attack commanded, degrees
β	angle of sideslip, degrees
γ	flight-path angle, degrees
δ_a	aileron deflection, positive for right roll command, degrees
$\delta_{a,int}$	aileron deflection beyond which asymmetric spoilers are to deflect with ailerons, degrees
δ_c	control-column deflection, positive for pull force, degrees
δ_{f1}	deflection of forward segment of trailing-edge flap, degrees
δ_{f2}	deflection of second segment of trailing-edge flap, degrees
δ_{f3}	deflection of rearward segment of trailing-edge flap, degrees
δ^*_{f3}	deflection of δ_{f3} from 60^o, degrees $\left(\delta^*_{f3} = \delta_{f3} - 60^o\right)$
δ_{lt}	cockpit controller for longitudinal trim
δ_p	pedal travel, centimeters (inches)
δ_{RT}	cockpit controller for roll trim
δ_r	rudder deflection, degrees
δ_s	asymmetric deflection of spoilers for roll control, positive for right roll command, degrees
$\delta_{s,int}$	asymmetric spoiler deflection beyond which the ailerons are slaved to deflect with asymmetric spoiler, degrees
δ_{sp}	symmetric deflection of spoilers for lift control, degrees

δ_t	horizontal-tail deflection, positive when trailing edge is deflected down, degrees
δ_{th}	throttle deflection
δ_V	pilot commanded airspeed controller
δ_w	wheel deflection, degrees
ϵ_y	localizer error, degrees
ϵ_z	glideslope error, degrees
ϵ_{zh}	glideslope error, meters (feet)
ζ_d	Dutch roll damping ratio
ζ_{ph}	phugoid damping ratio
ζ_R	damping ratio of roll mode
ζ_{sp}	longitudinal short-period damping ratio
ζ_ϕ	damping ratio of numerator quadratic of ϕ/δ_a transfer function
θ	pitch angle, degrees
θ_c	pitch angle commanded, degrees
ρ	air density, kilograms/meter^3 (slugs/foot^3)
$\sigma_u,\sigma_v,\sigma_w$	root-mean-square intensities of u_g, v_g, and w_g, respectively, meters/second (feet/second)
τ	time constant, seconds
τ_{ph}	time constant of phugoid mode, seconds
τ_R	time constant of roll mode, seconds

τ_{sp} time constant of longitudinal short-period mode, seconds

ϕ angle of roll, degrees

ψ angle of heading, degrees

ω_d undamped natural frequency of Dutch roll mode, radians/second

ω_{ph} undamped natural frequency of phugoid mode, radians/second

ω_R undamped natural frequency of roll mode, radians/second

ω_{sp} longitudinal short-period undamped natural frequency, radians/second

ω_ϕ undamped natural frequency appearing in numerator quadratic of ϕ/δ_a transfer function, radians/second

$$C_{l_\beta} = \frac{\partial C_l}{\partial \beta} \qquad C_{n_\beta} = \frac{\partial C_n}{\partial \beta} \qquad C_{Y_\beta} = \frac{\partial C_Y}{\partial \beta}$$

$$C_{X_{\delta^*_{f3}}} = \frac{\partial C_X}{\partial \delta^*_{f3}} \qquad C_{Z_{\delta^*_{f3}}} = \frac{\partial C_Z}{\partial \delta^*_{f3}} \qquad C_{m_{\delta^*_{f3}}} = \frac{\partial C_m}{\partial \delta^*_{f3}}$$

$$C_{X_{\delta_s}} = \frac{\partial C_X}{\partial \delta_s} \qquad C_{Z_{\delta_s}} = \frac{\partial C_Z}{\partial \delta_s} \qquad C_{m_{\delta_s}} = \frac{\partial C_m}{\partial \delta_s}$$

$$C_{l_{\delta_s}} = \frac{\partial C_l}{\partial \delta_s} \qquad C_{n_{\delta_s}} = \frac{\partial C_n}{\partial \delta_s} \qquad C_{Y_{\delta_s}} = \frac{\partial C_Y}{\partial \delta_s}$$

$$C_{X_{\delta_{sp}}} = \frac{\partial C_X}{\partial \delta_{sp}} \qquad C_{Z_{\delta_{sp}}} = \frac{\partial C_Z}{\partial \delta_{sp}} \qquad C_{m_{\delta_{sp}}} = \frac{\partial C_m}{\partial \delta_{sp}}$$

$$C_{X_{\delta_t}} = \frac{\partial C_X}{\partial \delta_t} \qquad C_{Z_{\delta_t}} = \frac{\partial C_Z}{\partial \delta_t} \qquad C_{m_{\delta_t}} = \frac{\partial C_m}{\partial \delta_t}$$

$$C_{l_{\delta_r}} = \frac{\partial C_l}{\partial \delta_r} \qquad C_{n_{\delta_r}} = \frac{\partial C_n}{\partial \delta_r} \qquad C_{Y_{\delta_r}} = \frac{\partial C_Y}{\partial \delta_r}$$

$$C_{l_{\delta_a}} = \frac{\partial C_l}{\partial \delta_a} \qquad C_{n_{\delta_a}} = \frac{\partial C_n}{\partial \delta_a} \qquad C_{Y_{\delta_a}} = \frac{\partial C_Y}{\partial \delta_a}$$

$$C_{l_p} = \frac{\partial C_l}{\partial \frac{pb}{2V}} \qquad C_{n_p} = \frac{\partial C_n}{\partial \frac{pb}{2V}} \qquad C_{Y_p} = \frac{\partial C_Y}{\partial \frac{pb}{2V}}$$

$$C_{l_r} = \frac{\partial C_l}{\partial \frac{rb}{2V}} \qquad C_{n_r} = \frac{\partial C_n}{\partial \frac{rb}{2V}} \qquad C_{Y_r} = \frac{\partial C_Y}{\partial \frac{rb}{2V}}$$

$$C_{m_q} = \frac{\partial C_m}{\partial \frac{q\bar{c}}{2V}} \qquad C_{m_{\dot{\alpha}}} = \frac{\partial C_m}{\partial \frac{\dot{\alpha}\bar{c}}{2V}} \qquad C_{L_\alpha} = \frac{\partial C_L}{\partial \alpha}$$

Subscripts:

max	maximum
rms	root mean square

Abbreviations:

BLC	boundary-layer control
CAS	command augmentation systems
CTOL	conventional take-off and landing
DLC	direct lift control
EBF	externally blown flap
IFR	instrument flight rules
ILS	instrument landing system
OASPL	overall sound pressure level
SAS	stability augmentation systems

STOL short take-off and landing

VFR visual flight rules

DESCRIPTION OF SIMULATED AIRPLANE

The airplane design used in this study was a four-engine subsonic jet transport with a high wing and high-bypass-ratio turbofan engines. A three-view drawing of the airplane is presented in figure 1, and a detailed description of the aerodynamic configuration is given in reference 3.

The engines were mounted in such a manner that the jet exhaust impinged directly on the trailing-edge flap system. (See fig. 2.) The inboard engines were always located along the wing at 0.22 semispan, but the investigation included two different spanwise locations for the outboard engines: 0.30 semispan in a clustered-engine arrangement and 0.42 semispan in a spread-engine arrangement. Most of the simulation program was for the clustered-engine arrangement and the results discussed in the text represent the clustered-engine arrangement unless otherwise noted. The simulated airplane had a gross weight of 245 096 N (55 100 lbf), a wing loading of 3142 N/m^2 (65.36 lbf/ft^2), and a thrust-weight ratio of 0.60 for the maximum thrust condition. An example of the engine thrust response characteristics used is presented in figure 3, and all the engine response characteristics are given in table I.

The wing incorporated leading-edge boundary-layer control (BLC), Kruger-type, leading-edge flaps, which were deflected 60^o, and full-span, triple-slotted trailing-edge flaps which were set at $\delta_{f1}/\delta_{f2}/\delta_{f3} = 25^o/10^o/60^o$ for the approach and landing condition. The trailing-edge flaps were divided into three spanwise segments on each wing semispan as indicated in figure 1. In the present investigation, only the rear flap element was varied, δ_{f1} and δ_{f2} remained at 25^o and 10^o, respectively. All three spanwise elements were deflected as a unit to represent flap deflection, and deflection of these elements is designated δ_{f3} throughout the text. In addition, deflection of the inboard elements or the midspan elements (inboard elements for the clustered-engine arrangement and midspan elements for the spread-engine arrangement) could be deflected differentially and used as ailerons. Such deflection of the rear flap element as ailerons is designated as δ_a throughout the text. Wind-tunnel investigations (ref. 3) have shown that for the clustered-engine arrangement, the inboard flap elements are far more effective in providing rolling moments than the other two elements. Thus, for the clustered-engine configuration, the inboard elements were used as ailerons despite their adverse yaw characteristics. For the spread-engine arrangement, the midspan flap element provides rolling moments comparable to those generated by the inboard element; and, at the same time, the midspan element does not exhibit the undesirable adverse yaw character-

istic. Therefore the midspan flap elements were used for roll control in the spread-engine configuration.

The static aerodynamic data used from reference 3 represent the condition where blowing over the wing leading edge and the rudder were utilized. The major effect of blowing over the wing was to increase the stall angle of attack, particularly for the lower engine-thrust conditions. Blowing on the rudder more than doubled the rudder effectiveness.

A block diagram showing the basic flight controls is presented in figure 4. Two roll-control surfaces are available on the airplane, asymmetric spoilers (δ_s) and the aforementioned asymmetric flaps (δ_a). For the basic (unaugmented) airplane, the spoiler was used as the primary roll control since the "aileron" exhibited an undesirable degree of adverse yaw. However, the aileron was slaved to the spoiler so that whenever δ_s exceeded 30^o, the ailerons were also driven. (The maximum deflection of the spoiler is 60^o.) This feature allowed the ailerons normally to remain inactive; the pilot could, however, quickly obtain maximum available roll control ($\delta_s + \delta_a$), if desired.

The mass and dimensional characteristics of the simulated STOL airplane are presented in table II, and the aerodynamic characteristics are presented in table III and figure 5.

DESCRIPTION OF SIMULATION EQUIPMENT

The fixed-base simulator had a transport-type cockpit which was equipped with conventional flight and engine-thrust controls and with a flight-instrument display representative of those found in current transport airplanes. (See fig. 6.) In addition, a direct-lift-control (DLC) thumb controller was mounted on the right horn of the control yoke. An instrument was installed in the display panel to indicate the direction and amount of DLC being commanded. (See fig. 6(b).) Instruments indicating angle of attack, sideslip, and flap angle were also provided. A conventional cross-pointer-type flight director instrument was used, but the command bars (cross pointers) were driven by the main computer program. (See appendix A for a detailed description of the flight director system used in this study.)

The simulator control forces were provided by a hydraulic servosystem and were functions of control displacement and rate. The control characteristics of the simulator are defined in table IV. Real-time digital simulation techniques were used wherein a digital computer was programed with equations of motion for six degrees of freedom. The simulator did not incorporate cockpit motion.

A visual display of a STOL airport (fig. 7) was used in order to provide visual cues for the flare and landing. The display consisted of a closed-circuit television presenta-

tion, viewed through a collimating lens in the pilot's windshield, of the simulated approach to a 914-meter (3000-ft) runway (see figs. 8 and 9). Although a 914-meter (3000-ft) runway was used, each pilot was instructed to land within an area that was clearly marked on the runway. It was assumed that if the pilot landed within the target area, he could easily turn off at the first runway exit, which meant that less than 610 meters (2000 ft) of the runway would be used for the landing. Each flight was terminated at touchdown; the rollout was not simulated.

TESTS AND PROCEDURES

The low-speed flight characteristics of the subject STOL airplane are presented and discussed in relation to pilot opinions and ratings. (See table V for pilot rating system.) Three research pilots participated in the simulation program and used standard flight-test procedures in the evaluation of the handling qualities.

The ILS approach was initiated with the airplane in the power-approach condition (power for level flight) with a lateral offset from the localizer, at an altitude below the glideslope, and at a variable distance from the runway. (The distance from the runway and the altitude varied with glideslope angle.) The initial flight conditions for this jet-flap STOL airplane were determined with the following considerations: (1) the angle of attack for the approach conditions should be at least 10° below the stall; and (2) the approach airspeed should be at least 15 knots greater than the one-engine-out stall speed (maximum power on three engines). Although most of the results discussed in the text pertain to the airplane being flown at $C_L = 3.5$ ($V \approx 75$ knots), the airplane was also evaluated at $C_L = 4.0$ ($V \approx 70$ knots), and $C_L = 4.5$ ($V \approx 65$ knots). Also, although most of the landing approaches were made on a 6° glideslope, the glideslope angle was varied from 4° to 9° during the test program. (All results discussed pertain to an airspeed of 75 knots and a glideslope of 6° unless otherwise noted.)

The logic employed for the flight director was varied to correspond to the flight condition and piloting technique being simulated. (See appendix A.) The pilot's task was to capture the localizer and glideslope and to maintain them as closely as possible while under IFR conditions. (The ILS glideslope beam was 2° ($\pm 1^{\circ}$) deep and the localizer beam was 5° $\left(\pm 2\frac{1}{2}^{\circ}\right)$ wide.) At an altitude of 61 meters (200 ft) a visual display of the STOL runway and surrounding area was displayed to the pilot, and from that altitude the pilot attempted to land the airplane visually (with limited reference to the flight director) on a prescribed area on the runway. (The 6° glideslope gave an altitude of 8 meters (26 ft) at the runway threshold and intercepted the runway 76 meters (250 ft) from the threshold.)

Three levels of turbulence were used during the subject simulation program: gusts having a root-mean-square value of approximately 0.6 m/sec (2 ft/sec) which were described by the pilots as "light" turbulence, gusts having a root-mean-square value of 1.2 m/sec (4 ft/sec) which were said to represent "moderate" turbulence, and 1.8 m/sec (6 ft/sec) root-mean-square gusts which were described as "heavy" turbulence.

RESULTS AND DISCUSSION

The results of the investigation are discussed in terms of the previously stated objectives. All results discussed pertain to an airspeed of 75 knots and a glideslope of 6^{o} unless otherwise noted. Also, throughout the discussion, the pilot ratings listed for the various conditions will be an average of the ratings from all pilots who "flew" that particular condition.

The dynamic stability and response characteristics of the simulated jet-flap STOL transport airplane for stability augmentation off and on are presented in tables VI, VII, and VIII.

Basic Airplane

The average pilot rating assigned to the longitudinal handling qualities of the unaugmented airplane was $6\frac{1}{2}$, the primary objections being (1) poor airspeed control; (2) sluggish initial pitch response; (3) unusually large pitch-attitude excursions associated with changes in thrust, flaps, spoilers, or bank angle; (4) a phugoid with a short period which caused pilot-induced oscillations; and (5) low apparent pitch damping.

A pilot rating of 9 was assigned to the lateral-directional handling qualities. The major objections were (1) poor roll control; (2) a highly divergent spiral mode; (3) unacceptably large sideslip excursions in turns; and (4) low roll damping.

Longitudinal characteristics.- At the approach speeds, the subject STOL airplane was flown on the "backside" of the power-required curve where precise control of pitch attitude was needed for speed control and where thrust was the principal control for glidepath. The variation of thrust required with airspeed $\frac{\partial T/W}{\partial V}$ is approximately -0.0019 per knot at 75 knots and -0.0038 per knot at 65 knots. However, this speed-thrust instability is not the major cause of the piloting difficulties; rather, it is the inability of the pilot to control pitch attitude precisely.

Table VI presents the airplane dynamic parameters for various airspeeds and augmentation modes. The phugoid mode which exhibits a highly undesirable short period (particularly at 65 knots) is superimposed on the short-period mode and was the dominant factor when attempting to control the airplane longitudinally. Even at a speed of

75 knots, the period of the phugoid is only about four times that of the short-period mode. (It is generally desired that the period of the phugoid be at least ten times that of the short-period mode.) Because of this characteristic, most of the longitudinal motion which the pilot saw following a control or disturbance input was that due to the phugoid. The airplane pitch motions therefore appeared to the pilot to be very poorly damped and he had to make control inputs constantly in attempting to damp the motion. This problem was aggravated by the sluggish initial pitch response which causes the pilot to overcontrol and thus further excite the phugoid. In addition, changes in thrust, flap, spoilers, or bank angle cause large pitch-attitude excursions. This pitch-coupling effect provided a source of disturbances which constantly excited the phugoid motion. The net result of all the aforementioned characteristics was poor pilot control of pitch attitude and hence poor control of airspeed. Figure 10 indicates that the pitch control power $\left(\ddot{\theta}_{max}\right)$ is satisfactory at $V = 75$ knots.

Lateral-directional characteristics.- As stated previously, the pilots assigned a rating of 9 to the lateral-directional handling qualities of the basic airplane. The dynamic parameters shown in table VI indicate acceptable roll and Dutch roll characteristics according to references 6 and 7. However, the pilots commented that the roll damping was slightly low and indicated that higher values of Dutch roll damping and frequency would be desirable. The spiral mode, on the other hand, was completely unsatisfactory and showed a time to double amplitude of less than 7 seconds. Another characteristic which contributed to the poor pilot rating was the large sideslip excursions experienced during turns. Table VII shows a $\Delta\beta/\Delta\phi$ of approximately 0.3; the maximum sideslip experienced in rolling the airplane to a bank angle of 30° was nominally about 8°. Roll-sideslip coupling caused objectionable roll oscillations which aggravated the roll control problem. This characteristic, in combination with the highly divergent spiral mode, required constant attention and considerable effort on the part of the pilot; even so, the lateral-directional control remained very poor.

Figures 11 and 12 indicate that the airplane has satisfactory roll and yaw control power.

Augmented Airplane

The airplane stability and control characteristics were augmented longitudinally by incorporating a pitch-attitude command system and an automatic speed controller. The lateral-directional augmentation consisted of a roll-rate command system and various feedback signals driving the rudder to attain good turn coordination. The development of these various systems is discussed in appendix B.

Longitudinal characteristics.- The pitch-attitude command system (fig. 13) provided pitch changes from trim proportional to column deflection; precise trim changes could

also be commanded through the trim controller. A pitch-rate command system was also evaluated. Either system (attitude or rate) provided the desired characteristics of rapid well-damped responses to pilot inputs as well as inherent attitude stability. That is, either system eliminated the pitch-attitude excursions associated with changes in thrust, flaps, spoilers, or bank angle. However, the pilots favored the attitude command system over the rate command system because "small" trim corrections could be more easily made with the attitude system and because a "reference" pitch attitude was thus provided. The attitude command system in conjunction with the autospeed system allowed the pilots to easily trim the aircraft to the pitch attitude required for touchdown early in the approach, and no other pitch changes were required since the command system automatically maintained this attitude throughout the remainder of the approach and landing.

The autospeed system drove the third segment flap (δ_{f3}) to maintain a selected airspeed. (See fig. 13.) To neutralize the lift increment resulting from flap deflection, an interconnect to the symmetric spoilers was provided. Since the spoilers were not uprigged, only negative lift increments were generated; however, this characteristic had no adverse effects on the speed control capability of the system during any part of this study. The autospeed system accomplished three objectives: (1) it eliminated the phugoid mode which was the source of much of the basic longitudinal handling difficulties; (2) it provided good speed control, which is essential to minimizing landing errors; and (3) it relieved the pilot of the speed control task and hence considerably reduced the pilot workload. The pilots concluded that an autospeed system would be a mandatory feature for the subject STOL airplane.

Table VIII shows that the normal-acceleration capability using only thrust for glidepath control is more than adequate with all engines operating and indicates that constant-attitude—thrust-only approaches are feasible for this STOL airplane.

Lateral-directional characteristics.- Figure 14 presents a block diagram of the lateral-directional augmentation system. Note that the primary roll control for the augmented airplane was a differential flap δ_a and not an asymmetric spoiler δ_s. The adverse yaw due to δ_a was eliminated by the rudder interconnect. In addition, δ_a is more desirable than δ_s in that the former does not involve the lift loss which is inherent to the use of spoilers for roll control. The asymmetric spoiler was slaved to the ailerons so that δ_s was driven whenever δ_a reached maximum deflection. Directionally, the system consisted of $\dot{\beta}$, a_y', p, and δ_a signals driving the rudder, whereas laterally a rate command system provided roll rate proportional to wheel position. Table VI shows that the Dutch roll characteristics were improved considerably; both damping ratio and frequency were increased over those of the basic airplane. The spiral divergence problem was eliminated since the roll-rate command system provided a slightly stable spiral mode. The sideslip excursions during turn entries were also reduced considerably; $\Delta\beta/\Delta\phi$ was reduced by a factor of 10, down to 0.033, and sideslip never exceeded 2^o for

bank-angle changes of more than 30°. The oscillations in roll were virtually eliminated, as shown by the parameters $\omega_\phi/\omega_d = 1.04$ and $\zeta_\phi/\zeta_d = 1.24$. The roll-rate command system also provided the very desirable roll-attitude-hold feature which proved to be very beneficial, particularly during the engine failure situation.

Pilot ratings for augmented airplane.- With the aforementioned stability-augmentation and command-control systems operative (θ command, autospeed, directional augmentation, and p command), the average pilot ratings of the longitudinal and lateral-directional handling qualities on the ILS approach were improved from $6\frac{1}{2}$ and 9 to $3\frac{1}{2}$ and 3, respectively, the pilot's remaining objection being that he still had to "chase" the glideslope and localizer with continuous thrust and bank-angle changes. In an attempt to overcome this problem, a flight director was developed to provide the pilot with guidance commands for the capture and tracking of the ILS beams. (See appendix A for discussion.) The pilots commented that with the addition of the flight-director system, the ILS approach could be flown much more precisely and with less pilot workload. The pilot rating was improved to $2\frac{1}{2}$ for the landing approach. The pilots concluded that a flight director would be mandatory for the subject STOL airplane.

Piloting Techniques

Throughout the study of the effects of various piloting techniques used in "flying" the landing approach on the subject externally blown flap STOL transport airplane, the previously discussed augmentation and command-control systems were used. Also, a flight director was provided to aid the pilot in all instances.

Although the handling qualities of the subject STOL were evaluated at airspeeds of 65 knots and 75 knots, it was determined early in the simulation program that the airplane should probably not be landed at speeds less than about 75 knots. For the one-engine-out condition, or for large head winds or crosswinds, an approach speed of 75 knots was considerably better than 65 knots as will be discussed later in this paper. Therefore, when evaluating various piloting techniques for flying the landing approach, the airplane was flown at an airspeed of 75 knots.

Backside operation without autospeed.- Although simultaneous changes in both column and throttles were generally used to maintain the proper airspeed and keep the glideslope error to a minimum, the piloting technique used to fly the approach was the same as that used for conventional airplanes that operate on the backside of the thrust-required curve during approach and landing. Basically, the technique used was as follows:

(1) When the glideslope was intercepted, the pilot used the throttles to initiate and stabilize on the desired rate of sink.

(2) The longitudinal trim and column were then used to control airspeed.

With the flaps set at 60° and V = 75 knots, the trim pitch attitude θ for straight and level flight was -4.1°. For a 6° approach this nose-down value essentially maintained the desired airspeed (V = 75 knots). Therefore, there was little pilot effort required in controlling airspeed. The pilots, however, did not like this technique (thrust for γ and θ for airspeed) for flying the landing approach because of the nose-down attitude which dictated a relatively large change in pitch attitude prior to landing. It should be noted that the airplane could have been flown at an airspeed of 75 knots in a nose-up pitch attitude if less than 60° of flap deflection were used.

Backside operation with autospeed.- The autospeed system used in this study consisted of driving the third segment of the triple-slotted flap as a function of changes in airspeed. The pilots commented that this autospeed-control system was very beneficial in that it held the desired airspeed closer than they could and, of course, because the longitudinal piloting task was now reduced to only one task – that of flying glideslope with throttles. Also, and most prevalent, since the autospeed system moved the flaps to maintain speed, the pilot could trim the airplane in a nose-up attitude prior to glideslope intercept and the pitch-attitude command system maintained this pitch attitude throughout the approach and landing. This constant pitch-attitude approach was said to be highly desirable from a piloting standpoint and was therefore used throughout the remainder of the simulation program.

Thrust modulation for direct lift control (DLC).- An attempt was made to use thrust modulation for direct lift control. In order to do this, the autospeed controller and pitch-attitude command were again used to balance any incremental drag and pitching moments due to thrust changes (DLC inputs). The pilot rating assigned to the longitudinal ILS task with this DLC system operative was 2, compared with a pilot rating of $2\frac{1}{2}$ when the pilot had to use throttles for thrust control. The improved pilot rating is due to the fact that pilot thrust inputs could be made with much less effort with the DLC controller and therefore small thrust corrections could be made more precisely.

Effects of Approach Angle

Although most of the simulated landing approaches were made with a glideslope angle of 6°, the approach angle was varied during the program. (Glideslope angles of 4°, $7\frac{1}{2}^{\circ}$, and 9° were also simulated.) In addition, a two-segment approach was mechanized so that the glideslope was transferred from 6° to 4°.

With the stability augmentation and control systems operating in modes that produced a pilot rating of $2\frac{1}{2}$ for the ILS approach and a pilot rating of $4\frac{1}{2}$ for the landing task on a glideslope of 6°, approaches were made on the aforementioned glideslope angles

$\left(4^{\circ}, 7\frac{1}{2}^{\circ}, \text{and } 9^{\circ}\right)$ at an airspeed of 75 knots. The pilots commented that they could easily capture and track the glideslope for any of the approach angles used and that the pilot rating for the approach would remain $2\frac{1}{2}$ for all glideslope angles. However, the pilots stated that the pilot rating would deteriorate for the flare and landing task as the approach angle increased and also commented that the breakout altitude would have to be increased as the approach angle increased above 6°. (The minimum acceptable breakout altitude when flying 6° approaches was 30 meters (100 ft).) The pilot ratings assigned to the landing task for approach angles of 4°, 6°, $7\frac{1}{2}^{\circ}$, and 9° were 3, $4\frac{1}{2}$, $5\frac{1}{2}$, and 6, respectively, the comments being that for the 4° approach, he could better judge when to initiate the flare. (The amount of thrust required to compensate for any adverse ground effects could be applied more slowly and confidently.) The pilot comments regarding the flare capability from glideslope angles greater than 6° were that (1) it was more difficult to judge when and how much thrust to apply for the flare; and (2) the engine-thrust response was slower because of the lower engine speed on the steeper approaches.

The pilots concluded that the maximum glideslope from which the airplane should be landed was 6°; and furthermore, in order to have any confidence in making consistently precise landings, the two-segment approach to a glideslope of 4° should be used.

Two-Segment Approach

In an effort to improve the pilot ratings assigned to the landing task from a 6° approach, two-segment approaches were made wherein the flight director (appendix A) was programed to transfer from a glideslope of 6° to a more shallow angle. It was determined during the simulation program that the minimum altitude from which the pilot wanted to initiate the transition from a 6° approach to a more shallow glideslope was approximately 60 meters (200 ft), and as the first segment of the two-segment approach was steepened above 6°, the "transition" altitude was increased. After considering the proposed criterion of reference 8 for STOL obstacle clearance during take-off and landing (fig. 15) and the aforementioned minimum transition altitudes, it was determined that the second segment of the two-segment approach had to be greater than 3.82° (15 to 1 slope). (See fig. 16.) Therefore, the minimum glideslope from which landings were made during the present STOL simulation program was 4°.

When flying the two-segment approaches, the pilots assigned a rating of 3 to the landing task $\left(\text{compared with a pilot rating of } 4\frac{1}{2} \text{ for the landing task from a } 6^{\circ} \text{ approach}\right)$.

Flare and Landing

During the present STOL simulation program, the primary requirements specified for a satisfactory landing were (1) touchdown within the prescribed landing area, a zone

137 meters (450 ft) long starting 76 meters (250 ft) from the runway threshold; and (2) touchdown with an acceptable rate of sink (no greater than 0.9 m/sec (3 ft/sec)). This task presented considerable difficulty to the pilots; and the difficulty can be attributed to three basic problems: (1) the lack of adequate visual height cues; (2) the brevity of the flare; and (3) the adverse ground effects.

The first problem (lack of height cues) is simply due to the failure of the visual presentation to provide the pilot with a good indication of altitude; thus, he could not consistently initiate the flare within the very small altitude tolerance "window."

The second problem (brevity of the flare) is dictated directly by the requirement of having to touchdown within the unusually short landing area. The geometry of the landing flare is presented in figure 17. The four important points in the landing flare maneuver are (1) flare initiation, the point at which the pilot moves his control or controls to initiate the flare; (2) flare point, the point of departure of the airplane's flight path from that of the straight ILS trajectory; (3) threshold conditions, the altitude and rate of sink as the airplane crosses the runway threshold; and (4) condition at touchdown, the rate of sink and runway touchdown point. Table IX presents a comparison of these flare parameters for a typical present-day subsonic jet transport with the subject STOL airplane. The most significant difference in the flare geometries of these two types of airplanes (CTOL and STOL) is that the flare of the STOL airplane is much shorter, both in distance and duration. For example, the flare of the CTOL airplane covers almost 700 meters (2300 ft) horizontally and lasts for more than 11 seconds; whereas, when the STOL airplane is flared from a 6^{o} glideslope, the horizontal distance covered is approximately 183 meters (600 ft) and the flare time is less than 5 seconds. Therefore, the STOL pilot has much less time for iteration and is thus allowed very little margin for error. One pilot described this demanding flare-maneuver task thusly: "It's a one-shot deal; if the pilot errs even a little, the consequences are foregone – either an immediate hard landing or a hard landing following a 'balloon' maneuver." Time histories of three typical landings, made at an airspeed of 75 knots from a 6^{o} glideslope, are presented in figure 18. For the first landing, the pilot added too much thrust and overflared. Upon realizing this, he reduced thrust, but landed very hard and long. On the second landing the flare was initiated only 0.8 second later and approximately 3 meters (10 ft) lower than for the first landing. At this flare-initiation altitude, 8.5 meters $\left(h_{lg} \approx 28 \text{ ft}\right)$, the adverse ground effects were already acting. Responding to this increase in sink rate, the pilot increased thrust rapidly, but the airplane landed with an unacceptably high rate of sink, approximately 1.5 m/sec (5 ft/sec). The third landing indicated in figure 18 shows a good flare and landing; the airplane landed in the middle of the prescribed runway area at a rate of sink of approximately 0.9 m/sec (3 ft/sec).

The thrust time histories of these three landings (fig. 18) emphasize the criticality of when and how much thrust is added to initiate the flare and thus are vivid examples of just how small the pilot's margin for error is when attempting to land this STOL airplane.

The flare and landing task was made all the more difficult by the adverse ground effects. The incremental changes in pitching-moment, lift, and drag coefficients due to ground effect are presented in figure 5, and as can be seen, the data indicate a nose-down pitching moment, a loss in lift, and a decrease in drag as the ground is approached. The effects of ground proximity on C_D and C_m begin at an altitude of approximately 18 meters (60 ft) and increase in severity to touchdown. These two effects were not noticeable to the pilots when the fully augmented airplane was flown, since the pitch-attitude command system closely maintained attitude and the autospeed controller negated the drag loss. The effects of ground proximity on C_L essentially begins at a much lower altitude $\left(h_{lg} \approx 10 \text{ meters } (30 \text{ ft})\right)$ and increases rapidly until touchdown. This characteristic made pilot compensation for the lift loss very difficult. When the "suck-down" is experienced, there is very little time left to counter it and, of course, this problem becomes more severe as landings are made from steeper approaches. (Table IX shows how the time spent in the ground effect t_{ge} decreases as the approach angle increases.) This is one major reason why the pilots preferred transition to a final approach of 4° which allowed more time to compensate for the lift loss due to ground effect.

The transitioning to a shallower approach angle, from which the landing flare is made, conflicts with the well-known fact that steeper final approaches result in smaller touchdown dispersions. However, several other factors should be considered. First, landings from steep approaches require unusually large reductions in sink rate during the flare. For example, a $\Delta\dot{h} \approx 4$ m/sec (13 ft/sec) is required to land from a $7\frac{1}{2}^\circ$ approach at 75 knots, compared with a $\Delta\dot{h} \approx 1.7$ m/sec (5.5 ft/sec) for a 4° approach at the same airspeed. Therefore, much larger and more sudden control inputs (throttles for this STOL airplane) are required for flaring from the steeper approaches. Second, because of the higher sink rates associated with the steeper approach angles, precise timing of the flare initiation becomes even more critical. Also, the previously mentioned suck-down effect appears to be more severe for the steeper approach angles, because of the higher rate of penetration of the ground effects. All these factors lead to a much more demanding pilot task for landing from steep final approaches as reflected by the degraded pilot ratings discussed earlier.

The effects of approach angle on pilot workload required to make a precise landing flare are indicated in figure 19, where some of the best simulated landings from approach angles of 4°, 6°, and $7\frac{1}{2}^\circ$ are presented. Note that for the $7\frac{1}{2}^\circ$ landing, the thrust time history is distinguished by a very large and sudden initial input, followed by some sizable overshooting and oscillating; these conditions indicate that the pilot experienced difficulty

in the closed-loop control of the flare. The landing made from the 4° approach, however, shows a much smoother and gradual thrust input for flaring, and indicates that the pilot had much better control throughout the flare maneuver. It can be seen from table IX that for the landing made from a 4° approach, the flare was initiated at an altitude where the lift loss due to ground proximity had already begun. Therefore, when landing from a 4° approach, the pilot could wait until he experienced the suck-down before he had to compensate for it; whereas, for the steeper approaches, the pilot had to anticipate the lift loss and start the flare before the loss in lift was actually realized. In general, the pilots concluded that unaided visual landings from approach angles greater than 6° was too demanding a task, and felt that they could not make acceptable landings from steeper approaches with any consistency.

It is believed that the use of a head-up display which would provide the pilot with some form of height and sink rate information, or maybe a flare command signal, could reduce the landing task difficulty to the extent that landing from steeper approach angles (greater than 6°) would be considered an acceptable procedure. To provide an initial examination of the concept, a flare mode was added to the flight director glideslope channel which gave thrust commands to follow an exponential altitude path to touchdown. It was determined that the use of this "flare" director helped the pilots to consistently make satisfactory landings, even from approach angles greater than 6°.

Based on the results of this STOL simulation program, wherein the pilots were required to land within the prescribed area and with a rate of sink no greater than 0.9 m/sec (3 ft/sec), it is concluded that unaided visual landings from approach angles greater than 6° constitute a pilot task that is both unsatisfactory and difficult. However, if the pilot is provided an adequate flare information display, such landings become feasible.

Crosswind Landings

As the landing speeds of airplanes decrease, the problems associated with landing in crosswinds increase. For example, when the pilot makes a crosswind approach with a STOL airplane, the crab or sideslip angle required to maintain a given ground track is considerably greater than he is normally used to on CTOL airplanes. For this reason, various piloting techniques were used to fly landing approaches in various crosswind conditions during the present simulation program and these piloting techniques are listed in the order of pilot preference:

(1) Crabbed approach and landing using crosswind landing gear

(2) Crabbed approach that changes to a sideslipping approach at some nominal altitude just prior to landing

(3) Pure wing-down—sideslipping approach and landing

(4) Crabbed approach, and assuming conventional landing gear, having to decrab with rudder just prior to touchdown

Both steady crosswinds (up to 25 knots) and crosswinds with horizontal shear were simulated, and the order of pilot preference of techniques for making the approach and landing remained the same for all crosswind conditions flown.

The configuration flown for all the wind conditions simulated incorporated what was considered to be the best augmentation and control systems (pilot rating is $2\frac{1}{2}$ for ILS approach and $4\frac{1}{2}$ for the landing task in calm air), and all approaches were made on a 6^{o} glideslope at airspeeds of 75 knots and 65 knots. Also, since the pilot ratings did not change for the ILS approach and landing when the crosswinds were present and crosswind landing gear was used, most of the crosswind landings were made by using the technique listed as the pilots' second preference – crabbed approach, and at some nominal altitude, usually about 15 meters (50 ft), changing to a sideslipping, wing-down condition.

Figure 20 indicates the amount of steady-state sideslip, bank angle, and rudder deflection required for sideslipping crosswind approaches at airspeeds of 75 knots and 65 knots. It can be seen that maximum rudder deflection ($\delta_r = 40^{o}$) was required for a crosswind component of 21 knots when the aircraft was flown at 65 knots. (For an airspeed of 75 knots, the maximum crosswind component that could be trimmed was 26.7 knots.) It is therefore obvious that this STOL airplane could not be landed (with an adequate rudder control margin) in 90^{o} crosswinds higher than approximately 20 knots. Also, from a piloting standpoint, the lateral-directional control coordination required for the transition from a crabbed-approach condition to a sideslipping, wing-down condition becomes increasingly difficult as the 90^{o} crosswind increases above 15 knots. The longitudinal task imposed upon the pilot for the flare and landing is in itself very demanding, even in calm air. Therefore, landing in crosswinds without crosswind gear creates an additional lateral-directional task which increases pilot workload tremendously. It is therefore concluded from these ground-based fixed-cockpit simulator results that the subject STOL airplane should be equipped with crosswind gear, and if this is not feasible, the other alternative, of course, is to provide several crossing runways to reduce the possibility of 90^{o} crosswind components greater than 20 knots.

It should be mentioned that although the accuracy of the control coordination was the prime factor that affected the pilot's ability to make "precise" landings in high crosswinds, deficiencies of the visual presentation (quality of picture and lack of peripheral vision) and possibly the lack of cockpit motion also affected the pilot's ability to make satisfactory landings in large crosswinds.

Effects of Turbulence on Landing Approach

Flight in rough air was evaluated by using a turbulence model based on the Dryden spectral form. (See appendix C.) Three gust intensity levels were evaluated by assigning specific values to σ_w, the root-mean-square value of the vertical-gust component, while maintaining the relationship between σ_w, σ_v, and σ_u shown in appendix C. Values of 0.6 m/sec (2 ft/sec), 1.2 m/sec (4 ft/sec), and 1.8 m/sec (6 ft/sec) were used for σ_w, and these values were described by the pilots as being representative of light, moderate, and heavy levels of turbulence, respectively.

Static normal acceleration gust sensitivity can be defined as $S_{a_n} = \frac{C_{L_\alpha} \rho V}{2W/S}$; that is, the vertical response of an airplane to turbulence is directly proportional to the product of lift-curve slope and velocity and is inversely proportional to the wing loading. Table X presents a comparison of S_{a_n} for the subject STOL airplane and a typical present-day subsonic CTOL transport during the landing approach. Note that the wing loadings of the two airplanes are essentially identical, and that the higher value of C_{L_α} for the STOL airplane is offset by its lower approach speed. Therefore, the two S_{a_n} values are nearly equal, the STOL actually showing a slightly lower value. From consideration of these points, the response of the subject STOL airplane to atmospheric turbulence would not be expected to be any worse than the response of CTOL transport airplanes, and the simulation results verify this point.

Figure 21 presents plots of the root-mean-square values of the vertical and lateral accelerations experienced during ILS approaches made in various levels of turbulence for both the subject STOL airplane and a typical CTOL airplane. (The root-mean-square values are compared with the ride quality criterion of ref. 9.) As can be seen, the normal acceleration responses of the two classes of aircraft are very nearly the same. The lateral acceleration root-mean-square values, however, are much lower for the STOL airplane because the STOL augmentation systems act to maintain low sideslip and a wings-level attitude. The pilots had no problems in tracking the localizer for any of the turbulence levels evaluated. (It should be mentioned that although the $(a_y)_{rms}$ is primarily affected by σ_v, $(a_y)_{rms}$ is plotted against σ_w for convenience; σ_v is calculated from σ_w as discussed in appendix C.)

The pilots commented that the pilot rating for the approach task on the subject STOL airplane with σ_w = 1.2 m/sec (4 ft/sec) was $3\frac{1}{2}$ to 4, and the pilot rating with σ_w = 1.8 m/sec (6 ft/sec) was 5 to $5\frac{1}{2}$. (The pilot rating of this STOL airplane in calm air was $2\frac{1}{2}$ for the approach task.) Figure 22 shows a typical approach made in moderate turbulence (σ_w = 1.2 m/sec (4 ft/sec)), and as can be seen, the pilot could track the glide-

slope very closely – the vertical displacement from the desired glideslope (ϵ_{zh}) never exceeded 8 meters (25 ft). However, the ILS glideslope tracking task required considerable pilot effort and resulted in the degraded pilot rating. The thrust time history indicates that the pilot had to constantly make large throttle changes which accounted for most of the pilot workload.

The pilots stated that σ_w = 1.8 m/sec (6 ft/sec) would be about the heaviest level of turbulence that would be acceptable from a pilot workload standpoint, and this statement tends to agree with the ride-quality criterion of reference 9 for normal acceleration. As shown in figure 21, for a σ_w = 1.8 m/sec (6 ft/sec), the root-mean-square value of a_n is approaching the limit for satisfactory ride qualities.

Engine Failure

Lateral-directional control with a critical engine (outboard) failed has always been a prime consideration in the rudder design for multiengine airplanes. For STOL airplanes with high thrust-weight ratios and low airspeeds, engine-out conditions demand serious attention.

Control of asymmetries due to engine failure can be easily analyzed from static conditions by calculating the steady-state sideslip angle, bank angle, and control deflections for a straight flight path over the ground. The transient response immediately following an engine failure, however, presents problems involving pilot reaction time, the manner in which controls are applied, and, of course, the altitude and configuration of the airplane at the time of the failure. Because of the large lift contribution produced by power for the subject externally blown flap STOL design, the rolling moments generated by the thrust asymmetry are more significant than the corresponding yawing moments. Therefore, it was known prior to flying the airplane on the simulator that the primary control problems would be roll control and, of course, altitude control.

The manner in which an engine was failed during the present program was that which would be considered the most severe; that is, the engine failed instantaneously (a step form of thrust loss).

Wave-off capability after engine failure.- Figure 23 shows the effects of engine thrust on trim lift coefficient and flight-path angle for several flap (δ_{f3}) positions. As can be seen, with $\delta_{f3} = 60^o$, it would be impossible to perform a "wave-off" maneuver after an engine failure, and even with $\delta_{f3} = 50^o$, there is essentially no climb capability. Therefore, during this simulation program an autospeed cutoff switch was mounted on the left horn of the pilot's control wheel that allowed the pilot to drive the flaps to the takeoff position ($\delta_{f3} = 35^o$) merely by actuating the autospeed cutoff controller. As can be seen from figure 23, with $\delta_{f3} = 35^o$, an angle of climb of approximately 6^o can be accomplished with the thrust of three engines.

The engine-out wave-off and climb performance of the subject STOL airplane was documented and then compared with the requirements for powered-lift aircraft presented in reference 10. In general, the requirements of reference 10 were "In the event of failure of one engine on approach, it should be possible to arrest the descent and maintain level flight without change in flap setting or airspeed. It should also be possible after arresting the descent to establish a sustained climb angle of 2° (3.5-percent gradient) by retraction of the flap and without change in airspeed." As can be seen from figure 24, the subject STOL airplane exceeds these requirements; with the airspeed being held at 75 knots throughout the flight, the rate of descent was arrested without a change in flap setting (for the approach condition where $V = 75$ knots, $\theta = 4^{\circ}$, and $\gamma = -6^{\circ}$, the δ_{f3} setting is 45°) and then once $\gamma = 0$ flight was attained and the flaps were retracted to 35°, a sustained climb angle of approximately 5° was accomplished.

An attempt was made to determine the minimum altitude from which a wave-off could be performed on three engines. With one engine inoperative, the landing approach was continued down to an altitude of approximately 21 meters (68 ft), at which time maximum thrust was applied on the remaining three engines and the autospeed control was deactivated (which automatically drove the flaps to 35°). This procedure was used for approaches made on glideslopes of 4°, 6°, and $7\frac{1}{2}^{\circ}$; as expected, the amount of ground clearance decreased as the approach angle increased. See figure 25. (From a $7\frac{1}{2}^{\circ}$ approach the ground clearance was 9 meters (30 ft) compared with 14 meters (46 ft) for a 4° approach.)

It is concluded from these results that the subject externally blown jet-flap STOL airplane meets and exceeds the one-engine inoperative wave-off capability requirements of reference 10. It is also concluded that the one-engine-out wave-off could be accomplished successfully if the engine failed at an altitude as low as 30 meters (100 ft), particularly if the previously suggested two-segment approach, with a 4° final segment, is used.

Continued approach and landing after engine failure.- Attempts were made to simulate a continued approach and landing following the loss of an outboard engine. The configuration flown incorporated what was considered to be the best augmentation and control systems. These systems included the previously discussed stability augmentation, pitch-attitude command, roll-rate command, autospeed control, and the flight director.

A typical approach, for which the number one engine was failed during the approach, is presented in figure 26. The most interesting points indicated in this figure are the excursions from the localizer and glideslope immediately following the engine failure. As can be seen, the amount of lateral displacement from the localizer beam was less than

8 meters (25 ft), and the amount of vertical displacement from the glideslope beam was less than 4 meters (13 ft).

The pilots commented that the loss of a critical engine during an ILS approach posed no problems (insofar as tracking localizer and glideslope) with all the aforementioned augmentation and control systems operative, and assigned a pilot rating of $2\frac{1}{2}$ to this condition. However, this engine-out condition definitely presented problems when attempting to touchdown within a designated area on the runway with a rate of sink no greater than 0.9 m/sec (3 ft/sec).

As discussed previously, the preferred piloting technique for flying the landing approach was to use a constant nose-up pitch attitude (which was possible with the autospeed control operative); this procedure leaves only one longitudinal control task for the pilot – the control of flight path with thrust. For the condition where one engine was inoperative, however, the amount of remaining thrust available for flaring appears as a new constraint on the pilot's capability to make acceptable landings.

Figure 27(a) shows a time history of a landing flare made from both a 6^{o} and a 4^{o} approach angle. As can be seen, maximum thrust from the remaining three engines was used in attempting to flare the airplane; however, the rate of sink at touchdown was greater than 0.9 m/sec (3 ft/sec) for both landings. This problem of not having enough reserve thrust to flare the airplane with one engine inoperative is amplified by the loss in angle of attack (and the corresponding loss in lift) which occurs when the pitch attitude is held constant while the glidepath angle is reduced. Therefore, it appeared that the logical solution to the flare problem (short of increasing the maximum T/W) would be for the pilot to rotate the airplane in the flare in order to maintain or gain angle of attack, and thus ΔC_L. The results of using this technique for the landing flare were favorable insofar as reducing the touchdown rate of sink below 0.9 m/sec (3 ft/sec), as can be seen from figure 27(b). However, the pilots objected to this piloting technique; they state that the task of judging when and how much thrust and pitch attitude to add for the flare was much too difficult and that it was thus impossible consistently to make acceptable landings with this technique. This piloting problem is reflected in the time histories of thrust and pitch attitude of figure 27(b). The control sequence was as follows: (1) the pilot increased the thrust to maximum and began to rotate the airplane; (2) then, fearing that he was overflaring and thus would miss the touchdown zone, he reduced thrust; (3) finally, just prior to touchdown, the pilot again increased thrust to soften the landing. It must be remembered that all this maneuvering occurred within a very short period of time, perhaps 4 or 5 seconds, and made the coordination and control of the flare very difficult.

In an attempt to reduce the pilot workload, and at the same time improve the consistency for which acceptable landings could be made with one engine inoperative, the rotation part of the flare was essentially made "automatic" by switching from a "pitch-attitude

command" control system to an "angle-of-attack command" control system at some nominal altitude just prior to the initiation of the flare. (A block diagram of this angle-of-attack command system is presented in fig. 28.) This angle-of-attack command system aids the pilot in two ways during the flare: (1) the pilot does not have to rotate the airplane manually in the flare; thus, the thrust-rotation coordination problem was eliminated. Whereas the pitch-attitude command system holds θ constant in the flare and allows α to decrease as thrust is added for the flare, the α command system holds α constant by pitching the airplane nose upward as thrust is added in the flare; (2) with the α command system operative, it appears to the pilot that the lift loss or suck-down effect due to ground proximity is less severe.

The α command control system produced acceptable results and favorable reactions from the pilots. The rate of sink at touchdown was less than 0.6 m/sec (2 ft/sec) for landings made with three engines from both 6° and 4° approach angles. See figure 27(c). Also, as can be seen from the thrust time histories, the thrust changes made to flare were made in a smooth and positive manner. It should be mentioned that although less than maximum three-engine thrust was required to flare the airplane when the α command system was operative, the pilots felt that the thrust margin was less than desired.

Spread-Engine Configuration

Simulated flights were made with the spread-engine configuration wherein the outboard engines are located at 0.42 semispan as compared with 0.30 semispan for the clustered configuration. Longitudinally, the aerodynamic characteristics of the two configurations were sufficiently similar that the differences were not simulated. Laterally, the differences were (1) larger engine-out moments for the spread-engine arrangement; and (2) the midspan flap elements are used for roll control (δ_a) in the spread-engine configuration whereas for the clustered configuration the inboard elements are used. (As discussed earlier, asymmetric spoiler is used for additional roll control after the ailerons reach maximum deflection.) The only change made to the augmentation system for the spread-engine arrangement was that the aileron-rudder interconnect gain was modified to reflect the fact that the ailerons provided proverse rather than adverse yaw. The lateral augmentation systems were thus not optimized for this configuration; however, the pilots commented that they could fly this configuration as easily and as well as the clustered-engine configuration. Thus, pilot ratings and comments for the normal (four-engine operation) approach and landing condition were the same for both configurations.

Only during the engine-out situation did the two configurations show differences. Because of the larger rolling moments caused by asymmetric thrust, the spread-engine configuration required more roll control to retrim the airplane following an engine failure. The increase in spoiler deflection δ_s thus required, after the ailerons have been satu-

rated, entails a greater lift loss which, in turn, degrades the normal acceleration capability of the airplane. This characteristic was reflected in the wave-off capability wherein the airplane lost about 3 meters (10 ft) more altitude and took about 1.5 seconds longer to return to level flight than the clustered-engine configuration. The lift loss due to increased spoiler deflection is most seriously reflected in the airplane's flare and landing capability. Figure 29 shows that the rate of sink at touchdown was not reduced below 1.5 m/sec (5 ft/sec) even when maximum thrust on the remaining engines were applied to flare the airplane. The pilots rated the three-engine landing performance of the spread-engine configuration unacceptable.

Ground Noise Considerations

The minimization of ground noise is an important factor that must be considered in the development of STOL transport airplanes. Therefore, during the present STOL landing approach simulation program, calculations were made of the overall sound pressure level (OASPL) at a number of ground stations in order to allow comparisons of various piloting techniques and approach geometries from a noise viewpoint. Incremental differences in computed noise levels between two flights provided a measure of how "noisy" one is with respect to the other. The reference flight, against which all others were compared, was one in which the piloting technique used was favored by the pilots (V = 75 knots, glideslope of 6^{o}, and $\theta = 4^{o}$). From this reference flight, a $\Delta OASPL = OASPL_i - OASPL_R$ was generated, where the subscript i refers to the flight under investigation and the subscript R refers to the reference flight. All flights were initiated from below the glideslope at an altitude of 366 meters (1200 ft) – from there, glideslope capture was accomplished and the airplane was landed.

The factors examined were (1) effect of approach speed; (2) effect of airplane pitch attitude; and (3) effect of glideslope angle. The sound pressure level was calculated as a function of four variables: (1) engine thrust; (2) range between airplane and ground station; (3) angle between the airplane and ground station line of sight and the engine axis; and (4) flap deflection. (See appendix D.) Although noise calculations were made for 10 ground station locations, all the results discussed pertain to the station alined with the runway center line and located 1524 meters (5000 ft) short of the runway threshold. It was considered valid to use the noise comparisons from only one ground station location since the variation of ΔOASPL between various stations was small.

Effect of airplane speed.- A landing approach made at an airspeed of 65 knots was, on the average, approximately 4 decibels more noisy than an approach made at 75 knots. (Fig. 30 shows a plot of the ΔOASPL between approaches flown at 65 knots and 75 knots.) There are two reasons for the higher noise level at 65 knots: (1) higher thrust – since the airplane is flown on the backside of the thrust-required curve, flight at 65 knots requires more thrust than at 75 knots, ΔT = 19 600 N (4400 lbf); and (2) for the 65-knot

approach, a greater flap deflection $(\Delta\delta_{f3} > 4^o)$ is required to maintain speed. A pitch attitude of 4^o was specified for both the 65-knot and 75-knot approach.

Effect of pitch attitude.- Landing approaches were made for which the airplane nose was left at the negative trim attitude; for $\gamma = 0^o$ flight and $\delta_{f3} = 60^o$, the trim attitude is -4.1^o for an airspeed of 75 knots. Approaches made with $\theta = -4.1^o$ produced considerably higher noise levels (about 5.4 dB more on the average) than the approaches made with the nose up, $\theta = 4^o$. (The ΔOASPL between approaches made with the airplane nose up and nose down is indicated in fig. 31.) The higher noise level measured for the nose-down approach is due to two factors: (1) higher thrust – since the airplane is flying at a lower angle of attack, more thrust (ΔT = 22 000 N (4900 lbf)) is required to generate the needed lift; and (2) a greater flap deflection $(\Delta\delta_{f3} > 13^o)$ is required to maintain airspeed. These results indicate that flying a constant nose-up attitude approach is desirable not only from a piloting standpoint but also for ground noise reduction.

Effect of glideslope angle.- Figure 32 shows the effect of flying steeper (greater than 6^o) approach angles on the calculated ground noise level. As would be expected, the steeper approaches are less noisy, approximately 2.6 dB quieter for an approach angle of $7\frac{1}{2}^o$ and 3.8 dB quieter for an approach angle of 9^o. The two principal factors are (1) less thrust is required for the steeper approach angles $(\Delta T = -11\,565$ N (-2600 lbf) for $7\frac{1}{2}^o$ and ΔT = -13 345 N (-3000 lbf) for $9^o)$; and (2) for a given ground track position, the airplane is at a higher altitude when on the steeper approach.

Figure 33 depicts the effect of a two-segment approach $(6^o/4^o)$ on the calculated ground noise level. As can be seen, while on the 6^o segment, this approach was slightly more noisy (ΔOASPL = 0.5 dB) than the standard 6^o single-segment approach because at a given point on the ground track, the airplane is at a lower altitude when flying the two-segment approach than when flying the single-segment approach. (See fig. 16.) Also, upon capturing the second segment of the two-segment glideslope (4^o), the noise difference becomes greater (ΔOASPL = 3 dB) because of the increase in thrust. This increase in noise is of short duration, however, since the transition is initiated at a low altitude ($h \approx 60$ meters (200 ft)) and is soon followed by the flare and landing.

Summation of calculated ground noise results.- Ground noise increases with decreasing approach speeds. Therefore, for this STOL simulation program, the 75-knot approach is favored over the 65-knot approach not only from piloting considerations (particularly for the crosswind conditions or the engine-out situation) but also from a minimum noise viewpoint. In addition, the constant nose-up attitude approach favored by the pilots also appears to be highly desirable for noise reduction.

Steeper approaches, greater than 6^o, afford improvements in ground noise at the price of a much more difficult landing task. It appears that of the approach techniques

used during this simulation program, the technique which best satisfies both requirements of piloting ease and "minimum" ground noise would be a two-segment approach consisting of a steep first segment $\left(7\frac{1}{2}^{\circ} \text{ to } 9^{\circ}\right)$ and then a 4° final segment. Such a two-segment approach, flown at 75 knots and with a constant nose-up attitude, should present no excessive piloting problems while the ground noise is kept to a minimum. In addition, it should be understood that although decelerating and/or curved approaches were not investigated during the present study, such techniques could be beneficial from both a noise-reduction and an operational standpoint.

SUMMARY OF RESULTS

A fixed-base simulator program was conducted to determine the flight characteristics of a representative short take-off and landing (STOL) transport having a high wing and equipped with an external-flow jet flap in combination with four high-bypass-ratio fan-jet engines during the approach and landing. The results may be summarized as follows:

1. The longitudinal and lateral-directional dynamic characteristics of the basic (unaugmented) airplane are unacceptable. The average pilot ratings assigned to the longitudinal and lateral-directional handling qualities were $6\frac{1}{2}$ and 9, respectively.

2. Longitudinal augmentation, consisting of a pitch-attitude command system and an autospeed controller, essentially eliminated the longitudinal control problems. Lateral-directional augmentation, consisting of a roll-rate command system, and of sideslip rate $\dot{\beta}$, lateral acceleration a_y', roll rate p, and aileron deflection δ_a feedback signals to the rudder, made the lateral-directional handling characteristics satisfactory. With these augmentation systems operative, the average pilot ratings for the instrument approach task were $3\frac{1}{2}$ and 3 for the longitudinal and lateral-directional tasks, respectively.

3. A flight director optimized for STOL flight considerably reduced the pilot workload in capturing and tracking the glideslope and localizer. $\left(\text{The pilot rating for the instrument approach task was reduced to } 2\frac{1}{2}.\right)$ It was concluded that a good flight director would be mandatory for the subject STOL airplane.

4. It was also concluded that an autospeed system would be a mandatory feature for the subject STOL airplane. The most prevalent feature of the autospeed system was that when used in conjunction with the pitch-attitude command system, the pilot could trim the airplane in a nose-up attitude prior to glideslope intercept, and this pitch attitude could be maintained throughout the approach and landing.

5. With the augmentation and flight director operative, the pilots could easily capture and track the glideslope for any of the simulated approach angles $\left(4^{\circ}, 6^{\circ}, 7\frac{1}{2}^{\circ}, \text{and } 9^{\circ}\right)$, and the pilot rating for the instrument approach task remained the same for all approach angles. They concluded, however, that the maximum glideslope from which the airplane should be landed was 6°; furthermore, in order to have any confidence in making consistently precise landings, a two-segment approach to a glideslope of 4° should be used.

6. The effects of crosswinds on the approach and landing, when crosswind landing gear was simulated, were negligible. However, if the pilot must exchange a crabbed condition for a sideslipping, wing-down final approach and landing, this STOL airplane could not be landed (with an adequate rudder control margin) in 90° crosswinds higher than approximately 20 knots. It was therefore concluded that the subject STOL airplane should be equipped with crosswind landing gear.

7. The response of the subject STOL transport airplane to atmospheric turbulence should not be any worse than the response of CTOL transport airplanes having the same wing loading. In addition, the pilots stated that a root-mean-square value for the vertical-gust component of about 1.8 m/sec (6 ft/sec), as evaluated in this simulation program, would be the heaviest level of turbulence that would be acceptable from a pilot workload standpoint.

8. The engine-out wave-off and climb performance of the subject STOL airplane seemed to be adequate.

9. The loss of a critical engine during an instrument approach posed no problems, insofar as tracking the localizer and glideslope, with all the augmentation and control systems operative. However, the engine-out condition did present problems when attempting to land the airplane within a designated area on the runway with a rate of sink no greater than 0.9 m/sec (3 ft/sec). The pilots felt that the thrust margin was less than desired.

10. It appears that of the approach techniques used during this investigation, the technique which best satisfies both requirements of piloting ease and "minimum" ground noise would be a two-segment approach consisting of a steep first segment $\left(7\frac{1}{2}^{\circ} \text{ to } 9^{\circ}\right)$, and then a 4° final segment. Such a two-segment approach, flown at 75 knots and with a constant nose-up attitude, should present no excessive piloting problems while the ground noise is kept to a minimum.

Langley Research Center,
National Aeronautics and Space Administration,
Hampton, Va., August 7, 1972.

APPENDIX A

DESCRIPTION OF FLIGHT DIRECTOR

A conventional cross-pointer type flight director instrument was used but the command bars (cross pointers) were driven by the main computer program. The logic and gains of the localizer glideslope channels of the program flight director and its performance are presented in the subsequent sections.

Localizer Channel

In general, the same logic that is used for the localizer channel on CTOL airplane flight directors was utilized. A block diagram of the localizer channel is presented in figure 34. This channel of the flight director was activated when the aircraft came within $\pm 2^{o}$ of the localizer beam ($\pm 2^{o}$ of the projected runway center line). When the localizer error ϵ_y was less than 0.3^{o}, a very slow integration of ϵ_y was added to counteract steady-state disturbances and to quicken the final segment of the localizer capture. In order to prevent excessive initial overshoot, this integrator was not active when ϵ_y was larger than 0.3^{o}. The coarse-cut limit (maximum intercept angle) was set at 45^{o} and the bank angle limit was set at 11.5^{o}. (At an airspeed of 75 knots, a bank angle of 11.5^{o} gives a standard (3^{o}/sec) turn rate.)

Glideslope Channel

A block diagram of the glideslope channel of the flight director is presented in figure 35. The two parameters that drive this channel are glideslope linear error ϵ_{zh} and incremental thrust ΔT. The use of a linear error signal ϵ_{zh}, as opposed to an angular error signal ϵ_z, eliminated the change in the sensitivity of the system as the distance from the runway changed. (The linear error can be extracted from the raw ILS angular error by using altitude measurement.) The use of the thrust parameter is compatible with backside operation, where thrust is the principal control for glideslope.

Computation for the glideslope channel of the flight director, for a typical approach, proceeded as follows: As the airplane approached the glideslope beam, the glideslope linear error decreased; and at the capture initiation point (some point prior to $\epsilon_{zh} = 0$), a thrust command ($T_{bias,1}$) was indicated. At the same time, the other computations involving ϵ_{zh} and thrust control were activated to maintain smooth capture and accurate tracking of the desired glideslope. If a two-segment approach was desired, a second thrust command ($T_{bias,2}$) was indicated, at the appropriate altitude, for a smooth capture of the second segment of the glideslope beam.

A flare mode of the glideslope channel was also developed and evaluated, and a block diagram of this mode is presented in figure 36. This system is of the exponential path controller type. At a prescribed altitude, the glideslope tracking modes were disengaged and the flare command signals (calling for an increase in thrust) were activated. By following these commands, the pilots were able to consistently make acceptable landings, even from steep approaches.

Performance of Program Flight Director

Plots of glideslope and localizer errors for a typical ILS approach are presented in figure 37. The data show that both channels of the flight director performed well. The capture of both localizer and glideslope was smooth and accurate; the errors remained small throughout the approach; and, at the 30-meter (100-ft) decision height, the airplane was only 1 meter (3 ft) from the projected runway center line and within 0.3 meter (1 ft) of the glideslope.

APPENDIX B

DEVELOPMENT OF AUGMENTATION SYSTEMS

Compared with CTOL operational requirements, STOL requirements dictate far more precise control capability. For example, the STOL airplane will be required to land on 610-meter (2000-ft) runways upon which the allowable dispersion may be as little as ±30 meters (±100 ft), as compared with -152 meters (-500 ft) to 304 meters (1000 ft) dispersions for CTOL airplanes. At the same time, the basic flying qualities of the STOL airplane are inherently poor relative to CTOL airplane characteristics. Therefore, in order to meet the more precise control requirements of the STOL airplane, more stringent demands are made on the STOL augmentation systems than those for CTOL airplanes.

One major aim of this study was to evaluate and compare various flight control and stability augmentation systems applied to the subject externally blown flap STOL airplane. These systems were formulated and incorporated into the computer program so that any combination of systems could be readily obtained for any given flight. Several basic assumptions were made in formulating these systems:

(1) All systems are completely deterministic; measurement noise or bias errors were not considered.

(2) All servoactuators were modeled as first-order lags with a 0.1-second time constant.

(3) All augmentation systems had 100-percent control authority.

(4) Some onboard computation capability was assumed to be available.

A description of the stability augmentation and flight-control systems evaluated is presented in the subsequent paragraphs.

Basic Augmentation

Longitudinal.- The "basic" longitudinal augmentation (fig. 38) was developed in an attempt to rectify the major longitudinal deficiencies of the unaugmented airplane. These deficiencies were: (1) sluggish initial pitch response; (2) low apparent pitch damping; (3) large pitch-attitude excursions associated with changes in thrust, flaps, spoilers, and bank angle; and (4) short-period phugoid which caused pilot-induced oscillations.

To improve the initial pitch response, the column deflection signal was fed through a prefilter. Basically a lead network, the filter amplified high-frequency signals relative to signals of lower frequency; therefore, more rapid pitch response for sudden maneuvers was provided, but the pitch sensitivity for small, slow maneuvers was not degraded. This prefiltering somewhat improved the initial pitch response, although the

pilots still described the response as less than that desired. An amplified pitch-rate signal was added to increase the pitch damping.

Filtered thrust, flap, spoiler, and bank-angle signals were fed into the tail servo in an attempt to nullify the pitch-attitude excursions associated with variations in these parameters. However, these interconnects never performed acceptably; without pilot compensation, pitch trim changes remained large.

An autospeed system, which maintained the desired airspeed by driving the third flap segment (δ_{f3}), was added. This system accomplished three objectives: (1) it eliminated the phugoid mode which was the source of much of the basic longitudinal handling difficulties; (2) it provided good speed control, which is essential to minimizing landing errors; and (3) it relieved the pilot of the speed control task and hence reduced pilot workload.

Lateral directional.- The basic lateral-directional augmentation was developed in an attempt to rectify the major lateral-directional deficiencies of the unaugmented airplane. These deficiencies were (1) unacceptably large sideslip excursions in turns; (2) a highly divergent spiral mode; and (3) low roll damping.

Figure 39 presents a block diagram of the basic lateral-directional augmentation system which consisted of $\dot{\beta}$, a_y', and p feedbacks to the rudder, and p and r feedbacks to the ailerons. The a_y' signal was generated from the raw lateral-acceleration measurement a_y by subtracting the contribution due to rudder deflection; thus, only the dominant contribution due to sideslip remains. (As an approximation to a_y' the following equation was used: $a_y' = a_y - 0.00286\delta_r$.) The $\dot{\beta}$ and a_y' feedbacks improved the Dutch roll characteristics of the airplane (both damping and frequency were increased) and, at the same time, much better turn coordination was obtained. Roll rate p feedback to the rudder was added to further reduce sideslip excursions during turn entry. Also, an interconnect between ailerons and rudder was added to compensate for the adverse yaw due to ailerons.

The yaw rate r signal being fed back to the ailerons served to stabilize the spiral root, which was highly unstable $(t_2 \approx 5$ seconds) for the unaugmented airplane. The roll rate p feedback to the ailerons provided additional roll damping.

This basic lateral-directional augmentation system provided excellent turn coordination; sideslip never exceeded 2^o for bank-angle changes of more than 30^o. Roll oscillations were also almost eliminated, since the Dutch roll pole was almost canceled by the numerator zero in the ϕ/δ_a transfer function.

It should be mentioned that direct measurement of $\dot{\beta}$ may prove to be difficult; therefore, a washed-out yaw damper was evaluated in place of the $\dot{\beta}$ feedback. (The remaining aforementioned feedbacks were the same.) The turn coordination was degraded

slightly with this system since the yaw damper applies a rudder deflection opposite to that required in the turn and therefore increases sideslip. Generally, the pilots degraded the lateral-directional handling qualities by one-half rating when the yaw damper was substituted for the $\dot{\beta}$ feedback.

It is believed that on an airplane with modest computational capability, $\dot{\beta}$ can be generated indirectly from measurements of more easily measured parameters $\left(\dot{\beta} \approx \frac{g}{V_a}\phi - r + \frac{g}{V_a}a_y\right)$; therefore, $\dot{\beta}$ feedback was used during the remainder of this simulation program.

Command Augmentation

Longitudinal.- The stringent task requirements for the STOL airplane during the approach and landing indicate the need for control strategies which are highly task oriented, in order to maximize pilot performance and minimize pilot workload. Longitudinally, the two basic piloting tasks are flight-path control and speed control. In addition, a constraint on pitch attitude is necessary since it is required that the airplane lands in a nose-up attitude. Ideally, the pilot would like to control all three parameters (V, γ, and θ) independently.

During the present STOL simulation program the autospeed controller afforded precise control of airspeed and thus relieved the pilot of the speed-control task; longitudinally, only γ and θ were left for the pilot to control. It was determined during the program that the preferred piloting technique was a constant-attitude approach, in which thrust is used for glidepath control while the nose of the airplane is maintained at some positive attitude ($\theta \approx 4^{\circ}$) throughout the approach and landing. To facilitate this piloting technique, an attitude command control system was incorporated which provided pitch changes from trim, proportional to column deflection. (See fig. 40.) Trim attitude was varied through the longitudinal trim controller δ_{lt}, a feature which allowed small, precise pitch corrections to be made very easily.

This pitch-attitude command control system provided the desired characteristics of rapid well-damped responses to pilot inputs, and inherent attitude stability for no pilot inputs. With this system operative, the pitch-attitude control task is eliminated and the pilot is left with the single task of glidepath control with thrust. Because of the decreased pilot workload and increased task precision, a pilot rating of $3\frac{1}{2}$ was assigned to the longitudinal control of this augmented configuration during unaided (no flight director) ILS approaches.

Lateral.- A rate command system was implemented which provided roll rate proportional to wheel position. (See fig. 41.) Because p, and not $\dot{\phi}$, feedback was used,

the system provides a slightly stable spiral mode rather than attitude hold upon removal of a pilot command. However, the system minimizes unwanted roll disturbances by commanding zero roll rate (p) for no pilot command. This feature is especially beneficial for the engine-out situation where the large roll disturbance torque is essentially automatically compensated for by the roll-rate command system, and therefore the "engine-failure" pilot task is considerably reduced.

APPENDIX C

SIMULATED ATMOSPHERIC TURBULENCE

The random turbulence model used in the subject STOL simulation program is based on the Dryden spectral form. Longitudinal, lateral, and vertical gust-velocity components were generated by feeding Gaussian white noise from three independent random number generators through three shaping filters. (See fig. 42.) Rotational gusts were not simulated.

The filter transfer functions are:

$$G_{u_g}(s) = \sigma_u \sqrt{\frac{2V_o}{\pi L_u \Phi_o}} \left(\frac{1}{s + \frac{V_o}{L_u}} \right)$$

$$G_{v_g}(s) = \sigma_v \sqrt{\frac{3V_o}{\pi L_v \Phi_o}} \left[\frac{s + \frac{1}{\sqrt{3}} \frac{V_o}{L_v}}{\left(s + \frac{V_o}{L_v} \right)^2} \right]$$

$$G_{w_g}(s) = \sigma_w \sqrt{\frac{3V_o}{\pi L_w \Phi_o}} \left[\frac{s + \frac{1}{\sqrt{3}} \frac{V_o}{L_w}}{\left(s + \frac{V_o}{L_w} \right)^2} \right]$$

where

$G_{u_g}, G_{v_g}, G_{w_g}$	shaping filter transfer functions for gust velocity components along the X, Y, and Z airplane body axes, respectively
σ	root-mean-square gust intensity, m/sec (ft/sec)
V_o	initial total velocity of airplane, m/sec (ft/sec)
L	scale for turbulence velocities, m (ft)
Φ_o	white noise power spectral density, seconds

The normal method of scaling the turbulence is as follows:

When $h \geqq 533.4$ meters (1750 ft), $L_u = L_v = L_w = 533.4$ meters (1750 ft), and when $h < 533.4$ meters (1750 ft),

$$L_w = h$$

$$L_u = L_v = 145h^{1/3}$$

However, for the subject STOL landing approach simulation program, the turbulence was scaled by using an average altitude of 152 meters (500 ft); that is, $L_w = 152$ meters (500 ft) and $L_u = L_v = 351$ meters (1151 ft).

Three levels of turbulence were simulated during the program by assigning specific values to σ_w. Values of 0.6 m/sec (2 ft/sec), 1.2 m/sec (4 ft/sec), and 1.8 m/sec (6 ft/sec) were used for σ_w, and these values were described by the pilots as being representative of light, moderate, and heavy levels of turbulence, respectively. The intensities of σ_u and σ_v were determined by using the following relationships:

$$\frac{\sigma_u^2}{L_u} = \frac{\sigma_v^2}{L_v} = \frac{\sigma_w^2}{L_w}$$

It was believed to be unrealistic to maintain a constant vertical gust intensity σ_w to touchdown; therefore, the following equation for σ_w was derived by using the aforementioned relationship

$$\sigma_w = \sigma_u\sqrt{\frac{L_w}{L_u}}$$

As stated previously, $L_w = h$ and $L_u = 145h^{1/3}$; therefore the σ_w equation can be written as

$$\sigma_w = \frac{\sigma_u}{\sqrt{145}}h^{1/3}$$

Under the assumption that σ_u is constant with altitude, this equation states that σ_w is a function of the cube root of altitude, and was therefore used to decrease σ_w smoothly to zero at some altitude below 30 meters (100 ft). Because of the lack of turbulence data at very low altitudes as well as insufficient knowledge as to how turbulence interacts with the flow induced by the jet-flap system in ground effect, the vertical-gust component of the turbulence was arbitrarily decreased to zero before the onset of the lift loss due to ground effect. The σ_w was "bled-off" to zero between 30 meters (100 ft) and 15 meters (50 ft). (See fig. 43.) The longitudinal σ_u and lateral σ_v gust intensities remained constant with altitude.

APPENDIX D

GROUND NOISE CALCULATIONS

A computer program was written which calculated overall sound pressure level (OASPL) at various stations on the ground. The sound pressure level was programed as a function of four variables: (1) engine thrust; (2) range between airplane and ground station; (3) angle between the airplane/ground station line of sight and the engine axis; and (4) flap deflection. The geometry of the problem is shown in figure 44.

Noise data for the basic TF-34 engine was obtained from the engine manufacturer. The data provided a reference overall sound pressure level (SPL) as a function of the variables (1), (2), and (3) listed in the preceding paragraph. (Extrapolation to the actual range was accomplished by using the basic spherical wave relationship that intensity is inversely proportional to the square of the range.) In addition, a factor was added to account for noise due to jet exhaust interaction with the flaps. Because of the lack of measured data, this "flap scrub" noise was roughly approximated to be linear with flap deflection, and a value of 0.167 decibel/degree was used.

The form of the final equation used to make the ground noise calculations was:

$$OASPL_N = OASPL_0 - 20 \log \frac{R_n}{R_0} + 10 \log(E) + K_{f3}\delta_{f3}$$

where

$OASPL_N$ overall sound pressure level at ground station N, decibels

$OASPL_0$ engine reference overall sound pressure level, decibels

R_0 reference range, meters (ft)

R_n actual range from airplane to ground station N, meters (ft)

E number of engines (four)

K_{f3} flap scrub noise, 0.167 decibel/degree

δ_{f3} deflection of third segment of wing trailing-edge flap, deg

It is obvious that the absolute values of sound pressure level ($OASPL_N$) calculated from this equation are not meaningful in themselves since the basic reference data are approximate and because the noise computation has been simplified. However, the results of these computations should provide a valid basis for comparing various piloting techniques from a ground noise viewpoint. That is, the incremental difference in the noise level $\Delta OASPL_N$ between various flight configurations or modes is a valid measure of how noisy one is with respect to the other.

REFERENCES

1. Grantham, William D.; Deal, Perry L.; and Sommer, Robert W.: Simulator Study of the Instrument Landing Approach of a Heavy Subsonic Jet Transport With an External-Flow Jet-Flap System Used for Additional Lift. NASA TN D-5862, 1970.

2. Grantham, William D.; Sommer, Robert W.; and Deal, Perry L.: Simulator Study of Flight Characteristics of a Jet-Flap STOL Transport Airplane During Approach and Landing. NASA TN D-6225, 1971.

3. Parlett, Lysle P.; Greer, H. Douglas; Henderson, Robert L.; and Carter, C. Robert: Wind-Tunnel Investigation of an External-Flow Jet-Flap Transport Configuration Having Full-Span Triple-Slotted Flaps. NASA TN D-6391, 1971.

4. Grafton, Sue B.; Parlett, Lysle P.; and Smith, Charles C., Jr.: Dynamic Stability Derivatives of a Jet Transport Configuration With High Thrust-Weight Ratio and an Externally Blown Jet Flap. NASA TN D-6440, 1971.

5. Vogler, Raymond D.: Wind-Tunnel Investigation of a Four-Engine Externally Blowing Jet-Flap STOL Airplane Model. NASA TN D-7034, 1970.

6. Innis, Robert C.; Holzhauser, Curt A.; and Quigley, Hervey C.: Airworthiness Considerations for STOL Aircraft. NASA TN D-5594, 1970.

7. Anon.: Flying Qualities of Piloted Airplanes. Mil. Specif. MIL-F-8785B(ASG); Aug. 7, 1969.

8. Anon.: Planning and Design Criterion of Metropolitan STOL Ports. AC 150/5300-8, FAA, Nov. 1970.

9. Anon.: Low-Wing-Loading STOL Transport Ride Smoothing Feasibility Study. D3-8514-2 (Contract NAS1-10410), Boeing Co., Feb. 8, 1971. (Available as NASA CR-111819.)

10. Parlett, Lysle P.; Fink, Marvin P.; and Freeman, Delma C., Jr.: (With appendix B by Marion O. McKinney and Joseph L. Johnson, Jr.): Wind-Tunnel Investigation of a Large Jet Transport Model Equipped With an External-Flow Jet Flap. NASA TN D-4928, 1968.

TABLE I.- SIMULATED ENGINE RESPONSE CHARACTERISTICS

[The thrust values are presented in units of newtons (pounds force)]

(a) Acceleration

Time, sec	Thrust response for T_c, N (lbf), of –										
	2611 (587)	6530 (1468)	13 625 (3063)	16 796 (3776)	22 023 (4951)	36 764 (8265)	6904 (1552)	14 741 (3314)	18 847 (4237)	21 649 (4867)	36 764 (8265)
0	1681 (378)	1681 (378)	1 681 (378)	1 681 (378)	1 681 (378)	1 681 (378)	2611 (587)	2 611 (587)	2 611 (587)	2 611 (587)	2 611 (587)
.2	1681 (378)	1681 (378)	1 681 (378)	1 681 (378)	1 681 (378)	1 681 (378)	2705 (608)	2 705 (608)	2 705 (608)	2 705 (608)	2 705 (608)
.4	1775 (399)	1775 (399)	1 775 (399)	1 775 (399)	1 775 (399)	1 775 (399)	2798 (629)	2 798 (629)	2 798 (629)	2 798 (629)	2 798 (629)
.6	1868 (420)	1868 (420)	1 868 (420)	1 868 (420)	1 868 (420)	1 868 (420)	2985 (671)	2 985 (671)	2 985 (671)	2 985 (671)	2 985 (671)
.8	2055 (462)	2055 (462)	2 055 (462)	2 055 (462)	2 055 (462)	2 055 (462)	3358 (755)	3 358 (755)	3 358 (755)	3 358 (755)	3 358 (755)
1.0	2144 (482)	2144 (482)	2 144 (482)	2 144 (482)	2 144 (482)	2 144 (482)	4106 (923)	4 106 (923)	4 106 (923)	4 106 (923)	4 106 (923)
1.2	2331 (524)	2331 (524)	2 331 (524)	2 331 (524)	2 331 (524)	2 331 (524)	5227 (1175)	5 227 (1175)	5 227 (1175)	5 227 (1175)	5 227 (1175)
1.4	2424 (545)	2611 (587)	2 611 (587)	2 611 (587)	2 611 (587)	2 611 (587)	5600 (1259)	7 090 (1594)	7 277 (1636)	7 277 (1636)	7 277 (1636)
1.6	2518 (566)	2985 (671)	2 985 (671)	2 985 (671)	2 985 (671)	2 985 (671)	5880 (1322)	10 449 (2349)	10 449 (2349)	10 449 (2349)	10 449 (2349)
1.8	2611 (587)	3545 (797)	3 545 (797)	3 545 (797)	3 545 (797)	3 545 (797)	6161 (1385)	11 196 (2517)	12 691 (2853)	12 691 (2853)	15 302 (3440)
2.0		4012 (902)	4 386 (986)	4 386 (986)	4 386 (986)	4 386 (986)	6343 (1426)	11 943 (2685)	14 372 (3231)	15 115 (3398)	18 473 (4153)
2.2		4666 (1049)	5 600 (1259)	5 600 (1259)	5 600 (1259)	5 600 (1259)	6437 (1447)	12 504 (2811)	15 489 (3482)	16 796 (3776)	21 649 (4867)
2.4		5040 (1133)	8 211 (1846)	8 211 (1846)	8 211 (1846)	8 211 (1846)	6623 (1489)	12 878 (2895)	16 329 (3671)	17 917 (4028)	24 447 (5496)
2.6		5600 (1259)	9 519 (2140)	11 383 (2559)	11 383 (2559)	11 383 (2559)	6717 (1510)	13 158 (2958)	16 983 (3818)	18 571 (4175)	26 876 (6042)
2.8		5974 (1343)	10 360 (2329)	12 686 (2852)	15 395 (3461)	16 610 (3734)	6810 (1531)	13 438 (3021)	17 357 (3902)	19 034 (4279)	28 740 (6461)
3.0		6250 (1405)	11 196 (2517)	13 812 (3105)	16 983 (3818)	21 276 (4783)	6904 (1552)	13 625 (3063)	17 637 (3965)	19 407 (4363)	30 048 (6755)
3.2		6437 (1447)	11 943 (2685)	14 741 (3314)	18 104 (4070)	24 634 (5538)		13 718 (3084)	17 824 (4007)	19 781 (4447)	31 258 (7027)
3.4		6530 (1468)	12 317 (2769)	15 302 (3440)	18 571 (4175)	27 619 (6209)		13 905 (3126)	18 011 (4049)	19 968 (4489)	32 378 (7279)
3.6			12 691 (2853)	15 675 (3524)	19 034 (4279)	29 487 (6629)		13 998 (3147)	18 104 (4070)	20 248 (4552)	33 126 (7447)
3.8			12 878 (2895)	15 956 (3587)	19 407 (4363)	31 164 (7006)		14 092 (3168)	18 198 (4091)	20 417 (4590)	33 780 (7594)
4.0			13 251 (2979)	16 143 (3629)	19 781 (4447)	32 472 (7300)		14 185 (3189)	18 384 (4133)	20 715 (4657)	34 340 (7720)
4.2			13 438 (3021)	16 236 (3650)	20 061 (4510)	33 499 (7531)		14 279 (3210)	18 473 (4153)	20 809 (4678)	34 807 (7825)
4.4			13 625 (3063)	16 423 (3692)	20 342 (4573)	34 153 (7678)		14 372 (3231)	18 571 (4175)	20 996 (4720)	35 270 (7929)
4.6				16 516 (3713)	20 435 (4594)	34 714 (7804)		14 466 (3252)	18 665 (4196)	21 089 (4741)	35 643 (8013)
4.8				16 610 (3734)	20 622 (4636)	35 270 (7929)		14 555 (3272)	18 754 (4216)	21 182 (4762)	35 924 (8076)
5.0				16 703 (3755)	20 715 (4657)	35 643 (8013)		14 648 (3293)	18 847 (4237)	21 276 (4783)	36 204 (8139)
5.2				16 796 (3776)	20 902 (4699)	36 017 (8097)		14 741 (3314)		21 463 (4825)	36 391 (8181)
5.4					20 996 (4720)	36 297 (8160)				21 556 (4846)	36 578 (8223)
5.6					21 089 (4741)	36 578 (8223)				21 649 (4867)	36 671 (8244)
5.8					21 276 (4783)	36 671 (8244)					36 764 (8265)
6.0					21 463 (4825)	36 764 (8265)					
6.2					21 556 (4846)						
6.4					21 649 (4867)						
6.6					21 930 (4930)						
6.8					22 023 (4951)						

TABLE I.- SIMULATED ENGINE RESPONSE CHARACTERISTICS – Continued

[The thrust values are presented in units of newtons (pounds force)]

(a) Acceleration – Concluded

Time, sec	Thrust response for T_c, N (lbf), of –											
	36 764 (8265)	18 198 (4091)	36 764 (8265)	13 905 (3126)	22 397 (5035)	36 764 (8265)	19 594 (4405)	22 953 (5160)	36 764 (8265)	22 953 (5160)	36 764 (8265)	36 764 (8265)
0	4 479 (1007)	11 196 (2517)	11 196 (2517)	12 317 (2769)	12 317 (2769)	12 317 (2769)	16 796 (3776)	16 796 (3776)	16 796 (3776)	20 715 (4657)	20 715 (4657)	24 447 (5496)
.2	4 853 (1091)	12 317 (2769)	12 317 (2769)	12 878 (2895)	13 998 (3147)	13 998 (3147)	18 291 (4112)	19 221 (4321)	19 221 (4321)	21 836 (4909)	24 074 (5412)	27 806 (6251)
.4	5 600 (1259)	14 555 (3272)	15 675 (3524)	13 251 (2979)	16 796 (3776)	16 796 (3776)	18 940 (4258)	20 342 (4573)	24 074 (5412)	22 116 (4972)	30 048 (6755)	31 912 (7174)
.6	7 090 (1594)	15 302 (3440)	20 528 (4615)	13 438 (3021)	18 291 (4112)	22 397 (5035)	19 127 (4300)	21 089 (4741)	27 993 (6293)	22 303 (5014)	32 472 (7300)	33 407 (7510)
.8	9 519 (2140)	16 049 (3608)	24 634 (5538)	13 531 (3042)	19 407 (4363)	26 129 (5874)	19 407 (4363)	21 836 (4909)	30 608 (6881)	22 490 (5056)	33 780 (7594)	34 528 (7762)
1.0	12 878 (2895)	16 610 (3734)	27 993 (6293)	13 625 (3063)	20 342 (4573)	29 113 (6545)	19 594 (4405)	22 397 (5035)	32 472 (7300)	22 677 (5098)	34 527 (7762)	35 644 (8013)
1.2	17 917 (4028)	17 170 (3860)	30 234 (6797)	13 718 (3084)	20 902 (4699)	30 888 (6944)		22 677 (5098)	33 593 (7552)	22 770 (5119)	35 087 (7888)	36 205 (8139)
1.4	22 397 (5035)	17 357 (3902)	31 538 (7090)	13 812 (3105)	21 463 (4825)	32 285 (7258)		22 953 (5160)	34 247 (7699)	22 953 (5160)	35 643 (8013)	36 764 (8265)
1.6	25 755 (5790)	17 637 (3965)	32 472 (7300)	13 905 (3126)	21 930 (4930)	33 219 (7468)			34 714 (7804)		36 017 (8097)	
1.8	28 553 (6419)	17 917 (4028)	33 219 (7468)		22 210 (4993)	33 966 (7636)			35 270 (7929)		36 391 (8181)	
2.0	30 421 (6839)	18 011 (4049)	33 780 (7594)		22 397 (5035)	34 527 (7762)			35 830 (8055)		36 764 (8265)	
2.2	31 444 (7069)	18 104 (4070)	34 340 (7720)			35 087 (7888)			36 204 (8139)			
2.4	32 285 (7258)	18 198 (4091)	34 714 (7804)			35 457 (7971)			36 578 (8223)			
2.6	32 846 (7384)		35 270 (7929)			35 830 (8055)			36 764 (8265)			
2.8	33 499 (7531)		35 830 (8055)			36 297 (8160)						
3.0	34 153 (7678)		36 204 (8139)			36 578 (8223)						
3.2	34 714 (7804)		36 484 (8202)			36 764 (8265)						
3.4	35 087 (7888)		36 671 (8244)									
3.6	35 457 (7971)		36 764 (8265)									
3.8	35 737 (8034)											
4.0	35 924 (8076)											
4.2	36 110 (8118)											
4.4	36 204 (8139)											
4.6	36 391 (8181)											
4.8	36 484 (8202)											
5.0	36 578 (8223)											
5.2	36 671 (8244)											
5.4	36 764 (8265)											

TABLE I.- SIMULATED ENGINE RESPONSE CHARACTERISTICS – Continued

[The thrust values are presented in units of newtons (pounds force)]

(b) Deceleration

Time, sec	Thrust response for T_c, N (lbf), of –									
	1 681 (378)	8 772 (1972)	17 357 (3902)	19 781 (4447)	24 447 (5496)	1 681 (378)	13 069 (2938)	16 796 (3776)	21 836 (4909)	1 681 (378)
0	36 764 (8265)	36 764 (8265)	36 764 (8265)	36 764 (8265)	36 764 (8265)	24 634 (5538)	24 634 (5538)	24 634 (5538)	23 513 (5286)	22 770 (5119)
.2	32 846 (7384)	32 846 (7384)	32 846 (7384)	32 846 (7384)	32 846 (7384)	21 743 (4888)	21 743 (4888)	22 210 (4993)	23 046 (5181)	20 155 (4531)
.4	26 876 (6042)	26 876 (6042)	26 876 (6042)	26 876 (6042)	26 876 (6042)	19 221 (4321)	19 221 (4321)	20 155 (4531)	22 677 (5098)	18 198 (4091)
.6	22 397 (5035)	22 397 (5035)	24 447 (5496)	24 634 (5538)	24 634 (5538)	17 170 (3860)	17 170 (3860)	19 034 (4279)	22 397 (5035)	16 049 (3608)
.8	18 847 (4237)	18 847 (4237)	22 584 (5077)	23 700 (5328)	24 447 (5496)	15 675 (3524)	15 675 (3524)	18 478 (4154)	22 210 (4993)	13 998 (3147)
1.0	16 610 (3734)	16 610 (3734)	21 463 (4825)	23 140 (5202)		14 092 (3168)	15 022 (3377)	18 104 (4070)	22 116 (4972)	12 504 (2811)
1.2	14 928 (3356)	15 302 (3440)	21 099 (4741)	22 770 (5119)		12 691 (2853)	14 555 (3272)	17 824 (4007)	21 930 (4930)	11 290 (2538)
1.4	13 812 (3105)	14 372 (3231)	20 715 (4657)	22 397 (5035)		11 196 (2517)	14 092 (3168)	17 637 (3965)	21 836 (4909)	10 449 (2349)
1.6	12 504 (2811)	13 812 (3105)	20 342 (4573)	22 210 (4993)		10 449 (2349)	13 812 (3105)	17 450 (3923)		9 706 (2182)
1.8	11 570 (2601)	13 438 (3021)	19 968 (4489)	22 023 (4951)		9 519 (2140)	13 438 (3021)	17 357 (3902)		8 959 (2014)
2.0	10 916 (2454)	12 971 (2916)	19 594 (4405)	21 836 (4909)		8 772 (1972)	13 251 (2979)	17 263 (3881)		8 398 (1888)
2.2	10 266 (2308)	12 691 (2853)	19 221 (4321)	21 649 (4867)		8 211 (1846)	13 069 (2938)	17 170 (3860)		7 838 (1762)
2.4	9 519 (2140)	12 410 (2790)	19 034 (4279)	21 463 (4825)		7 838 (1762)		17 077 (3839)		7 277 (1636)
2.6	8 772 (1972)	12 130 (2727)	18 847 (4237)	21 276 (4783)		7 371 (1657)		16 983 (3818)		6 904 (1552)
2.8	8 211 (1846)	11 943 (2685)	18 665 (4196)	21 089 (4741)		6 997 (1573)		16 890 (3797)		6 530 (1468)
3.0	7 838 (1762)	11 663 (2622)	18 478 (4154)	20 902 (4699)		6 717 (1510)		16 796 (3776)		6 161 (1385)
3.2	7 464 (1678)	11 478 (2580)	18 291 (4112)	20 809 (4678)		6 343 (1426)				5 787 (1301)
3.4	7 090 (1594)	11 290 (2538)	18 198 (4091)	20 715 (4657)		5 974 (1343)				5 600 (1259)
3.6	6 717 (1510)	11 103 (2496)	18 104 (4070)	20 528 (4615)		5 600 (1259)				5 320 (1196)
3.8	6 530 (1468)	11 009 (2475)	18 011 (4049)	20 435 (4594)		5 413 (1217)				5 133 (1154)
4.0	6 161 (1385)	10 822 (2433)	17 917 (4028)	20 342 (4573)		5 227 (1175)				4 853 (1091)
4.2	5 974 (1343)	10 636 (2391)	17 824 (4007)	20 248 (4552)		5 040 (1133)				4 573 (1028)
4.4	5 694 (1280)	10 449 (2349)	17 731 (3986)	20 155 (4531)		4 760 (1070)				4 386 (986)
4.6	5 413 (1217)	10 360 (2329)	17 637 (3965)	20 061 (4510)		4 479 (1007)				4 106 (923)
4.8	5 227 (1175)	10 266 (2308)	17 544 (3944)	19 968 (4489)		4 293 (965)				3 825 (860)
5.0	5 040 (1133)	10 080 (2266)	17 450 (3923)	19 875 (4468)		4 107 (923)				3 639 (818)
5.2	4 853 (1091)	9 986 (2245)	17 357 (3902)	19 781 (4447)		3 732 (839)				3 452 (776)
5.4	4 479 (1007)	9 893 (2224)				3 545 (797)				3 265 (734)
5.6	4 293 (965)	9 706 (2182)				3 358 (755)				3 172 (713)
5.8	4 106 (923)	9 613 (2161)				3 265 (734)				2 985 (671)
6.0	3 919 (881)	9 519 (2140)				3 078 (692)				2 798 (629)
6.2	3 732 (839)	9 426 (2119)				2 985 (671)				2 705 (608)
6.4	3 545 (797)	9 239 (2077)				2 798 (629)				2 518 (566)
6.6	3 172 (713)	9 145 (2056)				2 611 (587)				2 424 (545)
6.8	2 985 (671)	9 052 (2035)				2 424 (545)				2 237 (503)
7.0	2 798 (629)	8 959 (2014)				2 237 (503)				2 055 (462)
7.2	2 611 (587)	8 865 (1993)				2 055 (462)				1 962 (441)
7.4	2 424 (545)	8 772 (1972)				1 868 (420)				1 868 (420)
7.6	2 144 (482)					1 681 (378)				1 775 (399)
7.8	1 868 (420)									1 681 (378)
8.0	1 681 (378)									

TABLE I.- SIMULATED ENGINE RESPONSE CHARACTERISTICS – Concluded

[The thrust values are presented in units of newtons (pounds force)]

(b) Deceleration – Concluded

Time, sec	Thrust response for T_c, N (lbf), of –									
	3 732 (839)	17 917 (4028)	11 917 (2679)	1 681 (378)	7 464 (1678)	3 732 (839)	12 691 (2853)	1 681 (378)	3732 (839)	1681 (378)
0	20 155 (4531)	20 155 (4531)	18 754 (4216)	17 824 (4007)	17 824 (4007)	15 115 (3398)	13 998 (3147)	13 438 (3021)	7464 (1678)	5413 (1217)
.2	18 847 (4237)	19 034 (4279)	17 450 (3923)	16 423 (3692)	16 049 (3608)	14 372 (3231)	13 625 (3063)	12 504 (2811)	7184 (1615)	5133 (1154)
.4	17 170 (3860)	18 665 (4196)	15 862 (3566)	14 555 (3272)	14 741 (3314)	13 438 (3021)	13 345 (3000)	11 570 (2601)	6810 (1531)	4853 (1091)
.6	15 302 (3440)	18 478 (4154)	14 555 (3272)	13 158 (2958)	13 812 (3105)	12 130 (2727)	13 158 (2958)	10 636 (2391)	6437 (1447)	4573 (1028)
.8	13 438 (3021)	18 291 (4112)	13 812 (3105)	11 757 (2643)	12 878 (2895)	10 822 (2433)	12 971 (2916)	9 706 (2182)	6067 (1364)	4293 (965)
1.0	11 943 (2685)	18 104 (4070)	13 345 (3000)	10 449 (2349)	11 943 (2685)	9 706 (2182)	12 913 (2903)	8 772 (1972)	5694 (1280)	4012 (902)
1.2	10 822 (2433)	17 917 (4028)	12 971 (2916)	9 332 (2098)	11 383 (2559)	8 959 (2014)	12 878 (2895)	8 025 (1804)	5320 (1196)	3732 (839)
1.4	9 893 (2224)		12 691 (2853)	8 398 (1888)	10 822 (2433)	8 211 (1846)	12 784 (2874)	7 277 (1636)	5040 (1133)	3545 (797)
1.6	9 145 (2056)		12 504 (2811)	7 838 (1762)	10 449 (2349)	7 464 (1678)	12 726 (2861)	6 717 (1510)	4760 (1070)	3358 (755)
1.8	8 492 (1909)		12 410 (2790)	7 090 (1594)	10 080 (2266)	6 904 (1552)	12 691 (2853)	6 161 (1385)	4573 (1028)	3078 (692)
2.0	7 838 (1762)		11 917 (2679)	6 530 (1468)	9 706 (2182)	6 437 (1447)		5 787 (1301)	4293 (965)	2891 (650)
2.2	7 277 (1636)			6 067 (1364)	9 332 (2098)	5 974 (1343)		5 413 (1217)	4199 (944)	2611 (587)
2.4	6 904 (1552)			5 600 (1259)	9 145 (2056)	5 600 (1259)		5 040 (1133)	4106 (923)	2424 (545)
2.6	6 530 (1468)			5 227 (1175)	8 865 (1993)	5 413 (1217)		4 666 (1049)	4012 (902)	2237 (503)
2.8	6 161 (1385)			4 853 (1091)	8 585 (1930)	5 040 (1133)		4 293 (965)	3919 (881)	2144 (482)
3.0	5 787 (1301)			4 479 (1007)	8 398 (1888)	4 760 (1070)		4 012 (902)	3825 (860)	1962 (441)
3.2	5 413 (1217)			4 293 (965)	8 118 (1825)	4 479 (1007)		3 732 (839)	3732 (839)	1868 (420)
3.4	5 133 (1154)			3 919 (881)	7 838 (1762)	4 293 (965)		3 452 (776)		1775 (399)
3.6	4 853 (1091)			3 732 (839)	7 650 (1720)	4 106 (923)		3 172 (713)		1681 (378)
3.8	4 666 (1049)			3 545 (797)	7 557 (1699)	3 919 (881)		2 985 (671)		
4.0	4 386 (986)			3 265 (734)	7 464 (1678)	3 732 (839)		2 798 (629)		
4.2	4 106 (923)			2 985 (671)				2 611 (587)		
4.4	3 919 (881)			2 798 (629)				2 424 (545)		
4.6	3 732 (839)			2 611 (587)				2 237 (503)		
4.8				2 518 (566)				2 055 (462)		
5.0				2 331 (524)				1 868 (420)		
5.2				2 237 (503)				1 775 (399)		
5.4				2 055 (462)				1 681 (378)		
5.6				1 868 (420)						
5.8				1 775 (399)						
6.0				1 681 (378)						

TABLE II.- MASS AND DIMENSIONAL CHARACTERISTICS

Weight, N (lbf)	245 096	(55 100)
Wing area, m^2 (ft^2)	78	(843)
Wing span, m (ft)	24	(78)
Mean aerodynamic chord, m (ft)	3.58	(11.74)
Center-of-gravity location, percent $\bar{c}$		40
I_X, kg-m^2 (slug-ft^2)	331 103	(244 212)
I_Y, kg-m^2 (slug-ft^2)	334 637	(246 819)
I_Z, kg-m^2 (slug-ft^2)	625 677	(461 482)
I_{XZ}, kg-m^2 (slug-ft^2)	27 690	(20 423)
Maximum control-surface deflections:		
δ_t, deg		±10
δ_{f3}, deg		0 to 90
δ_{sp}, deg		0 to 60
δ_s, deg		±60
δ_a, deg		±20
δ_r, deg		±40
Maximum control-surface deflection rates:		
$\dot{\delta}_t$, deg/sec		50
$\dot{\delta}_{f3}$, deg/sec		5
$\dot{\delta}_{sp}$, deg/sec		50
$\dot{\delta}_s$, deg/sec		50
$\dot{\delta}_a$, deg/sec		50
$\dot{\delta}_r$, deg/sec		50

TABLE III.- BASIC AERODYNAMIC INPUTS USED IN SIMULATION

$[\delta_{f3}^* = \delta_{f3} - 60]$

(a) Clustered engines

α, deg	C_T=0	C_T=1.87	C_T=3.74	C_T=0	C_T=1.87	C_T=3.74	C_T=0	C_T=1.87	C_T=3.74	C_T=0	C_T=1.87	C_T=3.74	C_T=0	C_T=1.87	C_T=3.74	C_T=0	C_T=1.87	C_T=3.74	C_T=0	C_T=1.87	C_T=3.74	C_T=0	C_T=1.87	C_T=3.74
	C_X			C_Z			C_m			$C_{X_{\delta_{f3}^*}}$, per deg			$C_{Z_{\delta_{f3}^*}}$, per deg			$C_{m_{\delta_{f3}^*}}$, per deg			C_{m_q}, per rad			$C_{m_{\dot{\alpha}}}$, per rad		
-10	-0.330	-0.211	0.383	-0.145	-3.212	-4.739	0.80	0.25	-0.50	-0.0038	-0.0460	-0.0760	-0.0180	-0.0550	-0.0400	-0.0001	0.0016	-0.0036	-28.60	-17.86	-28.60	-11.40	-7.14	-11.40
-5	-.366	-.232	.285	-.741	-3.794	-5.345	.45	.10	-.50	-.0033	-.0435	-.0736	-.0134	-.0580	-.0610	.0006	.0021	-.0023	-28.60	-26.80	-28.60	-11.40	-10.70	-11.40
0	-.340	-.250	.300	-1.400	-4.500	-6.130	.12	-.07	-.53	-.0026	-.0403	-.0700	-.0086	-.0611	-.0861	.0013	.0026	-.0010	-28.60	-32.15	-29.30	-11.40	-12.85	-11.70
5	-.249	-.119	.432	-2.090	-5.180	-6.889	-.14	-.25	-.60	-.0029	-.0388	-.0690	-.0089	-.0593	-.0832	.0019	.0022	0	-26.45	-34.30	-30.00	-10.55	-13.70	-12.00
10	-.094	.095	.594	-2.518	-5.781	-7.572	-.23	-.37	-.68	-.0040	-.0371	-.0674	-.0040	-.0534	-.0784	.0019	.0034	.0003	-21.44	-32.86	-30.36	-8.56	-13.14	-12.14
15	.017	.344	.932	-2.770	-6.306	-8.116	-.27	-.45	-.78	-.0041	-.0360	-.0649	.0009	-.0490	-.0759	.0033	.0030	.0005	-10.72	-30.72	-31.45	-4.28	-12.28	-12.55
20	.019	.632	1.162	-2.851	-6.708	-8.601	-.27	-.50	-.84	-.0051	-.0350	-.0627	.0054	-.0492	-.0737	.0026	.0020	-.0005	-3.57	-30.00	-31.45	-1.43	-12.00	-12.55
25	.078	.864	1.535	-2.700	-7.033	-8.972	-.30	-.49	-.83	-.0046	-.0320	-.0591	.0040	-.0455	-.0734	.0030	.0016	-.0004	-5.00	-28.60	-30.36	-2.00	-11.40	-12.14
30	.111	.798	1.765	-2.592	-5.602	-9.258	-.32	-.40	-.75	-.0055	-.0099	-.0514	.0060	-.0527	-.0683	.0022	.0042	-.0006	-9.29	-39.30	-48.60	-3.71	-15.70	-19.40
	$C_{X_{\delta_s}}$, per deg			$C_{Z_{\delta_s}}$, per deg			$C_{m_{\delta_s}}$, per deg			$C_{Y_{\delta_s}}$, per deg			$C_{n_{\delta_s}}$, per deg			$C_{l_{\delta_s}}$, per deg			C_{Y_p}, per rad			C_{n_p}, per rad		
-10	-0.0012	-0.0024	-0.0026	0.0093	0.0140	0.0148	-0.0012	0.0006	0.0052	-0.0002	0	0.0002	0.0007	0.0007	0.0005	0.0015	0.0023	0.0024	-0.02	-0.09	-0.49	-0.15	-0.11	0.38
-5	-.0016	-.0016	-.0028	.0105	.0165	.0161	-.0017	-.0007	.0025	-.0002	-.0001	.0002	.0008	.0008	.0009	.0020	.0029	.0028	-.04	-.04	-.10	-.04	-.15	-.12
0	-.0020	-.0008	-.0030	.0117	.0192	.0173	-.0022	-.0020	-.0002	-.0002	-.0002	0	.0009	.0009	.0013	.0025	.0035	.0032	0	.05	.11	-.02	-.22	-.30
5	-.0026	-.0013	-.0032	.0128	.0209	.0173	-.0008	-.0022	-.0017	-.0002	-.0002	-.0001	.0009	.0010	.0015	.0027	.0038	.0033	.07	.19	.10	-.20	-.28	-.25
10	-.0033	-.0021	-.0028	.0119	.0217	.0185	-.0002	-.0020	-.0020	-.0003	-.0003	-.0002	.0009	.0011	.0015	.0026	.0038	.0032	.05	.25	.53	-.16	-.33	-.40
15	-.0035	-.0033	-.0046	.0099	.0219	.0186	.0008	-.0012	-.0012	-.0002	-.0003	-.0002	.0009	.0011	.0015	.0022	.0036	.0031	.24	.45	.80	-.20	-.45	-.52
20	-.0028	-.0037	-.0033	.0078	.0210	.0176	.0013	-.0008	-.0005	-.0002	-.0003	-.0002	.0008	.0011	.0014	.0017	.0035	.0029	.30	.80	1.20	-.22	-.50	-.57
25	-.0017	-.0032	-.0048	.0036	.0209	.0163	.0017	-.0008	-.0002	-.0002	-.0004	-.0002	.0008	.0010	.0013	.0011	.0037	.0028	.06	.89	1.25	-.15	-.40	-.59
30	0	-.0068	-.0029	.0015	.0117	.0160	.0020	-.0012	-.0005	-.0002	-.0004	-.0003	.0007	.0010	.0012	.0008	.0038	.0028	.13	.75	1.03	-.14	-.22	-.15
	$C_{X_{\delta_t}}$, per deg			$C_{Z_{\delta_t}}$, per deg			$C_{m_{\delta_t}}$, per deg			$C_{Y_{\delta_r}}$, per deg			$C_{n_{\delta_r}}$, per deg			$C_{l_{\delta_r}}$, per deg			C_{l_p}, per rad			C_{Y_r}, per rad		
-10	-0.0092	0.0072	-0.0049	-0.0242	-0.0160	-0.0102	-0.090	-0.084	-0.028	0.012	0.010	0.009	-0.0043	-0.0051	-0.0046	0.0020	0.0016	0.0019	-0.05	-1.13	-0.78	0.76	0.88	0.94
-5	-.0062	.0042	-.0019	-.0246	-.0204	-.0101	-.085	-.087	-.044	.012	.010	.009	-.0041	-.0047	-.0046	.0018	.0016	.0020	-.60	-.88	-.75	.76	.86	.92
0	-.0030	.0010	.0010	-.0250	-.0250	-.0100	-.080	-.090	-.060	.012	.010	.009	-.0039	-.0043	-.0046	.0016	.0016	.0021	-.98	-.68	-.72	.77	.90	1.00
5	-.0002	-.0012	.0004	-.0201	-.0202	-.0050	-.065	-.097	-.076	.011	.010	.009	-.0038	-.0041	-.0046	.0016	.0017	.0022	-.68	-.50	-.68	.77	1.03	1.20
10	-.0036	-.0044	-.0070	-.0138	-.0211	-.0174	-.040	-.092	-.088	.010	.010	.009	-.0036	-.0040	-.0046	.0016	.0017	.0022	-.40	-.50	-.63	.78	1.08	1.60
15	-.0018	-.0071	-.0015	-.0088	-.0122	-.0252	-.013	-.078	-.098	.010	.010	.010	-.0034	-.0040	-.0046	.0011	.0017	.0022	-.37	-.50	-.55	.80	1.00	1.35
20	-.0006	-.0011	.0002	-.0042	-.0057	-.0180	.002	-.069	-.089	.009	.011	.010	-.0024	-.0040	-.0046	.0003	.0016	.0020	-.32	-.33	-.42	.59	.70	1.24
25	-.0042	-.0051	-.0030	-.0053	-.0079	-.0124	.002	-.060	-.080	.006	.012	.012	-.0020	-.0041	-.0047	-.0003	.0010	.0017	-.26	-.17	-.33	.33	.32	.93
30	-.0002	-.0152	.0339	-.0036	-.0312	-.0728	-.005	-.050	-.079	.002	.010	.012	-.0002	-.0033	-.0042	.0006	.0008	.0014	-.26	-.08	-.25	-.08	1.70	2.55
	C_{Y_β}, per deg			C_{n_β}, per deg			C_{l_β}, per deg			$C_{X_{\delta_{sp}}}$, per deg			$C_{Z_{\delta_{sp}}}$, per deg			$C_{m_{\delta_{sp}}}$, per deg			C_{n_r}, per rad			C_{l_r}, per rad		
-10	-0.020	-0.022	-0.050	0.0030	0.0035	0.0053	0.0012	0	0	0	-0.0060	-0.0044	0.0260	0.0430	0.0300	-0.006	0	0.008	-0.45	-0.33	-0.37	0.32	0.57	0.55
-5	-.020	-.050	-.050	.0038	.0052	.0070	-.0006	-.0020	-.0020	-.0016	-.0043	-.0042	.0272	.0425	.0325	-.004	0	.005	-.35	-.38	-.42	.48	.70	.77
0	-.020	-.050	-.055	.0042	.0078	.0081	-.0024	-.0036	-.0031	-.0040	-.0010	-.0040	.0290	.0420	.0380	-.002	0	.002	-.30	-.42	-.45	.67	.80	.86
5	-.020	-.050	-.055	.0043	.0082	.0086	-.0034	-.0048	-.0044	-.0048	-.0018	-.0056	.0317	.0440	.0417	0	0	.001	-.33	-.41	-.45	.77	.85	.85
10	-.020	-.050	-.055	.0043	.0080	.0081	-.0023	-.0051	-.0053	-.0052	-.0016	-.0045	.0296	.0434	.0429	.001	0	.001	-.34	-.42	-.54	.83	.80	.80
15	-.023	-.050	-.055	.0047	.0082	.0089	-.0028	-.0051	-.0061	-.0046	-.0012	-.0080	.0247	.0432	.0414	.004	.001	.002	-.38	-.42	-.52	.88	.82	.83
20	-.024	-.050	-.055	.0050	.0084	.0092	-.0029	-.0062	-.0066	-.0036	-.0046	-.0070	.0157	.0420	.0387	.005	.001	.002	-.35	-.40	-.52	.73	.90	.90
25	-.020	-.050	-.055	.0021	.0083	.0088	-.0070	-.0067	-.0072	.0001	-.0025	-.0085	.0045	.0408	.0347	.004	.001	.003	-.30	-.34	-.47	.83	1.10	.93
30	-.024	-.020	-.055	.0018	-.0040	.0082	-.0050	-.0070	-.0090	.0012	-.0082	-.0024	.0019	-.0022	.0321	.004	.001	.003	-.20	-.42	-.70	.62	-.20	-.50

TABLE III.- BASIC AERODYNAMIC INPUTS USED IN SIMULATION - Continued

(a) Clustered engines – Concluded

α, deg	C_T=0	C_T=0.70	C_T=1.40	C_T=2.10	C_T=2.81	C_T=0	C_T=0.70	C_T=1.40	C_T=2.10	C_T=2.81	C_T=0	C_T=0.70	C_T=1.40	C_T=2.10	C_T=2.81	C_T=0	C_T=0.70	C_T=1.40	C_T=2.10	C_T=2.81	C_T=0	C_T=0.70	C_T=1.40	C_T=2.10	C_T=2.81
	$\Delta C_{Y,E1}$					$\Delta C_{n,E1}$					$\Delta C_{l,E1}$					$C_{X,E1}$					$C_{Z,E1}$				
-10	0	0.009	0.011	0.005	0.005	0	-0.026	-0.032	-0.038	-0.059	-0.004	-0.030	-0.102	-0.118	-0.162	-0.42	-0.58	-0.62	-0.51	-0.40	-0.07	-1.86	-2.73	-3.28	-3.82
-5	0	.007	.008	.005	0	0	-.021	-.030	-.043	-.055	-.001	-.040	-.100	-.133	-.171	-.36	-.52	-.49	-.38	-.25	-.76	-2.45	-3.30	-3.94	-4.55
0	0	.005	.005	.005	-.005	0	-.016	-.028	-.048	-.051	.002	-.050	-.098	-.148	-.180	-.30	-.46	-.36	-.25	-.10	-1.45	-3.04	-3.87	-4.60	-5.28
5	0	.002	.002	.005	.001	0	-.014	-.023	-.045	-.048	0	-.064	-.104	-.160	-.195	-.20	-.28	-.22	-.14	-.01	-2.05	-3.68	-4.46	-5.35	-6.02
10	-.001	.006	.006	.007	.003	0	-.010	-.020	-.040	-.048	0	-.075	-.115	-.165	-.210	-.07	-.12	-.05	.10	.20	-2.46	-4.17	-5.08	-5.96	-6.55
15	.001	.008	.008	.010	.006	-.002	-.012	-.024	-.043	-.052	-.003	-.086	-.127	-.229	-.228	.03	.11	.18	.31	.42	-2.72	-4.55	-5.44	-6.20	-6.91
20	.004	.013	.024	.025	.015	.005	-.036	-.069	-.087	-.085	.002	-.186	-.355	-.367	-.365	.09	.31	.46	.62	.73	-2.73	-4.34	-5.39	-6.49	-7.38
25	.003	.012	.023	.026	.029	-.002	-.021	-.044	-.065	-.098	-.003	-.134	-.266	-.348	-.490	.09	.53	.88	1.20	1.12	-2.59	-4.04	-5.26	-6.59	-7.56
30	.004	.008	.010	.019	.021	0	.003	-.005	-.027	-.040	-.001	-.048	-.125	-.237	-.373	.12	.64	1.15	1.44	1.32	-2.51	-3.89	-5.06	-6.20	-6.76
	$C_{Y_{\delta_a}}$, per deg					$C_{n_{\delta_a}}$, per deg					$C_{l_{\delta_a}}$, per deg														
-10	-0.0016	-0.0010	-0.0004	0.0002	0.0008	-0.0014	-0.0028	-0.0040	-0.0052	-0.0064	0.0082	0.0083	0.0084	0.0085	0.0086										
-5	-.0012	-.0007	-.0002	.0003	.0008	-.0001	-.0017	-.0032	-.0047	-.0062	.0048	.0058	.0068	.0078	.0088										
0	-.0008	-.0004	0	.0004	.0008	.0012	-.0006	-.0024	-.0042	-.0060	.0014	.0033	.0052	.0071	.0090										
5	-.0004	-.0002	0	.0002	.0004	-.0010	-.0022	-.0034	-.0046	-.0058	.0014	.0033	.0052	.0071	.0090										
10	-.0006	-.0004	-.0002	0	.0002	-.0010	-.0022	-.0034	-.0046	-.0058	.0010	.0030	.0050	.0070	.0090										
15	-.0008	-.0006	-.0004	-.0002	.0001	.0004	-.0011	-.0026	-.0041	-.0056	.0027	.0044	.0061	.0078	.0096										
20	-.0022	-.0018	-.0014	-.0010	-.0005	.0045	.0026	.0007	-.0012	-.0032	.0207	.0197	.0187	.0177	.0168										
25	-.0036	-.0024	-.0012	0	-.0012	.0036	.0024	.0010	-.0002	-.0014	-.0010	.0050	.0110	.0170	.0240										
30	-.0007	-.0006	-.0005	-.0004	-.0003	.0024	.0008	-.0008	-.0024	-.0040	-.0076	-.0012	.0052	.0116	.0180										

TABLE III.- BASIC AERODYNAMIC INPUTS USED IN SIMULATION – Concluded

(b) Spread engines. (Inputs same as for clustered engines except for coefficients herein.)

α, deg	C_T=0	C_T=1.40	C_T=2.81	C_T=0	C_T=1.40	C_T=2.81	C_T=0	C_T=1.40	C_T=2.81
	$\Delta C_{Y,E1}$			$\Delta C_{n,E1}$			$\Delta C_{l,E1}$		
-10	-0.010	0.065	-0.017	-0.002	-0.040	-0.060	-0.042	-0.135	-0.190
-5	0	.045	-.029	-.002	-.040	-.069	-.020	-.130	-.192
0	-.005	.032	-.035	-.003	-.038	-.073	-.003	-.129	-.200
5	0	.048	.003	-.001	-.041	-.083	.002	-.146	-.223
10	0	.055	.025	-.001	-.038	-.088	0	-.161	-.251
15	0	.050	.037	-.001	-.044	-.095	.002	-.185	-.278
20	.015	.070	.125	-.002	-.049	-.102	.002	-.178	-.318
25	.015	.185	.225	0	-.061	-.114	.002	-.253	-.392
30	.020	.075	.175	-.004	-.036	-.077	0	-.133	-.270
	$C_{Y_{\delta_a}}$, per deg			$C_{n_{\delta_a}}$, per deg			$C_{l_{\delta_a}}$, per deg		
-10	0.0005	-0.0058	-0.0042	0.0008	0.0002	-0.0010	0.0024	0.0038	0.0041
-5	-.0025	-.0022	-.0050	.0008	.0002	.0002	.0013	.0035	.0046
0	-.0032	-.0051	-.0068	.0009	.0002	.0008	.0003	.0034	.0049
5	-.0055	-.0074	-.0082	.0008	.0006	.0010	-.0001	.0038	.0056
10	-.0050	-.0078	-.0088	.0008	.0004	.0014	0	.0041	.0058
15	-.0050	-.0075	-.0094	.0010	.0006	.0018	.0020	.0052	.0068
20	-.0062	-.0085	-.0134	.0018	.0006	.0020	.0044	.0046	.0084
25	-.0062	-.0112	-.0182	.0018	.0019	.0021	.0045	.0116	.0120
30	-.0075	-.0068	-.0128	.0016	.0011	.0004	.0026	.0033	.0108

TABLE IV.- SIMULATOR CONTROL CHARACTERISTICS

Control	Maximum travel in –			Breakout force		Force gradient	
	deg	cm	in.	N	lbf	N/cm	lbf/in.
Column:							
Forward	9.9	13.97	5.50	13.3	3.0	14.0	8.0
Aft	20.5	25.25	9.94				
Wheel	±130.0	±37.34	±14.70	11.1	2.5	5.3	3.0
Pedal		10.80	4.25	31.1	7.0	28.9	16.5

TABLE V.- PILOT RATING SYSTEM

CONTROLLABLE Capable of being controlled or managed in context of mission, with available pilot attention.	ACCEPTABLE May have deficiencies which warrant improvement, but adequate for mission. Pilot compensation, if required to achieve acceptable performance, is feasible.	SATISFACTORY Meets all requirements and expectations; good enough without improvement. Clearly adequate for mission.	Excellent; highly desirable.	1
			Good, pleasant, well behaved.	2
			Fair. Some mildly unpleasant characteristics. Good enough for mission without improvement.	3
		UNSATISFACTORY Reluctantly acceptable. Deficiencies which warrant improvement. Performance adequate for mission with feasible pilot compensation.	Some minor but annoying deficiencies. Improvement is requested. Effect on performance is easily compensated for by pilot.	4
			Moderately objectionable deficiencies. Improvement is needed. Reasonable performance requires considerable pilot compensation.	5
			Very objectionable deficiencies. Major improvements are needed. Requires best available pilot compensation to achieve acceptable performance.	6
	UNACCEPTABLE Deficiencies which require improvement. Inadequate performance for mission even with maximum feasible pilot compensation.		Major deficiencies which require improvement for acceptance. Controllable. Performance inadequate for mission, or pilot compensation required for minimum acceptable performance in mission is too high.	7
			Controllable with difficulty. Requires substantial pilot skill and attention to retain control and continue mission.	8
			Marginally controllable in mission. Requires maximum available pilot skill and attention to retain control.	9
UNCONTROLLABLE Control will be lost during some portion of mission.			Uncontrollable in mission.	10

TABLE VI.- DYNAMIC STABILITY CHARACTERISTICS OF SIMULATED JET-FLAP STOL AIRPLANE

Parameter	Simulated STOL airplane					Breguet 941	Level for satisfactory operation	
	Clustered engines				Spread engines			
	Basic airplane		Command augmentation		CAS		Ref. 6	Ref. 7
Airspeed, knots	65	75	65	75	75	60		
Short-period mode								
ω_{sp}, rad/sec	1.23	1.41	-----	-----	-----	-----	------	------
P_{sp}, sec	8.16	6.32	-----	-----	-----	-----	------	------
ζ_{sp}	.78	.71	-----	-----	-----	-----	------	>0.35
τ_{sp}, sec	------	------	0.56	0.57	0.57	-----	------	------
Long-period (phugoid) mode								
ω_{ph}, rad/sec	0.39	0.24	0.4	-----	-----	-----	------	------
P_{ph}, sec	16.00	26.5	78.5	-----	-----	-----	------	------
ζ_{ph}	.065	.088	.98	-----	-----	-----	------	>0.04
τ_{ph}, sec	------	------	-----	9.63	9.63	-----	------	------
Roll mode								
τ_R, sec	0.83	0.71	-----	-----	-----	1.0	<2.0	<1.4
ζ_R	------	------	0.96	0.93	0.96	-----	------	------
ω_R, rad/sec	------	------	8.5	8.5	5.0	-----	------	------
Spiral mode								
$t_{1/2}$, sec	------	------	69	34	32	10.00	------	------
t_2, sec	5.25	6.83	-----	-----	-----	-----	>20.00	>20.00
Dutch roll mode								
ω_d, rad/sec	1.09	1.06	2.0	2.45	2.29	0.7	>0.53	>0.4
ζ_d	.19	.22	.47	.45	.5	.1	>.16	>.08
$\zeta_d\omega_d$, rad/sec	.21	.23	.94	1.1	1.15	.07	------	>.15
P, sec	5.87	6.07	3.57	2.86	3.16	8.5	<12.00	------
Roll-control parameters								
ω_ϕ/ω_d	0.90	0.93	1.04	1.04	1.1	-----	------	------
ζ_ϕ/ζ_d	1.72	1.56	1.15	1.24	1.12	-----	------	------

TABLE VII.- CONTROL RESPONSE CHARACTERISTICS OF SIMULATED JET-FLAP STOL AIRPLANE

Parameter	Simulated STOL airplane					Breguet 941	Level for satisfactory operation (ref. 6)	Level for safe operation (ref. 6)
	Clustered engines				Spread engines			
	Basic		CAS		CAS			
Airspeed, knots	65	75	65	75	75	60		
Longitudinal								
$\ddot{\theta}_{max}$, rad/sec^2	0.34	0.58	0.38	0.58	0.58	0.50	See fig. 10	Insufficient
$\ddot{\theta}$ in 1 sec, rad/sec^2	.34	.58	.38	.58	.58	----	>0.5	information
$\Delta\theta_{t=1}$, deg	6.25	8.06	6.24	9.5	9.5	6.6	---------	to provide
$t_{\Delta\theta=10^o}$, sec	1.38	1.1	1.33	1.03	1.03	1.2	<1.2	criteria
Lateral								
$\ddot{\phi}_{max}$, rad/sec^2	0.53	1.0	0.60	0.74	0.78	0.48	See fig. 11	----------
$\ddot{\phi}$ in 0.5 sec, rad/sec^2	.27	.33	.38	.40	.35	----	>0.4	>0.3
$\Delta\phi_{t=1}$, deg	5.0	6.0	7.7	8.2	7.6	4.0	---------	----------
$t_{\phi=30^o}$, sec	1.93	1.6	1.75	1.65	1.7	2.2	≦2.4	≦2.9
$\Delta\beta/\Delta\phi$, deg/deg	.3	.28	.06	.033	.04	.4	≦.3	≦.6
$\Delta a_{n_{\delta_w=max}}$, g	-.2	-.2	-.2	-.2	-.2		>-.1	>-.2
Directional								
$\ddot{\psi}_{max}$, rad/sec^2	0.32	0.4	0.33	0.37	0.38	0.18	See fig. 12	----------
$\Delta\psi_{t=1}$, deg	4.6	4.6	3.8	5.5	5.1	3.0	---------	----------
$t_{\Delta\psi=15^o}$, sec	1.68	1.57	1.75	1.53	1.46	2.0	≦2.2	≦3.1

TABLE VIII.- INDICATION OF SIMULATED AUGMENTED STOL AIRPLANE RESPONSE

TO THRUST INPUTS FOR FLIGHT-PATH CONTROL

Item	Mode (*)	Parameter	Simulated external flow jet-flap STOL airplane (airspeed 75 knots, command control systems)								Level for satisfactory operation (ref. 6)
			Clustered engines				Spread engines				
			Four engines operating, glideslope of –		Three engines operating, glideslope of –		Four engines operating, glideslope of –		Three engines operating, glideslope of –		
			6°	4°	6°	4°	6°	4°	6°	4°	
Control power	A	$\Delta a_{n(max)}$, g	>0.25	>0.25	>0.1	<0.1	>0.25	>0.25	<0.1	<0.1	No less than ±0.1g
	B	$\Delta a_{n(max)}$, g	>.3	>.25	>.1	>.1	>.3	>.25	≈.1	<.1	No less than ±0.1g
Airplane response	A	$\Delta a_{n,t=0.5}$, g	0.12	0.10	<0.1	<0.1	0.12	0.10	<0.1	<0.1	No less than ±0.1g
	B	$\Delta a_{n,t=1.5}$, g	.33	.24	.15	.11	.33	.24	<.1	<.1	No less than ±0.1g
Cross coupling	A	$\Delta\theta$, deg	<1.0	<1.0	<1.0	<1.0	<1.0	<1.0	<1.0	<1.0	Not noticeable
	B	$\Delta\theta$, deg	<1.0	<1.0	<1.0	<1.0	<1.0	<1.0	<1.0	<1.0	Not noticeable

*Mode A – Flare and touchdown control; mode B – Flight-path tracking.

TABLE IX.- COMPARISON OF FLARE AND TOUCHDOWN PARAMETERS FOR A TYPICAL CTOL AND THE SIMULATED EBF STOL

[Refer to fig. 17]

Airplane	V, m/sec (ft/sec)	$\dot{h}_{gs}$, m/sec (ft/sec)	Flare initiation		Flare point		Runway threshold		Touchdown		t_{flare}, sec	t_{ge}, sec
			h_{lg}, m (ft)	X, m (ft)	h_{lg}, m (ft)	X, m (ft)	h_{lg}, m (ft)	$\dot{h}$, m/sec (ft/sec)	$\dot{h}$, m/sec (ft/sec)	X, m (ft)		
CTOL, glideslope, 2.8°	64 (210)	-3.05 (-10)	15.24 (50)	-230.1 (-755)	9.75 (32)	-100.6 (-330)	6.1 (20)	-1.77 (-5.8)	-0.61 (-2)	461.5 (1514)	11.4	
EBF STOL, glideslope, 4°	38.2 (125.3)	-2.68 (-8.8)	8.84 (29)	-43.9 (-144)	4.88 (16)	22.86 (75)	6.1 (20)	-2.23 (-7.3)	-0.52 (-1.7)	182.9 (600)	6.0	6.3
EBF STOL, glideslope, 6°	38.2 (125.3)	-4 (-13.1)	11 (36)	-28.7 (-94)	6.4 (21)	19.2 (63)	7.9 (26)	-3.5 (-11.5)	-0.91 (-3)	155.4 (510)	4.8	4.6
EBF STOL, glideslope, $7\frac{1}{2}$°	38.2 (125.3)	-5 (-16.3)	13.1 (43)	-26.8 (-88)	6.4 (21)	27.4 (90)	9.75 (32)	-4.75 (-15.6)	-0.79 (-2.6)	158.5 (520)	4.8	4.1

TABLE X.- COMPARISON OF EXTERNALLY BLOWN FLAP (EBF)

STOL AND CTOL GUST SENSITIVITY PARAMETERS

Airplane	W, kN (lbf)	S, m^2 (ft^2)	W/S, kN/m^2 (lbf/ft^2)	C_{L_α}, rad^{-1}	V, m/sec (ft/sec)	S_{a_n}, g/(m/sec) (g/(ft/sec))
CTOL	800.7 (180 000)	256.2 (2758)	3.13 (65.3)	4.85	72.1 (236.5)	0.069 (.021)
EBF STOL	245.1 (55 100)	78.3 (843)	3.13 (65.4)	8.0	38.2 (125.3)	.059 (.018)

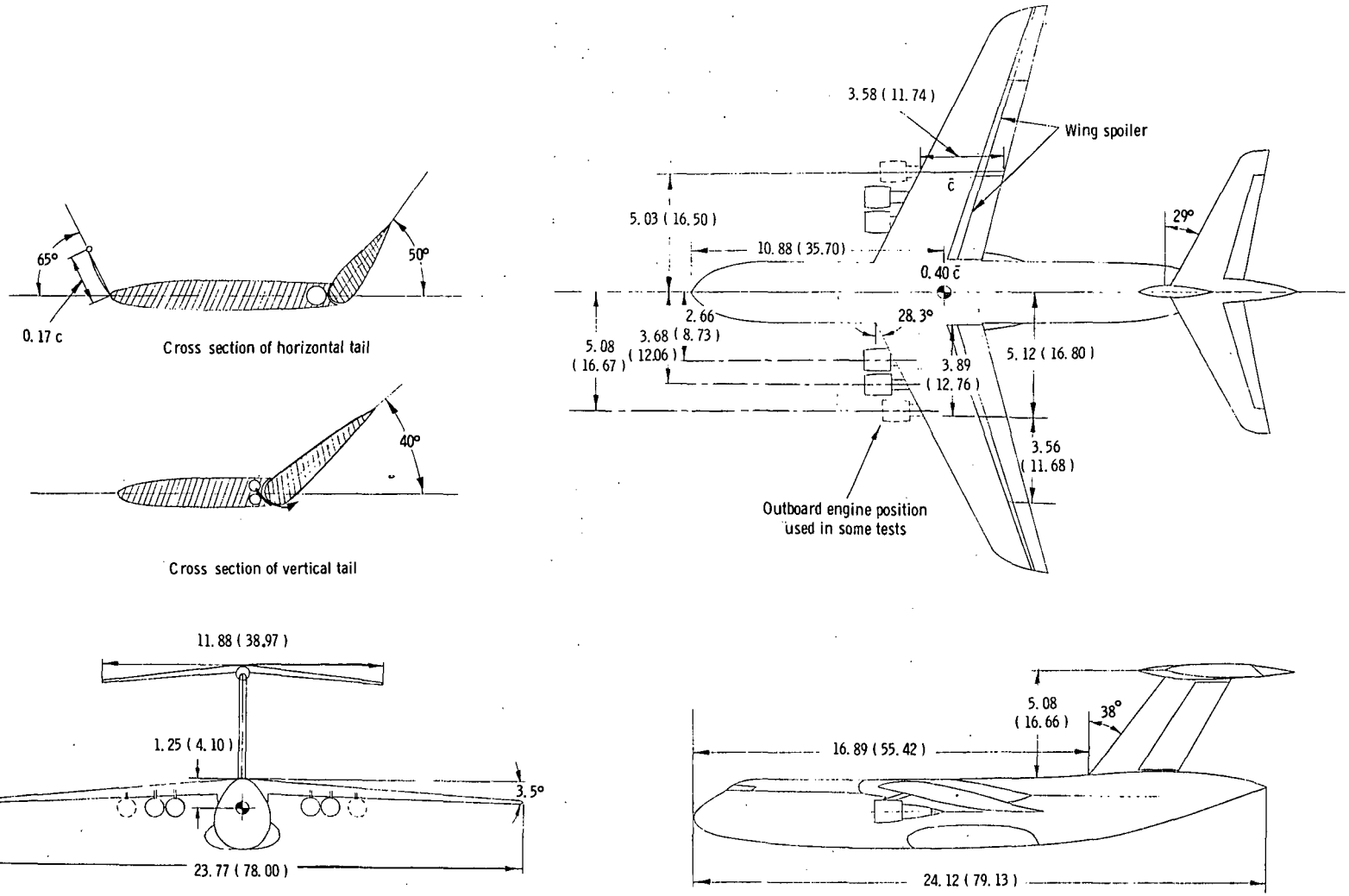

Figure 1.- Three-view drawing of simulated airplane. All linear dimensions are in meters (feet).

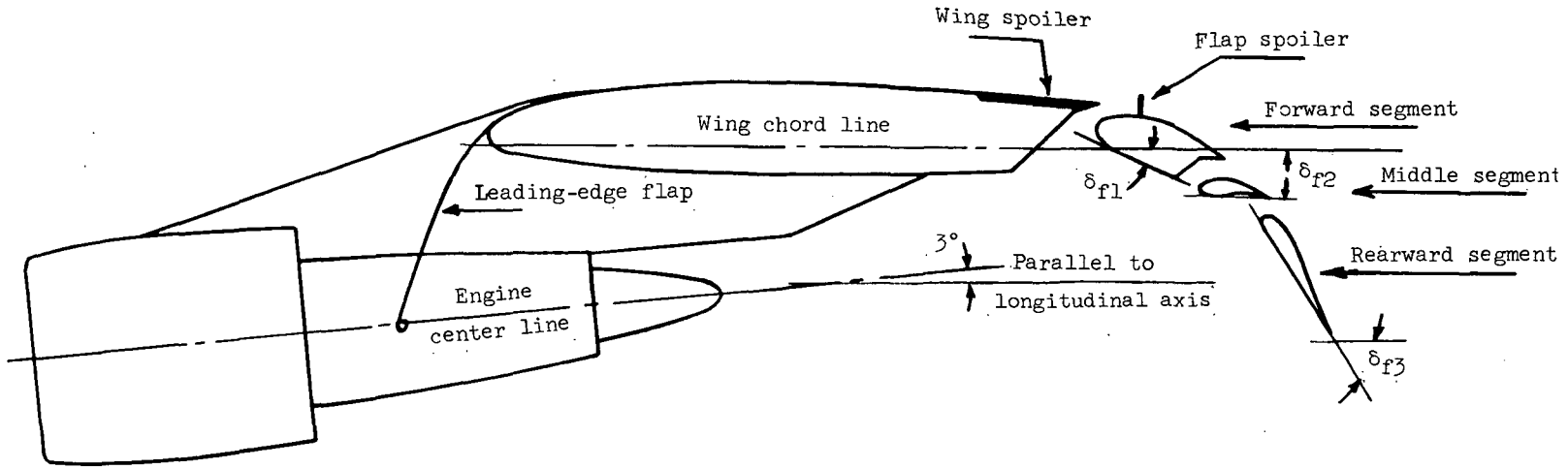

Figure 2.- Flap assembly and engine pylon detail. $\delta_{f1}/\delta_{f2}/\delta_{f3} = 25/10/60$.

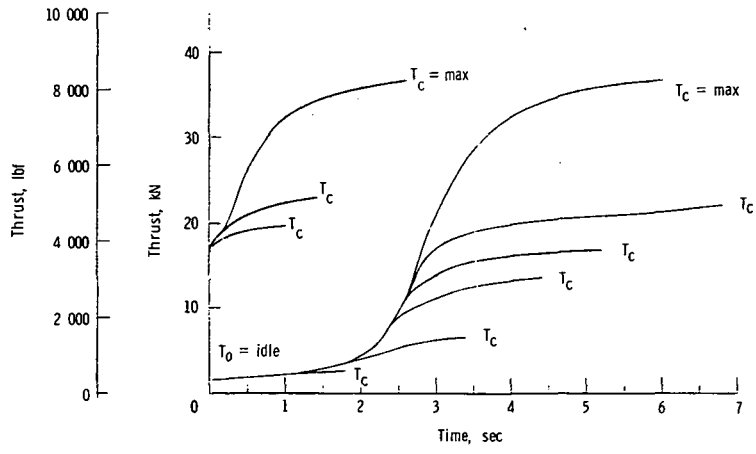

(a) Acceleration.

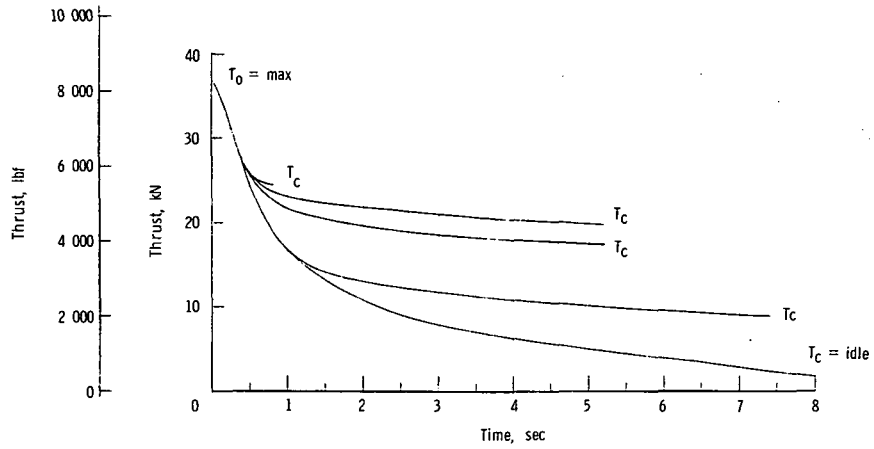

(b) Deceleration.

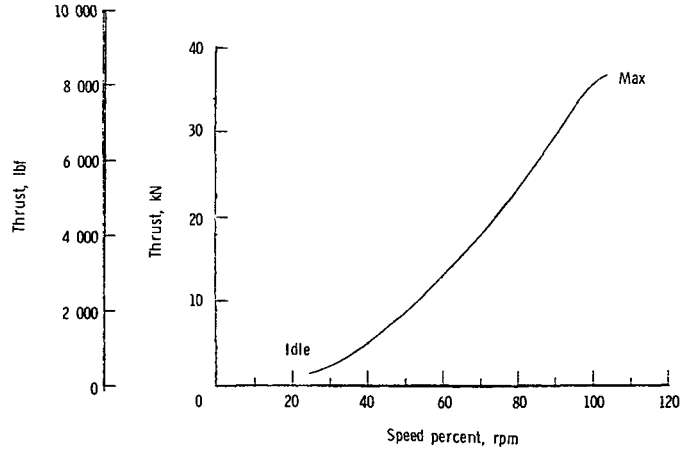

(c) Engine rotational speed, thrust relationship.

Figure 3.- Example of engine thrust characteristics used in simulation.

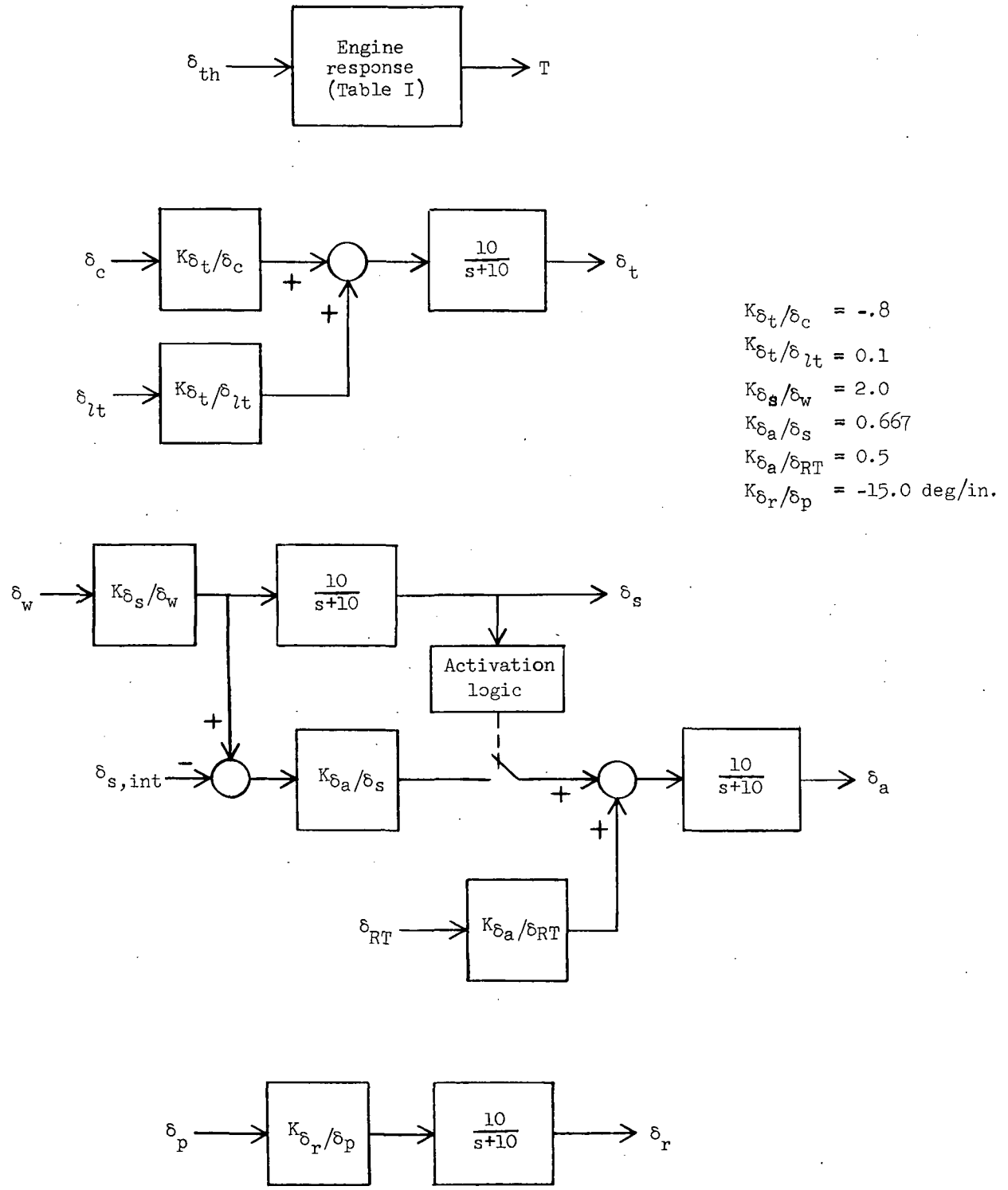

Figure 4.- Basic flight controls.

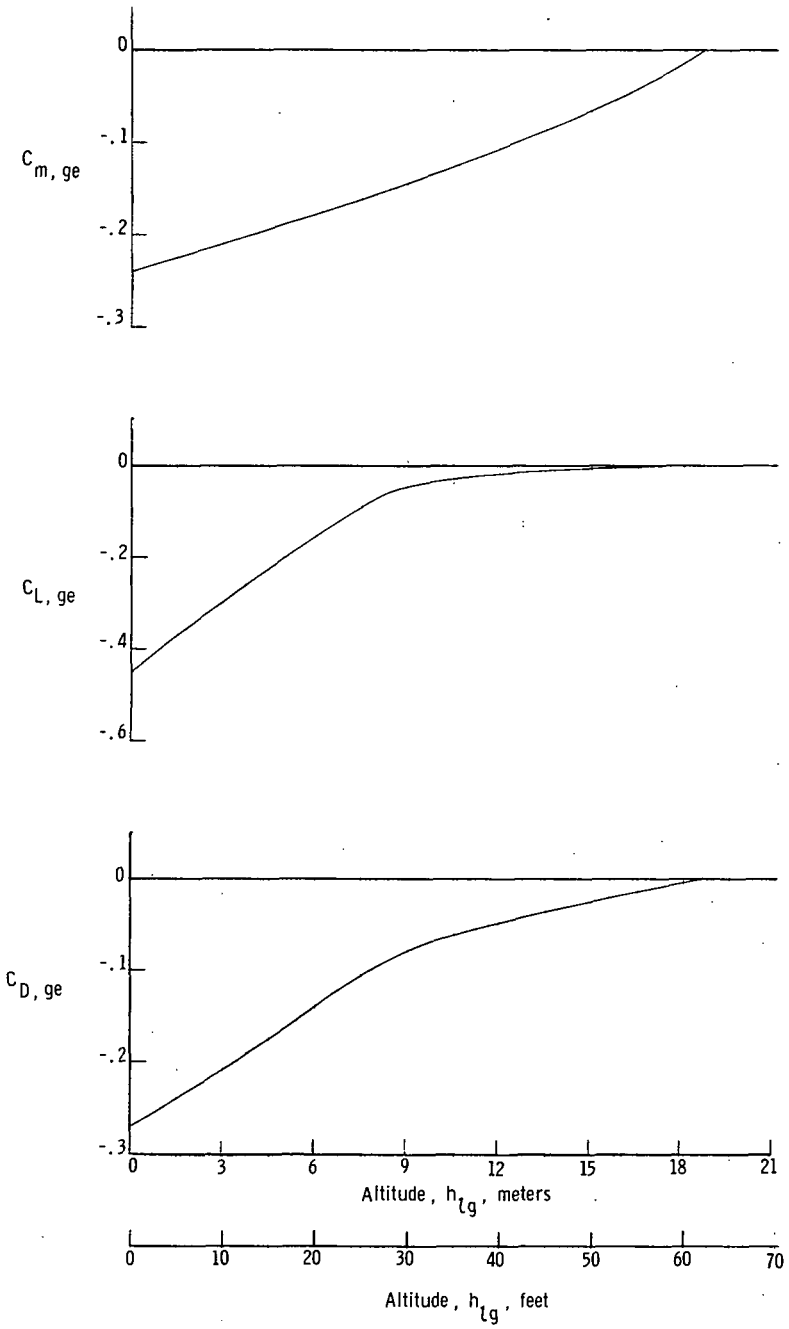

Figure 5.- Incremental changes in pitching-moment, lift, and drag coefficients due to ground effects.

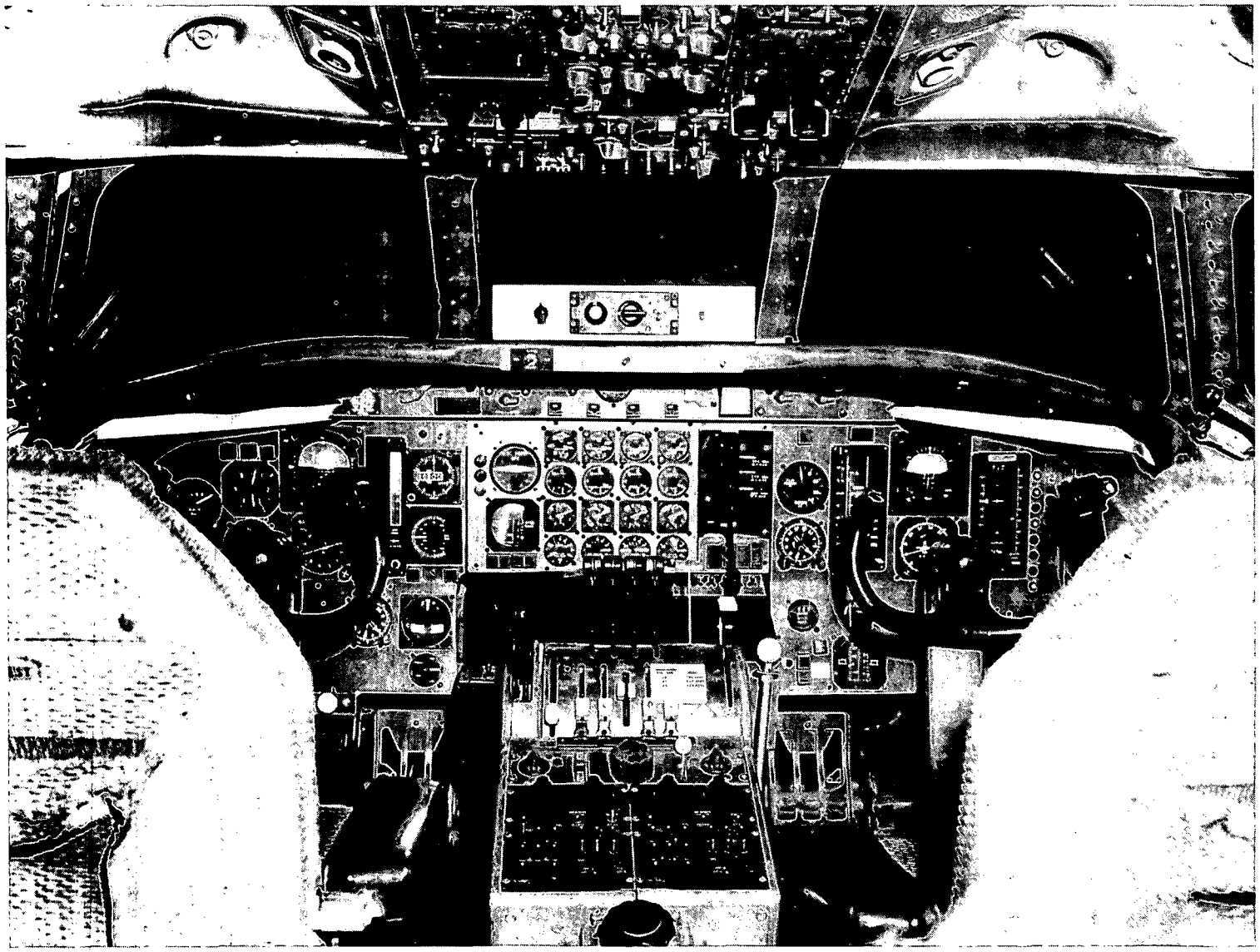

L-69-4124

(a) Simulator cockpit.

Figure 6.- Simulator cockpit and instrument display.

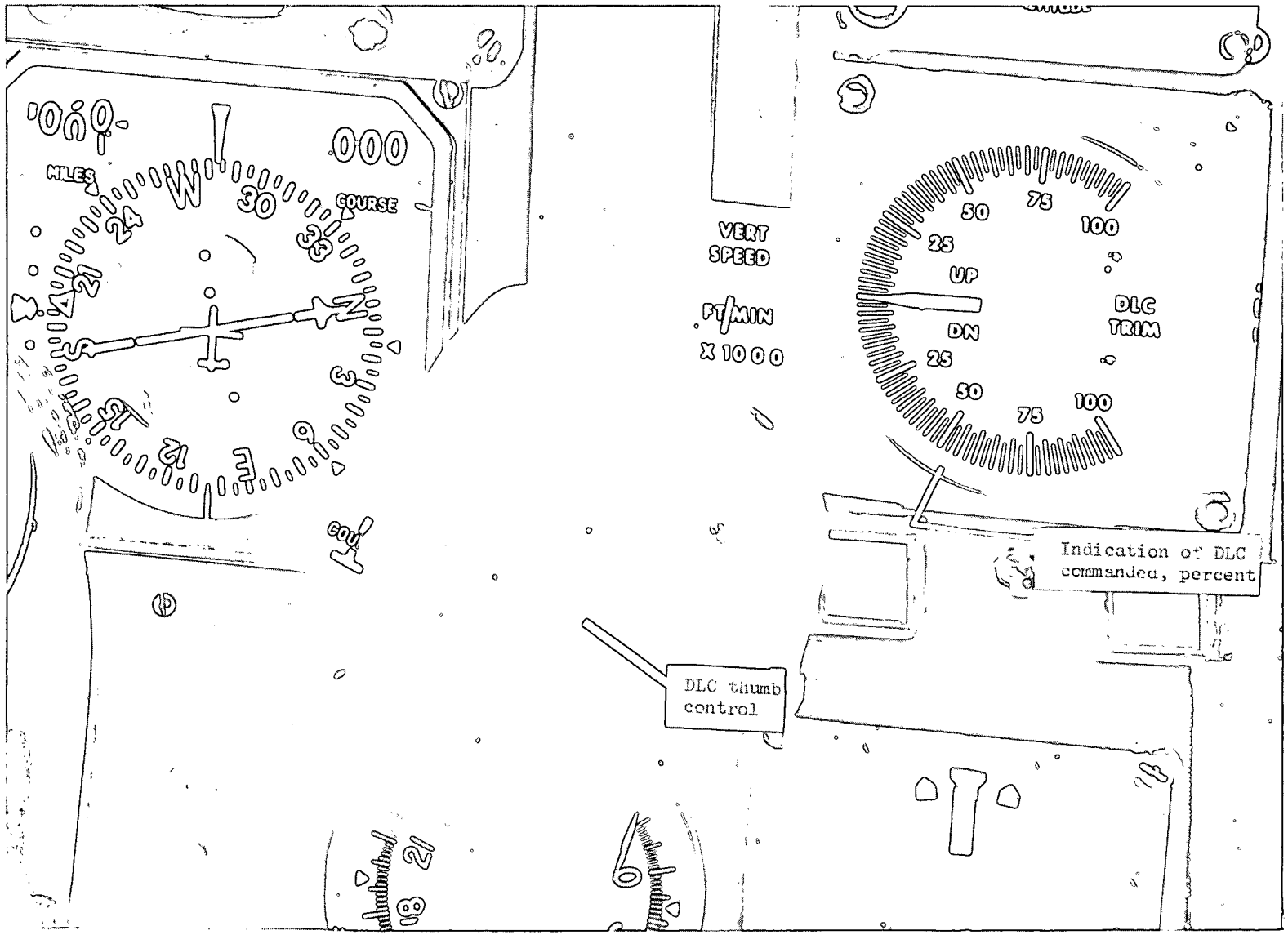

(b) Direct lift controller and amount of direct lift control (DLC) commanded.

Figure 6.- Concluded.

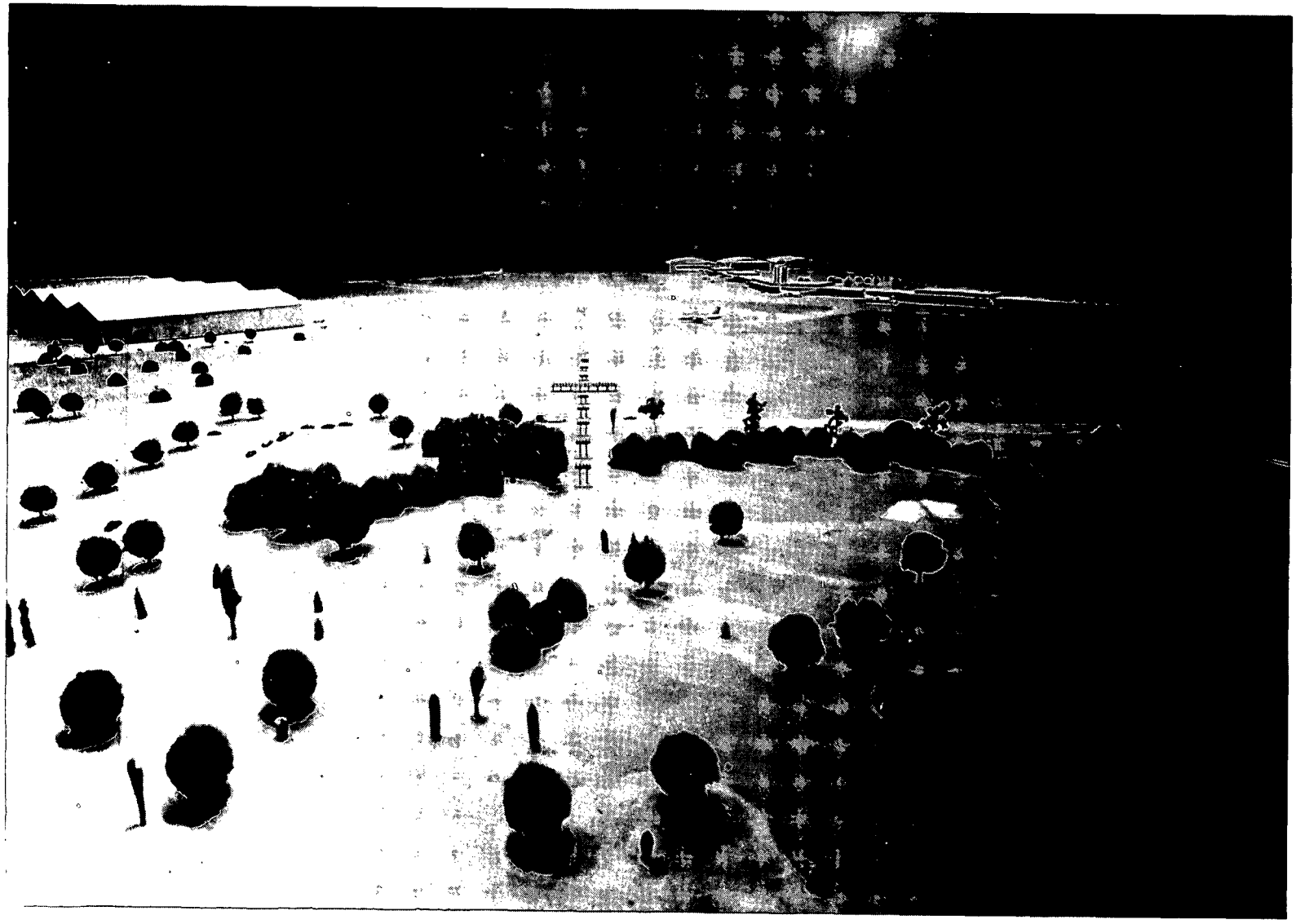

L-71-4272

Figure 7.- Photograph of 1/300-scale airport model.

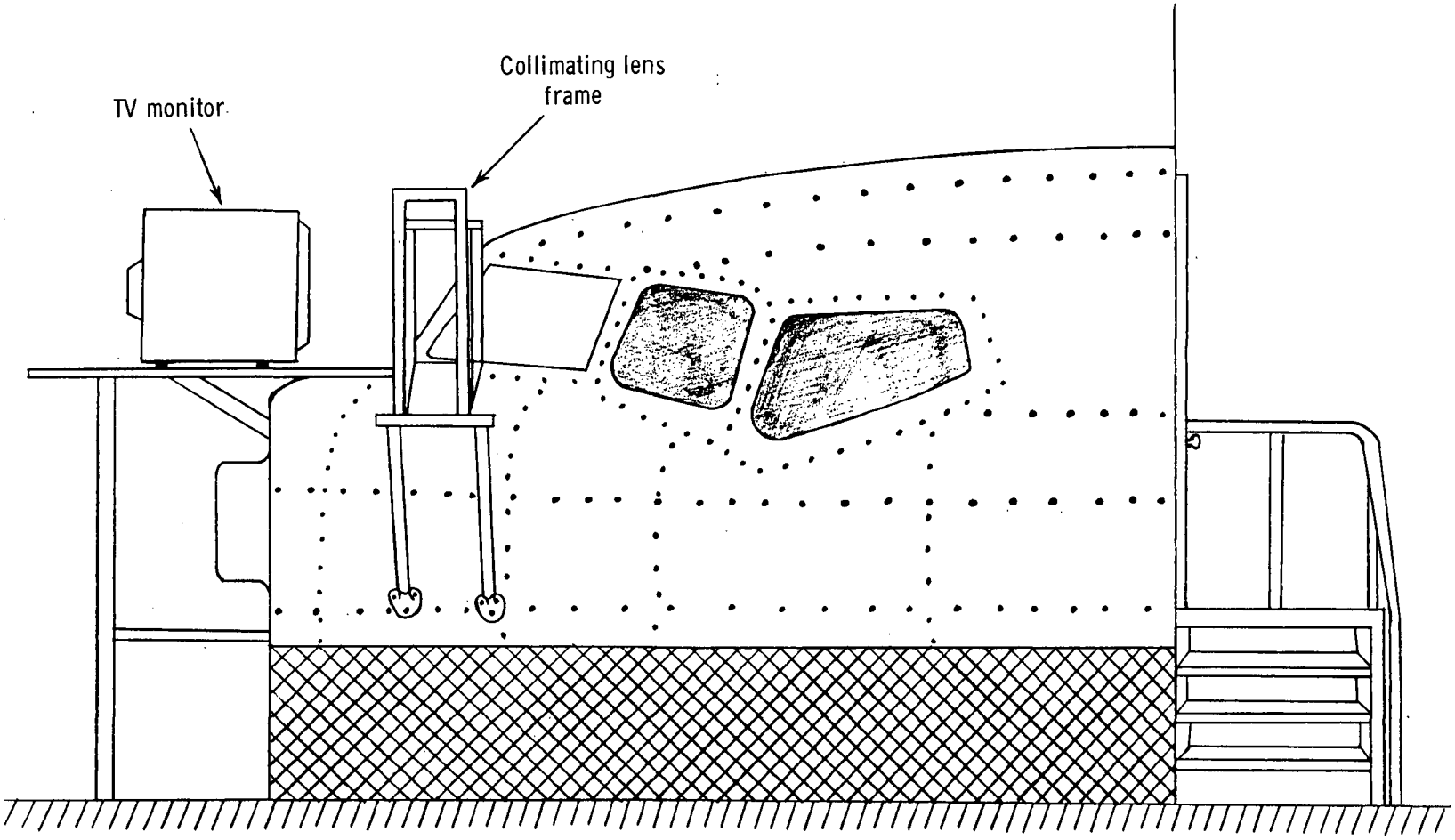

Figure 8.- Sketch showing TV monitor and collimating lens location with respect to cockpit window.

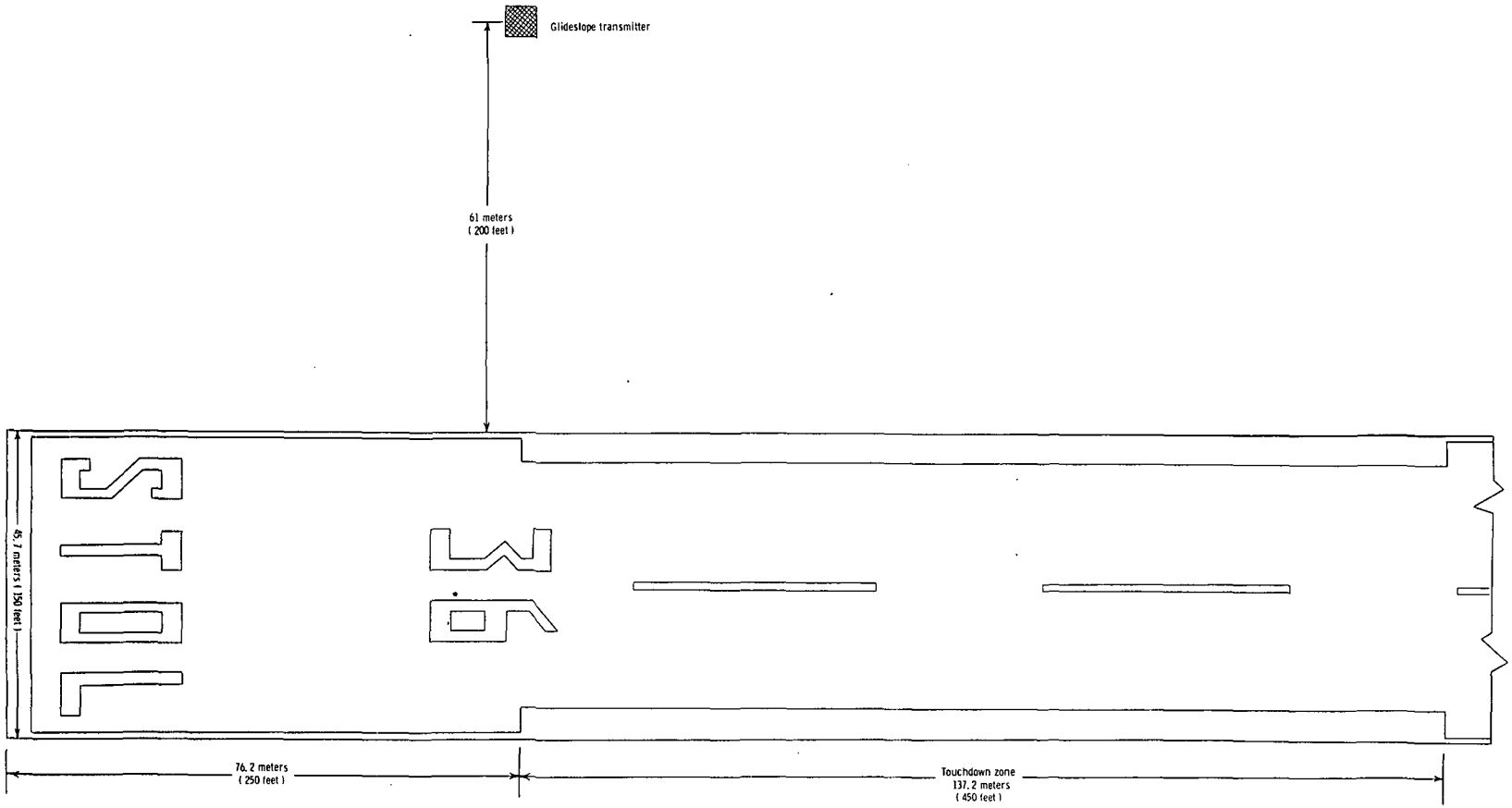

Figure 9.- Sketch of approach end of simulated runway.

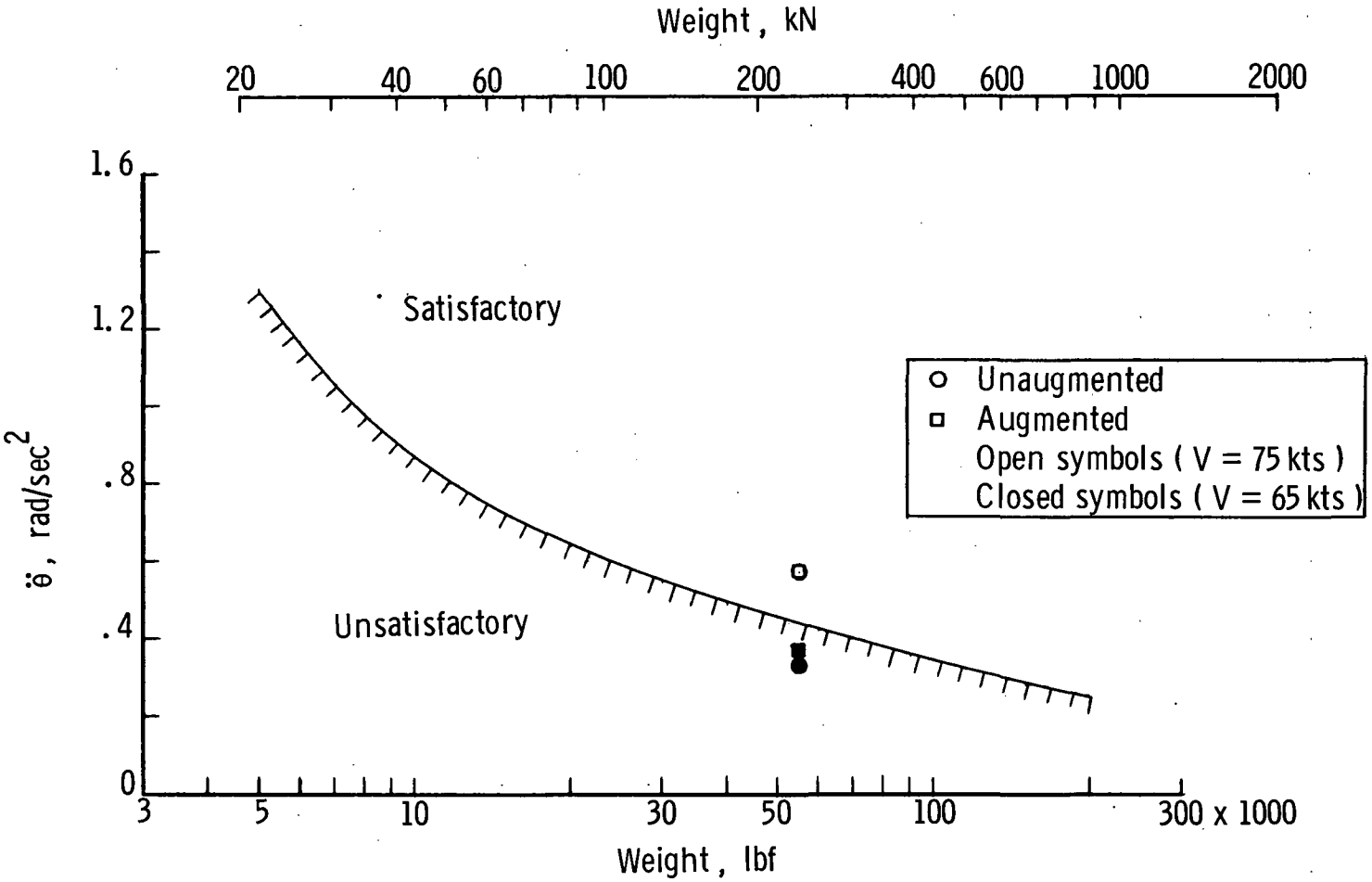

Figure 10.- Indication of pitch acceleration capability required for various size STOL airplanes. Boundary from reference 6.

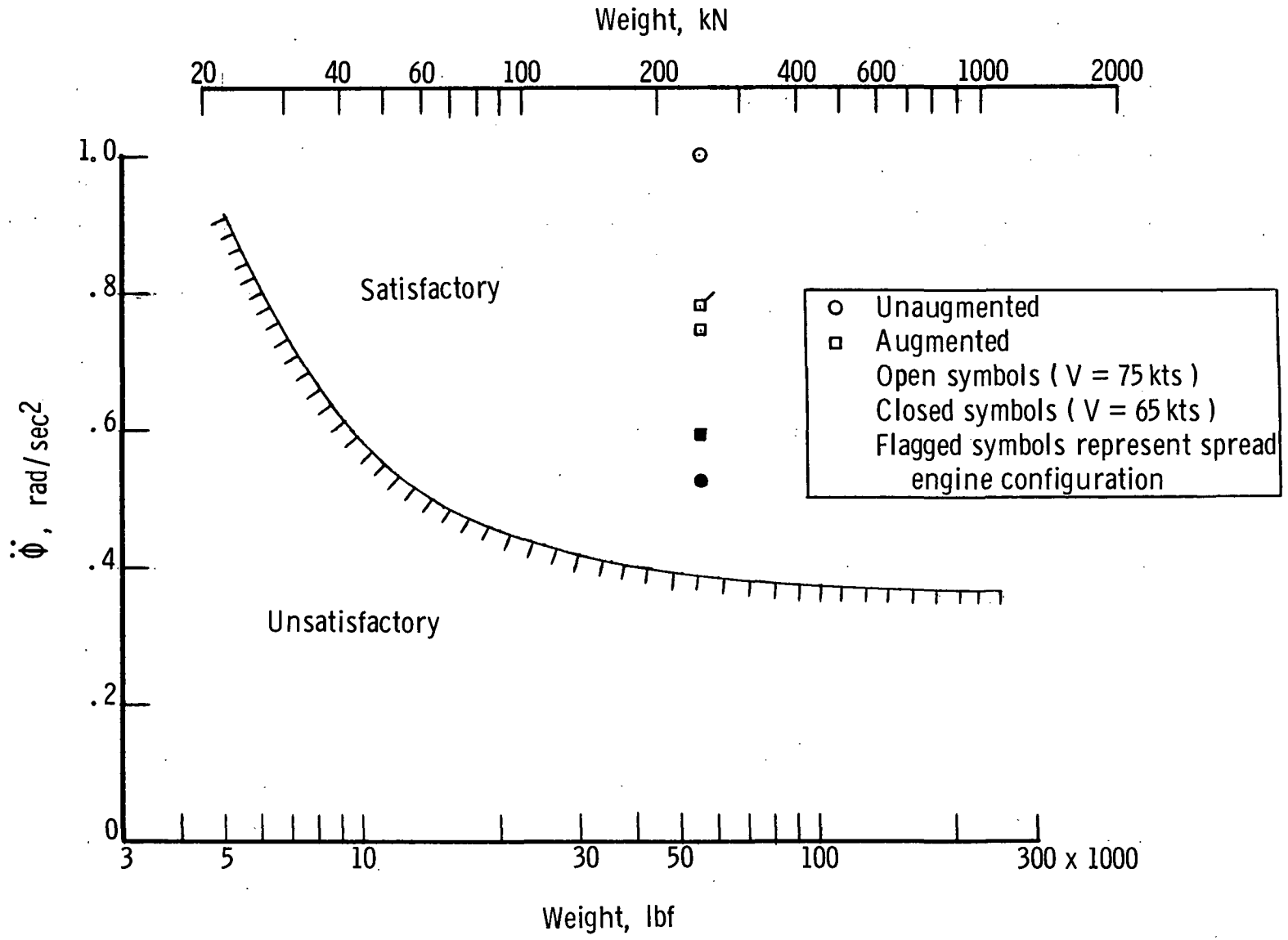

Figure 11.- Indication of roll acceleration capability required for various size STOL airplanes. Boundary from reference 6.

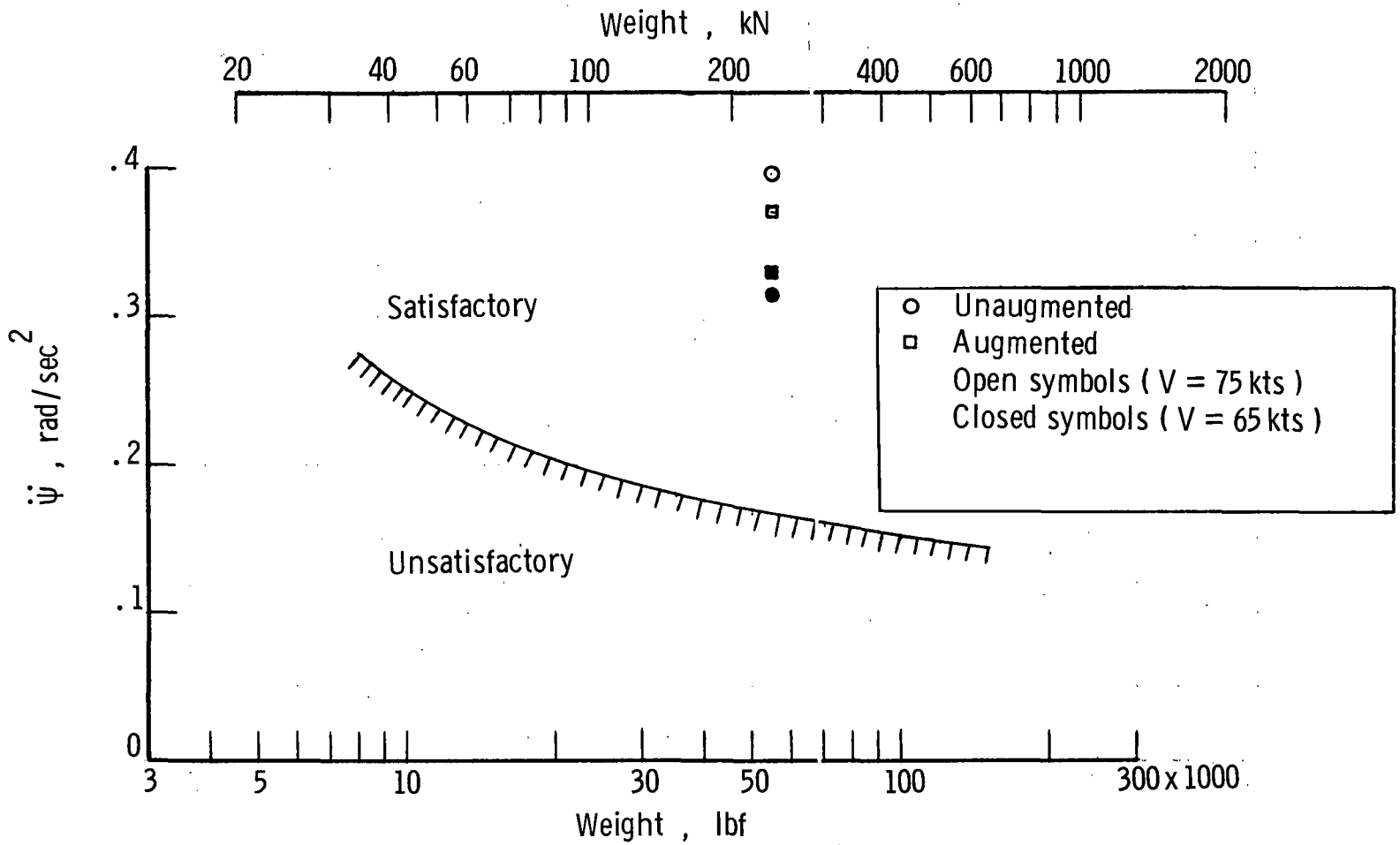

Figure 12.- Indication of yaw acceleration capability required for various size STOL airplanes. Boundary from reference 6.

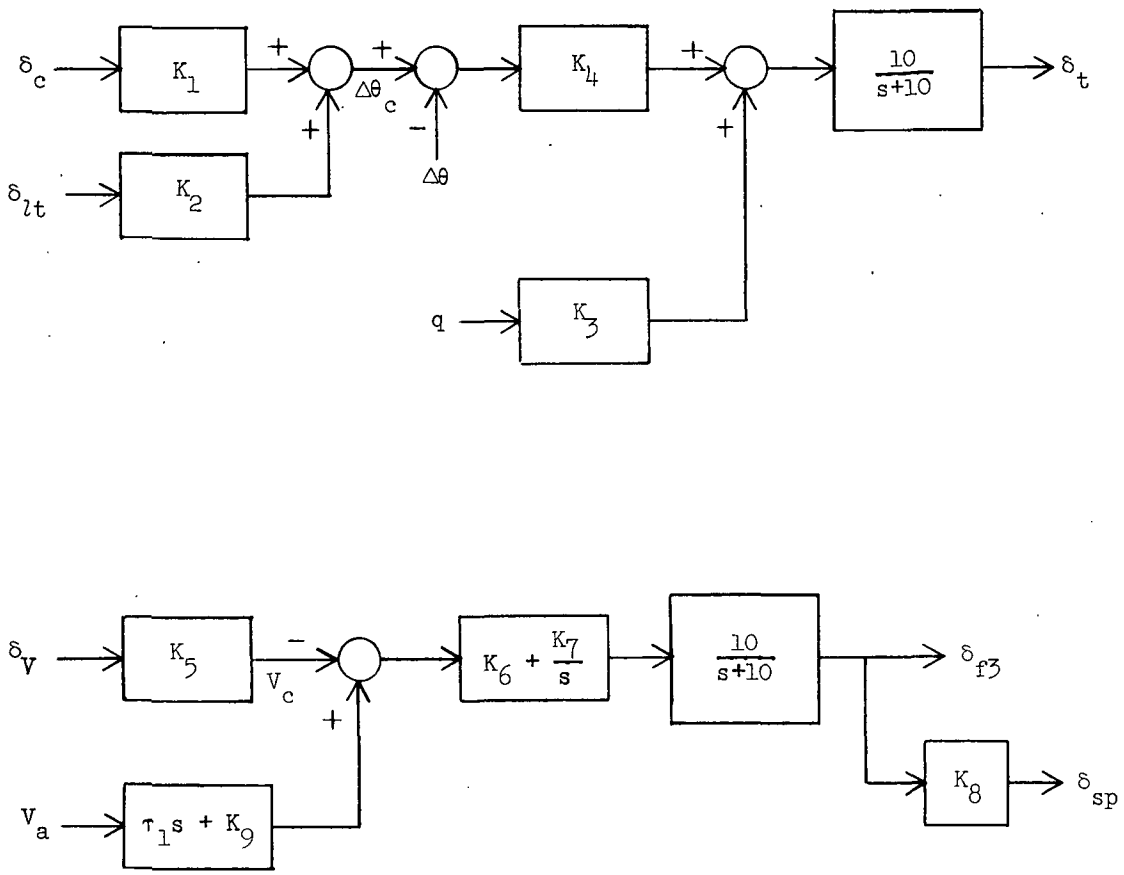

$K_1 = 2.0$	$K_5 = 1$
$K_2 = -0.5$	$K_6 = 19.7$ deg/m/sec (6.0 deg/ft/sec)
$K_3 = 2.0$ sec	$K_7 = 1.97$ deg/m (.6 deg/ft)
$K_4 = -3$	$K_8 = 1.6$
$\tau_1 = 2.5$ sec	$K_9 = 3.28$ deg/m/sec (1.0 deg/ft/sec)

Figure 13.- Longitudinal command augmentation system.

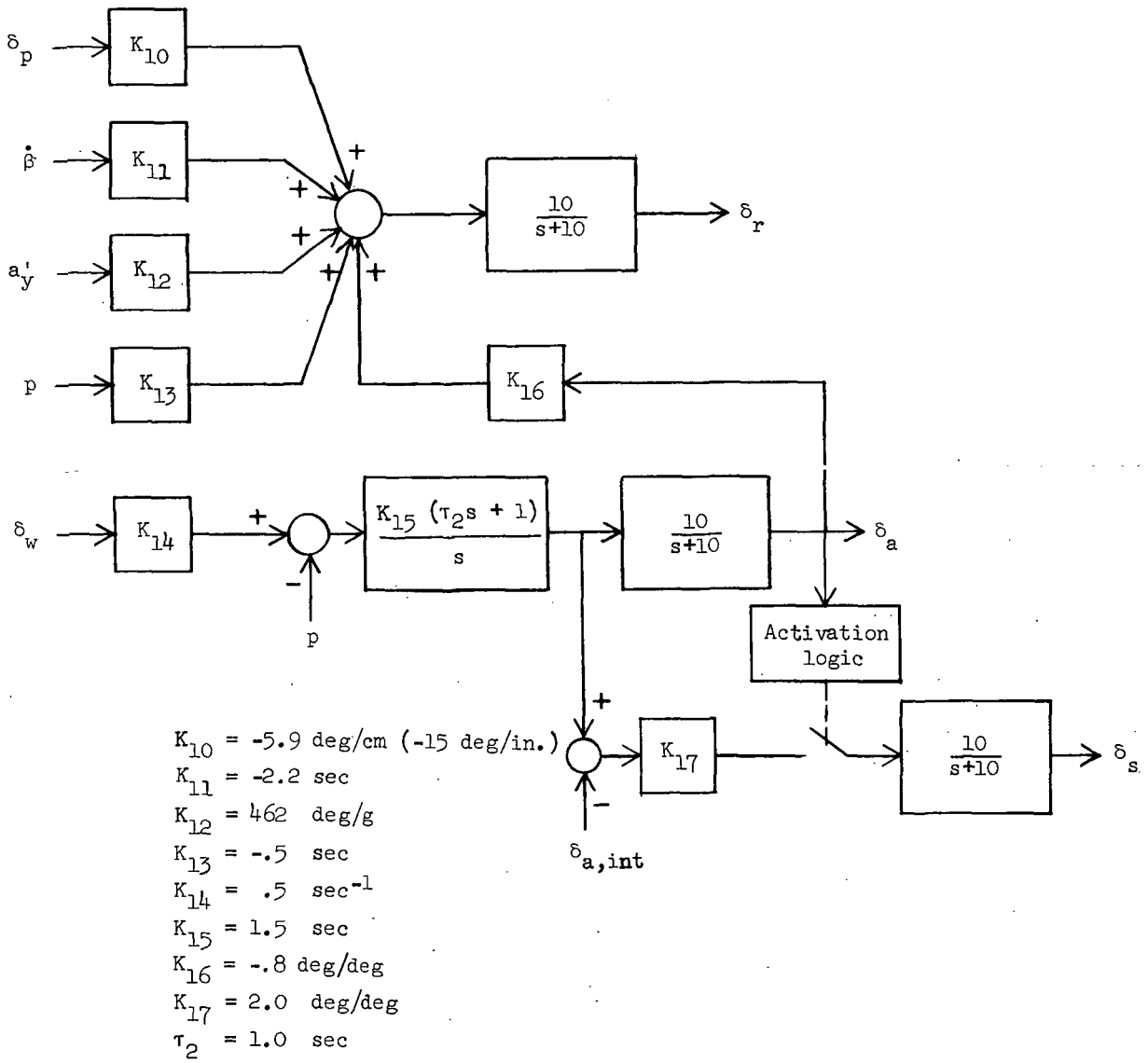

K_{10} = -5.9 deg/cm (-15 deg/in.)
K_{11} = -2.2 sec
K_{12} = 462 deg/g
K_{13} = -.5 sec
K_{14} = .5 sec^{-1}
K_{15} = 1.5 sec
K_{16} = -.8 deg/deg
K_{17} = 2.0 deg/deg
τ_2 = 1.0 sec

Figure 14.- Lateral-directional command augmentation system.

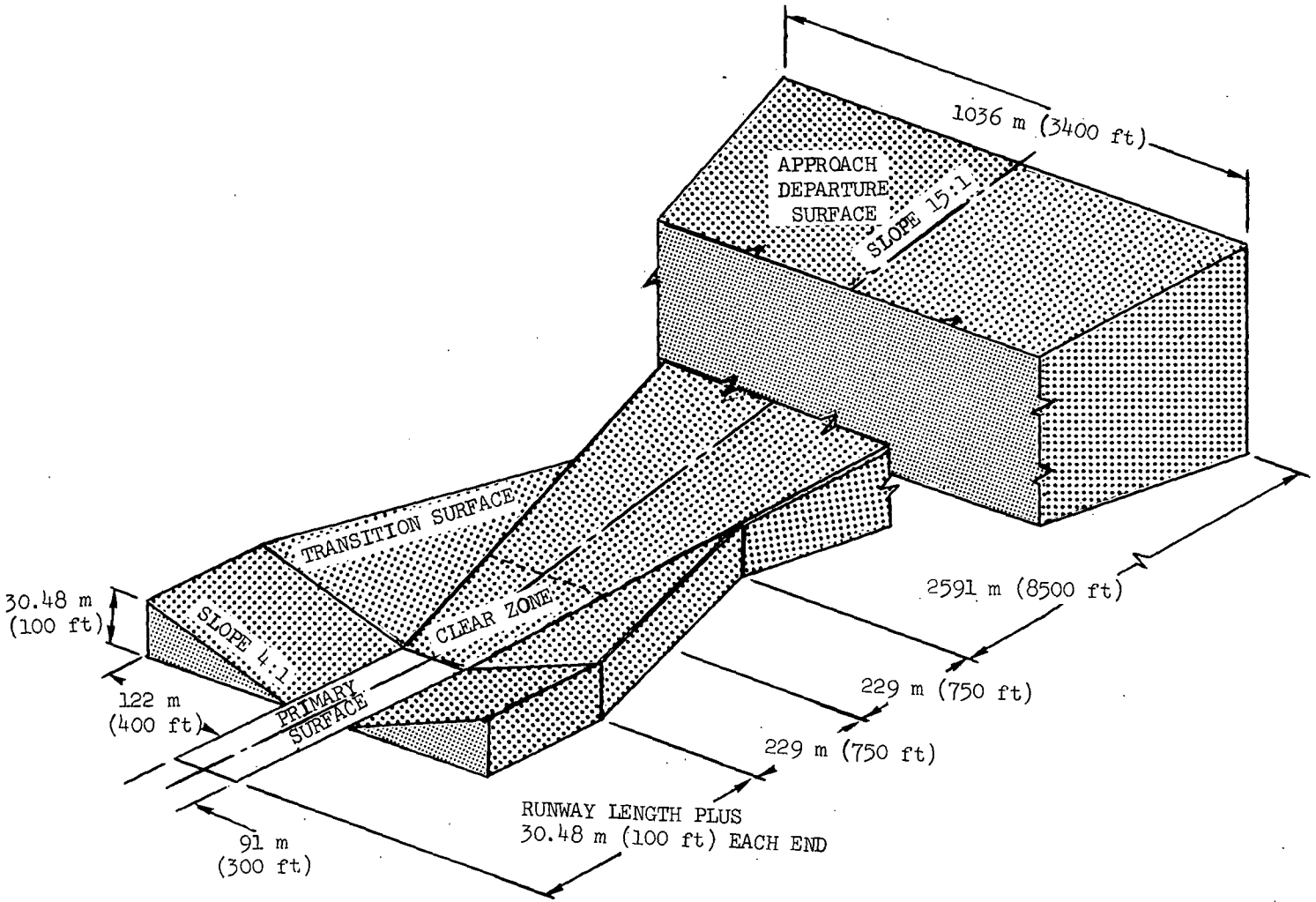

Figure 15.- Isometric of protection surfaces. (From ref. 8.)

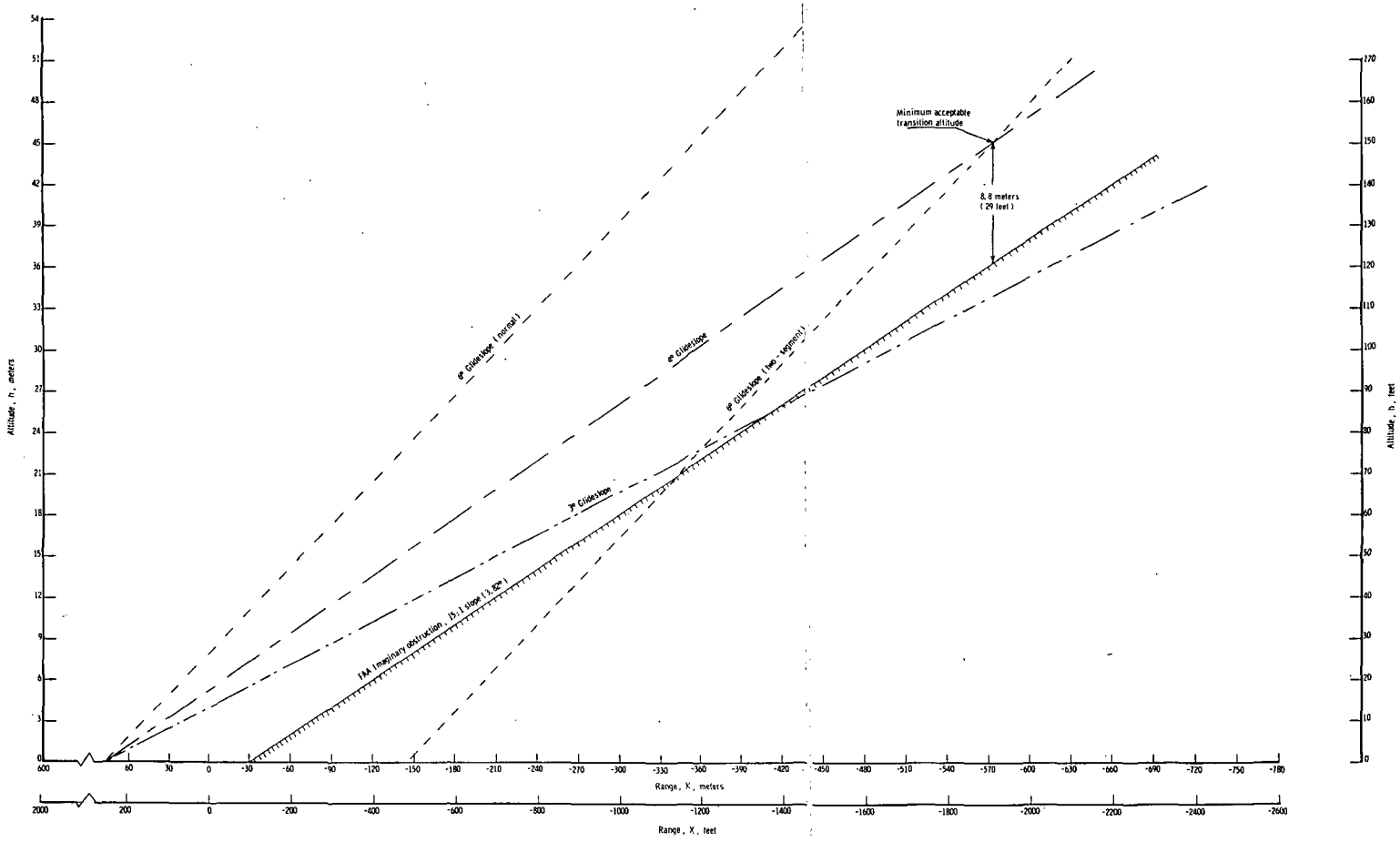

Figure 16.- Sketch indicating why 4° glideslope was minimum considered for STOL airplane.

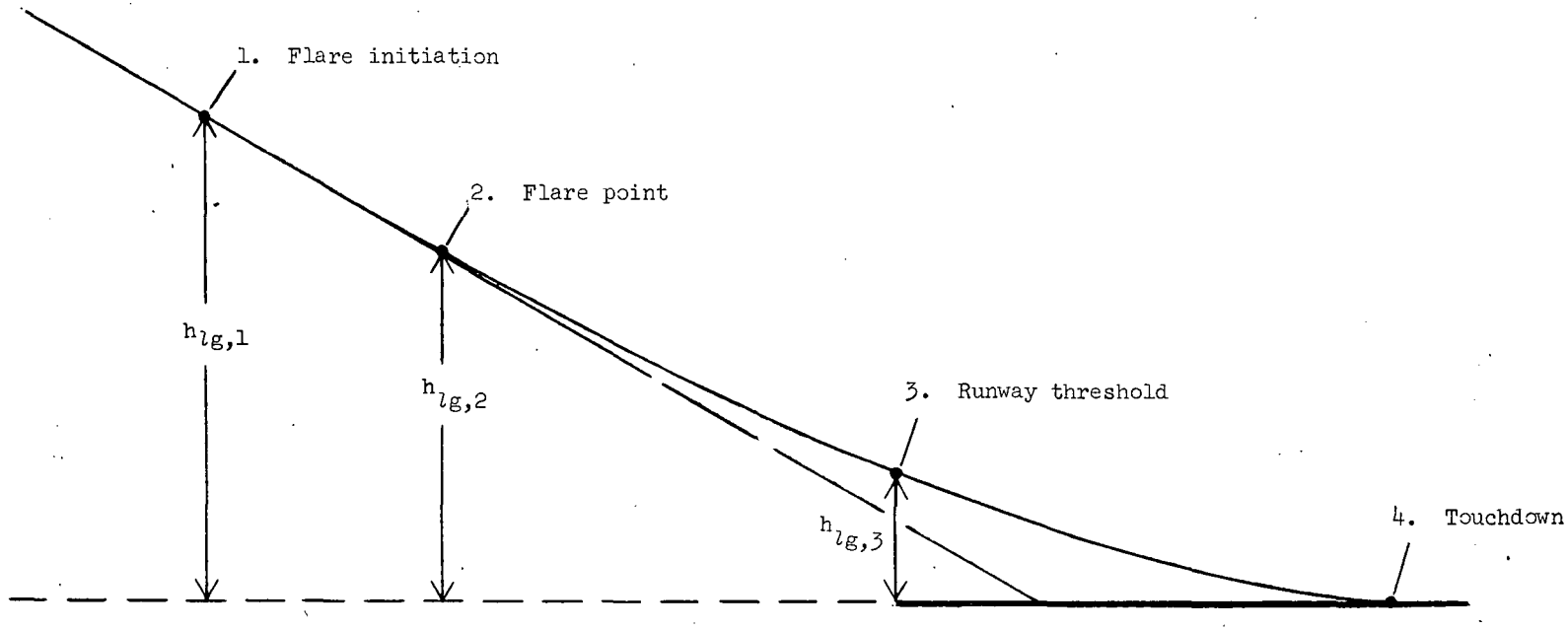

Figure 17.- Flare and touchdown geometry.

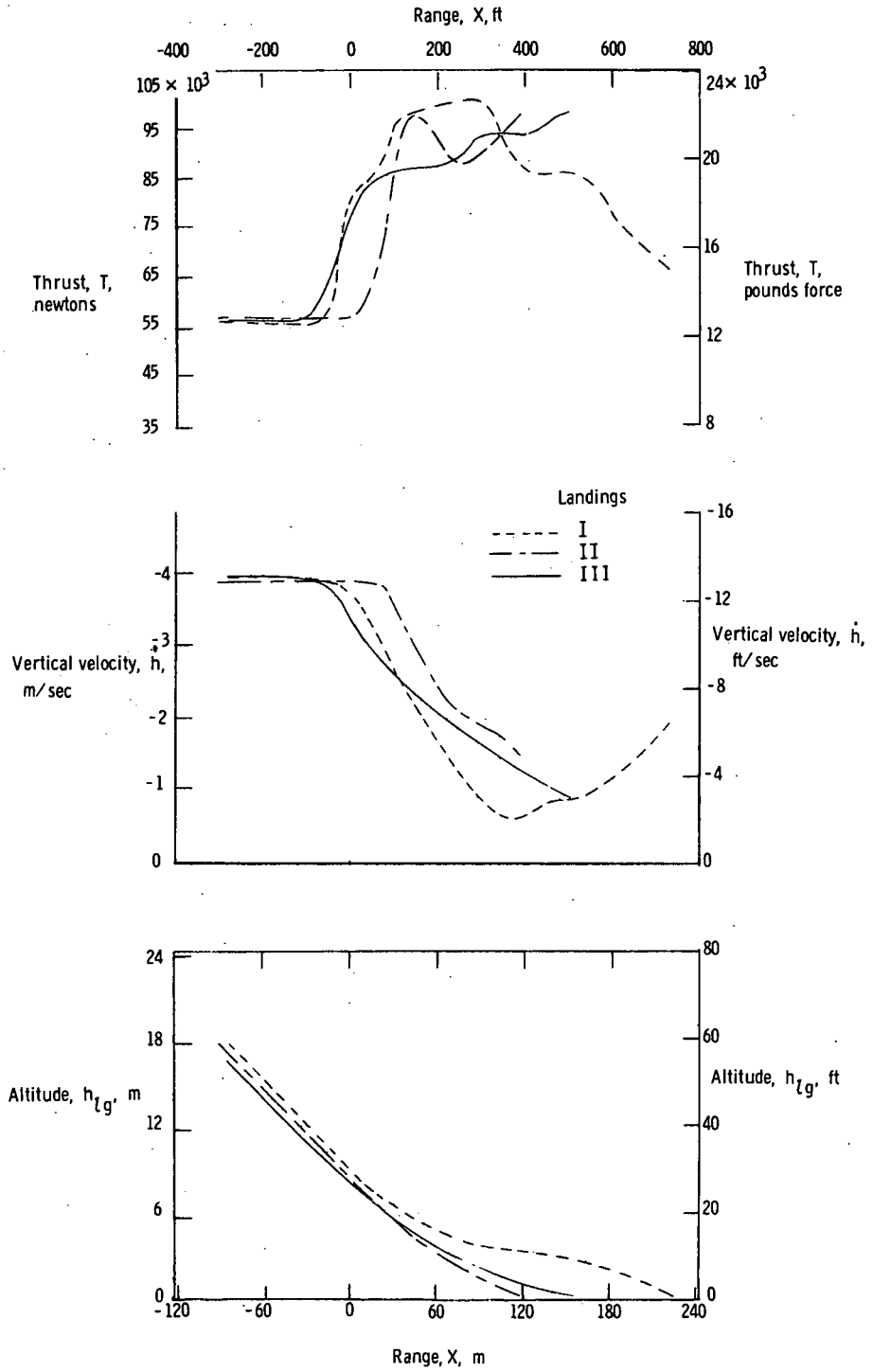

Figure 18.- Typical landings from a 6° glideslope. V = 75 knots.

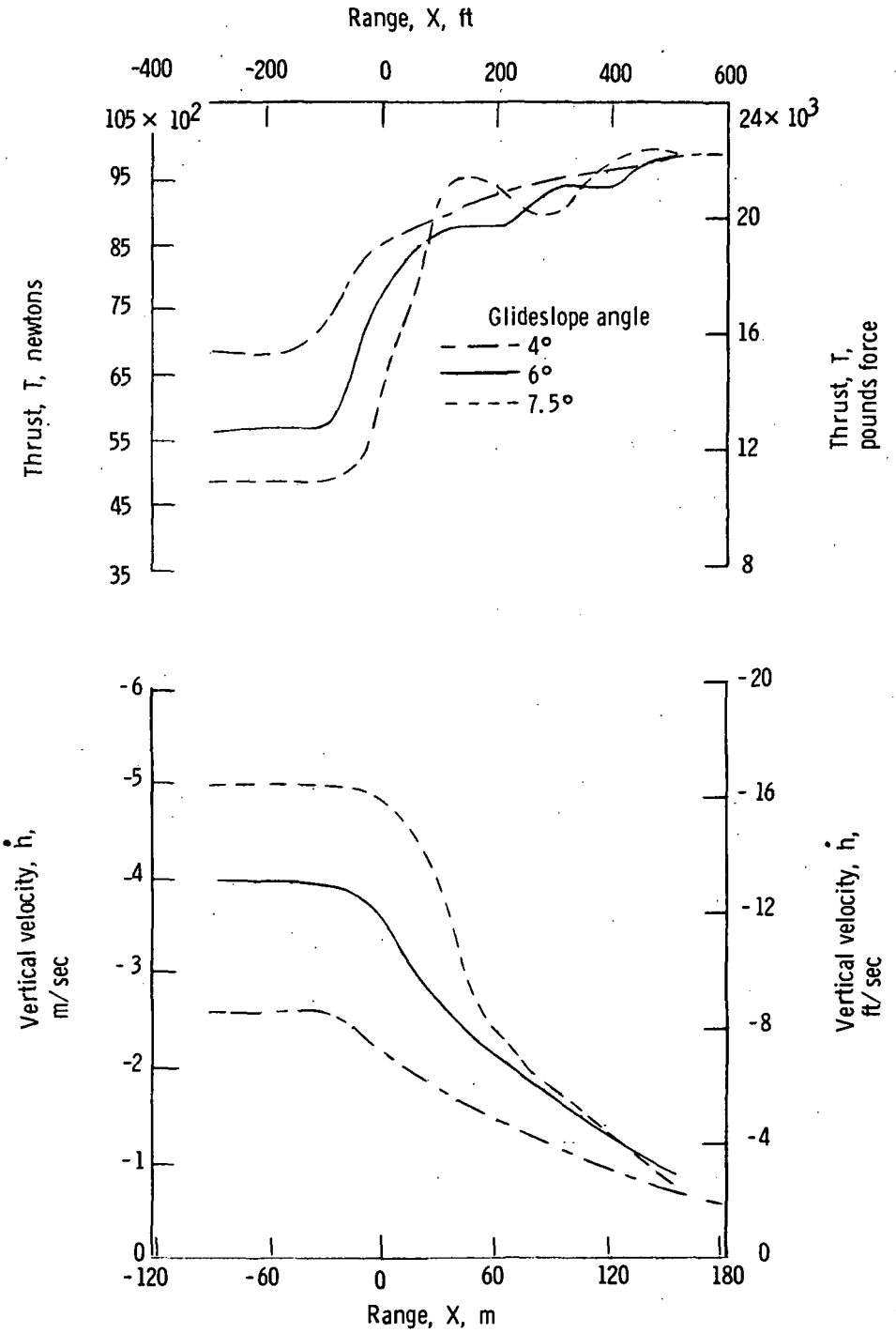

Figure 19.- Acceptable landings from 4°, 6°, and 7.5° approaches. V = 75 knots.

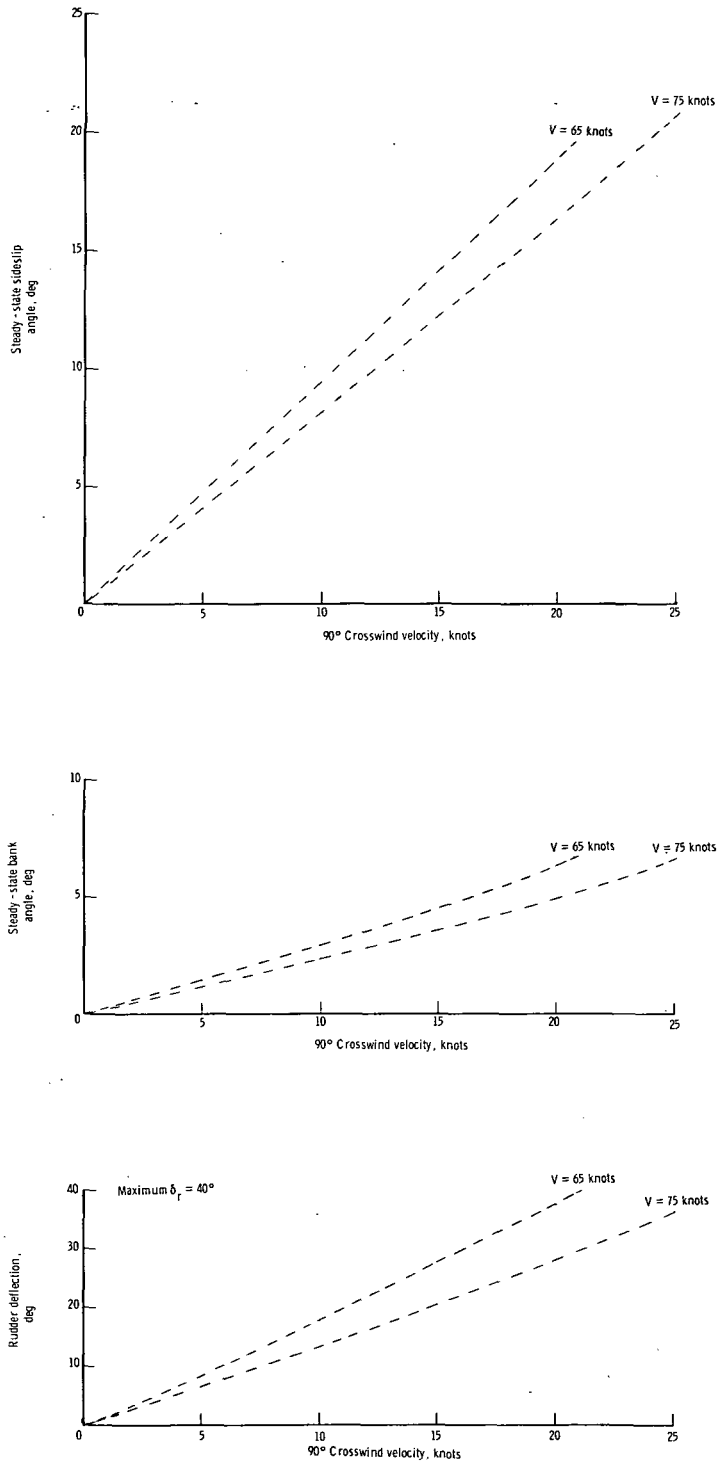

Figure 20.- Indication of amount of steady-state sideslip, bank angle, and rudder deflection required for sideslipping crosswind approaches.

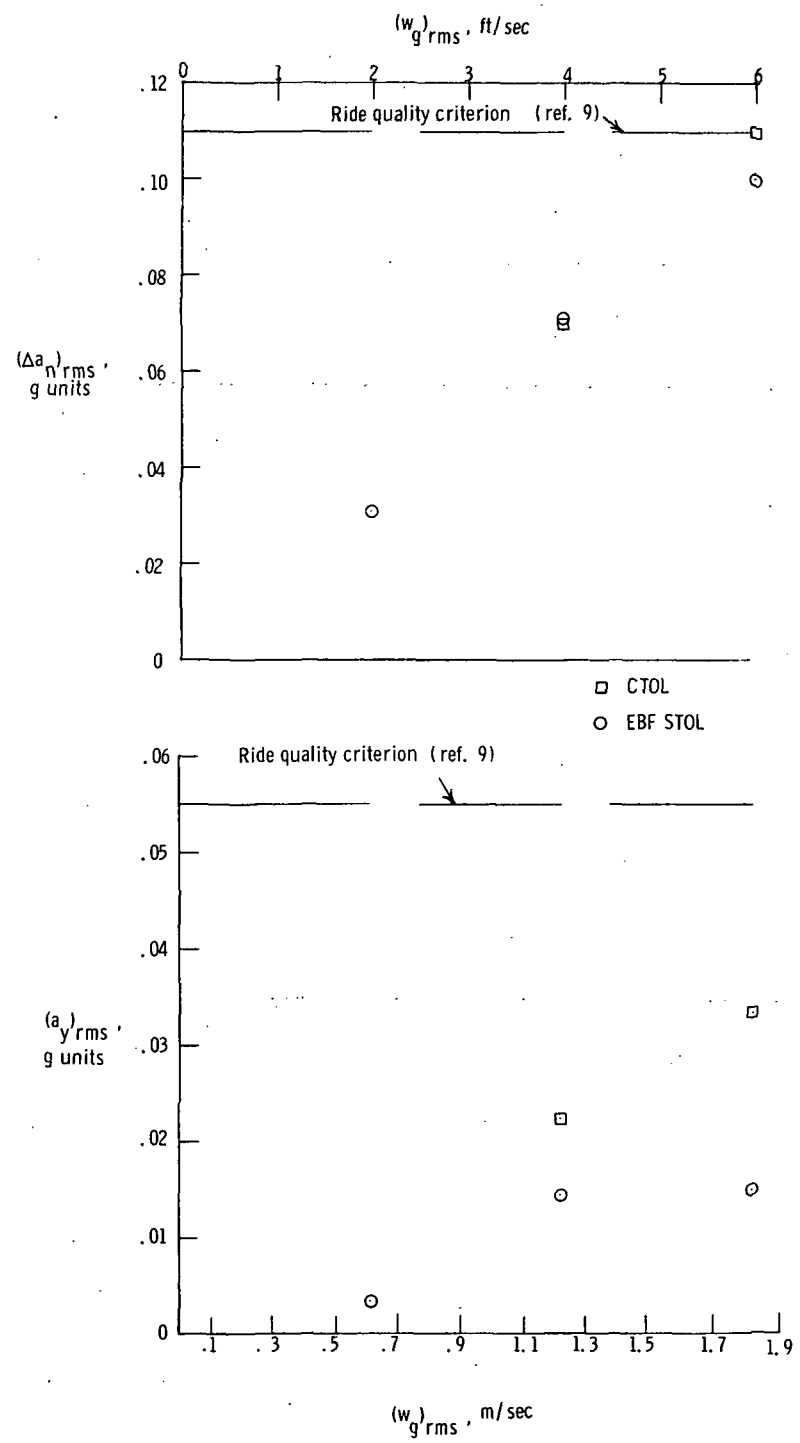

Figure 21.- Normal and lateral acceleration responses to continuous turbulence.

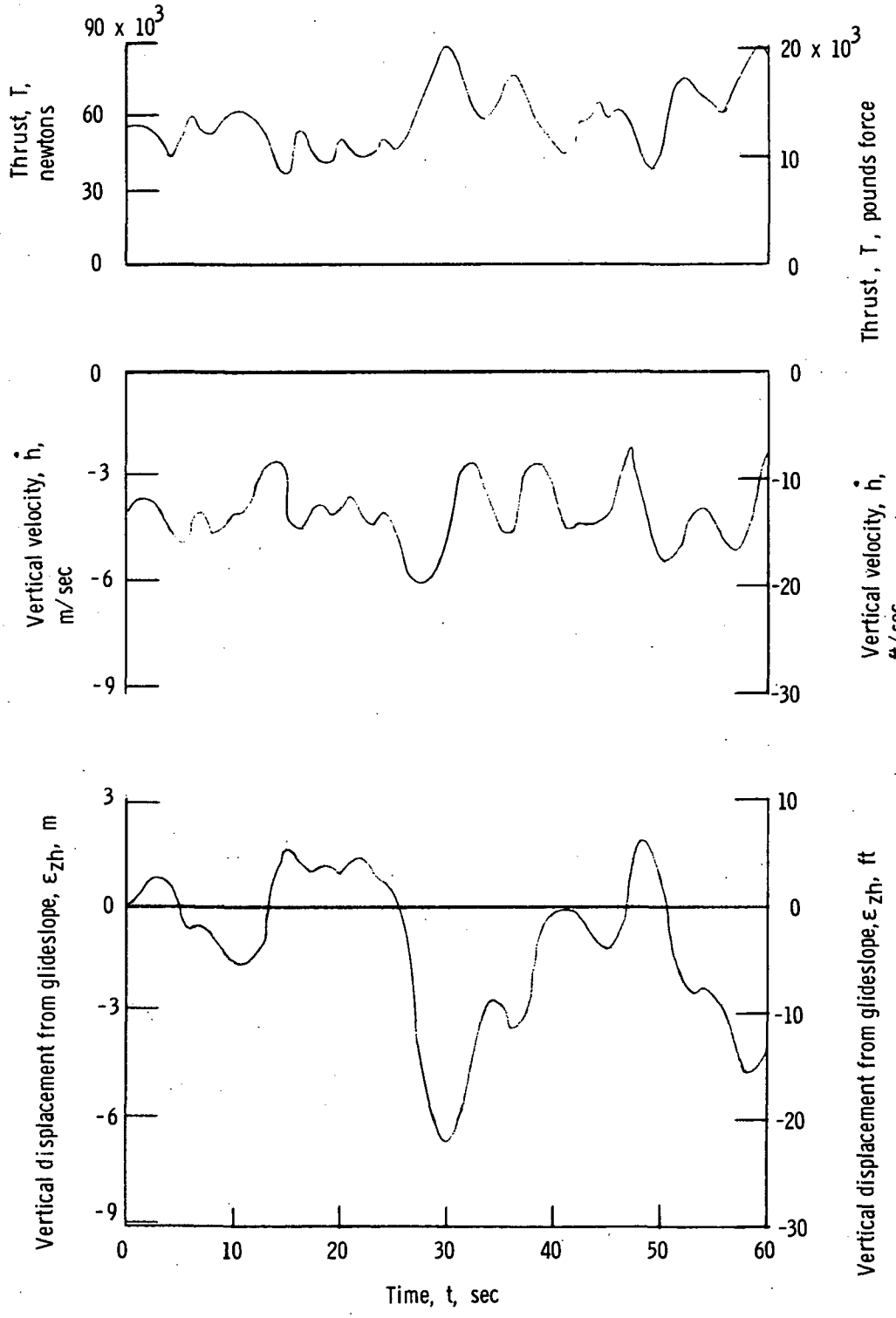

Figure 22.- A typical approach made in moderate turbulence. σ_w = 1.2 m/sec (4 ft/sec).

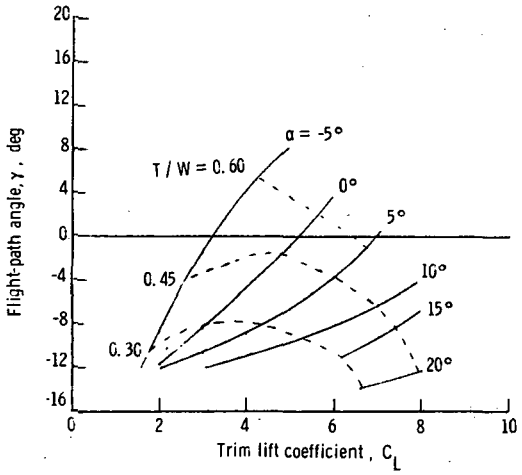

(a) $\delta_{f3} = 60^{o}$.

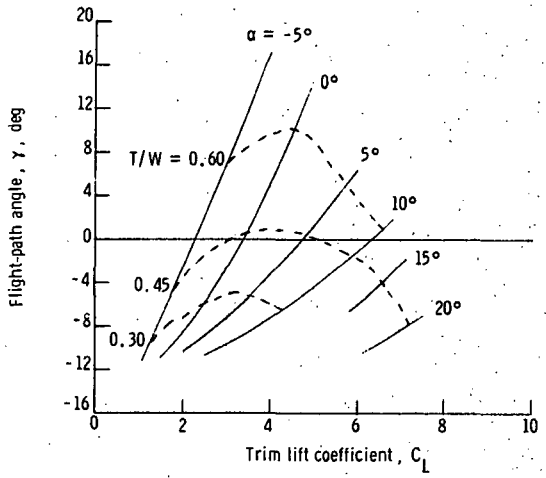

(b) $\delta_{f3} = 50^{o}$.

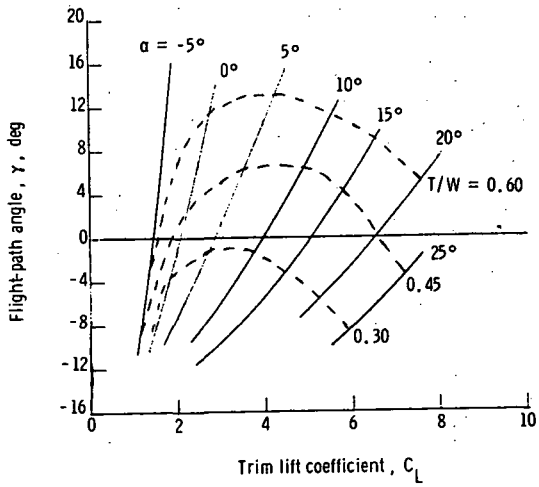

(c) $\delta_{f3} = 35^{o}$.

Figure 23.- Indication of effects of engine thrust on trim lift coefficient and flight-path angle for various flap (δ_{f3}) positions.

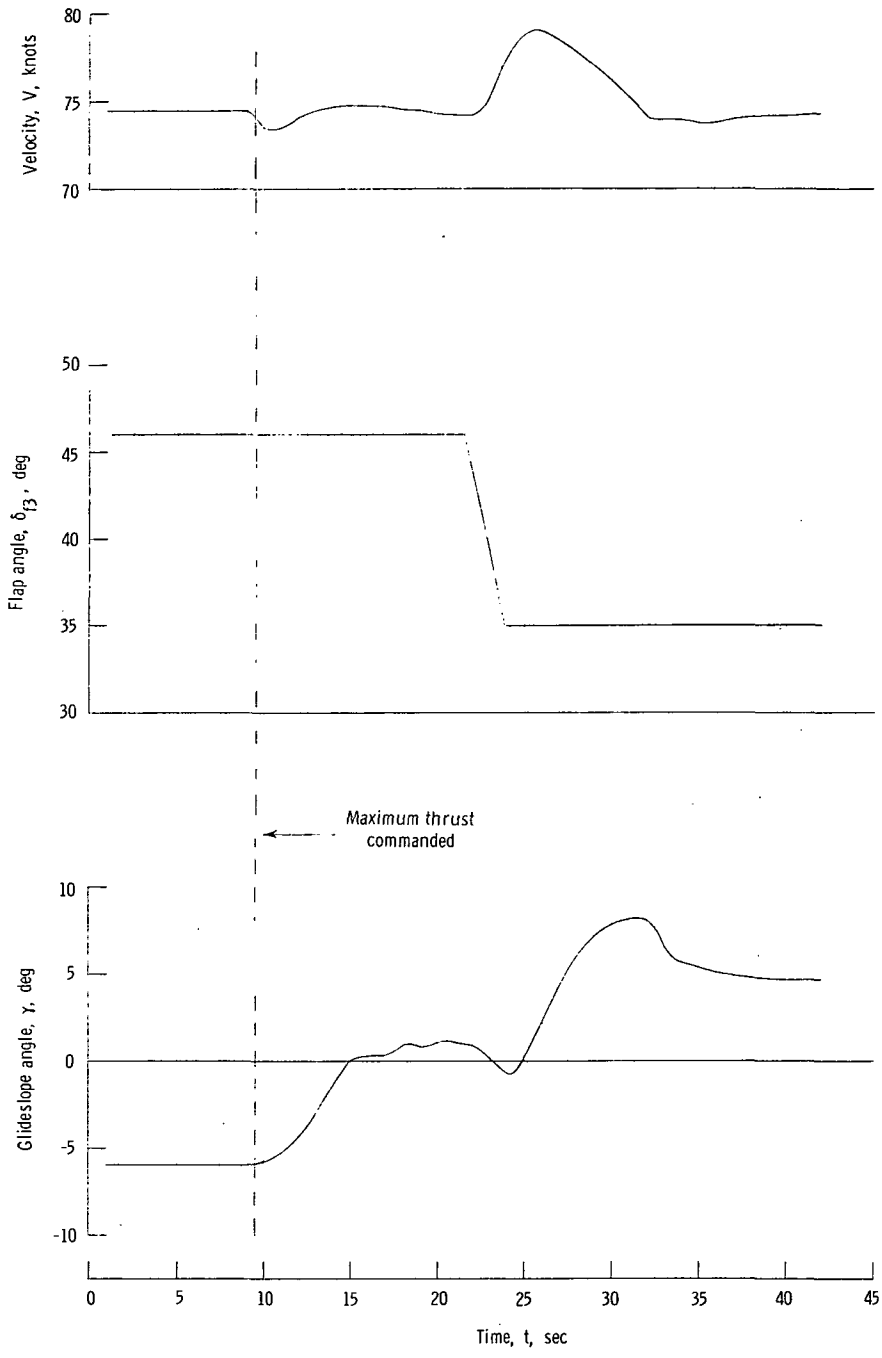

Figure 24.- Indication of wave-off capability from an approach angle of 6^{o} with only three engines operating.

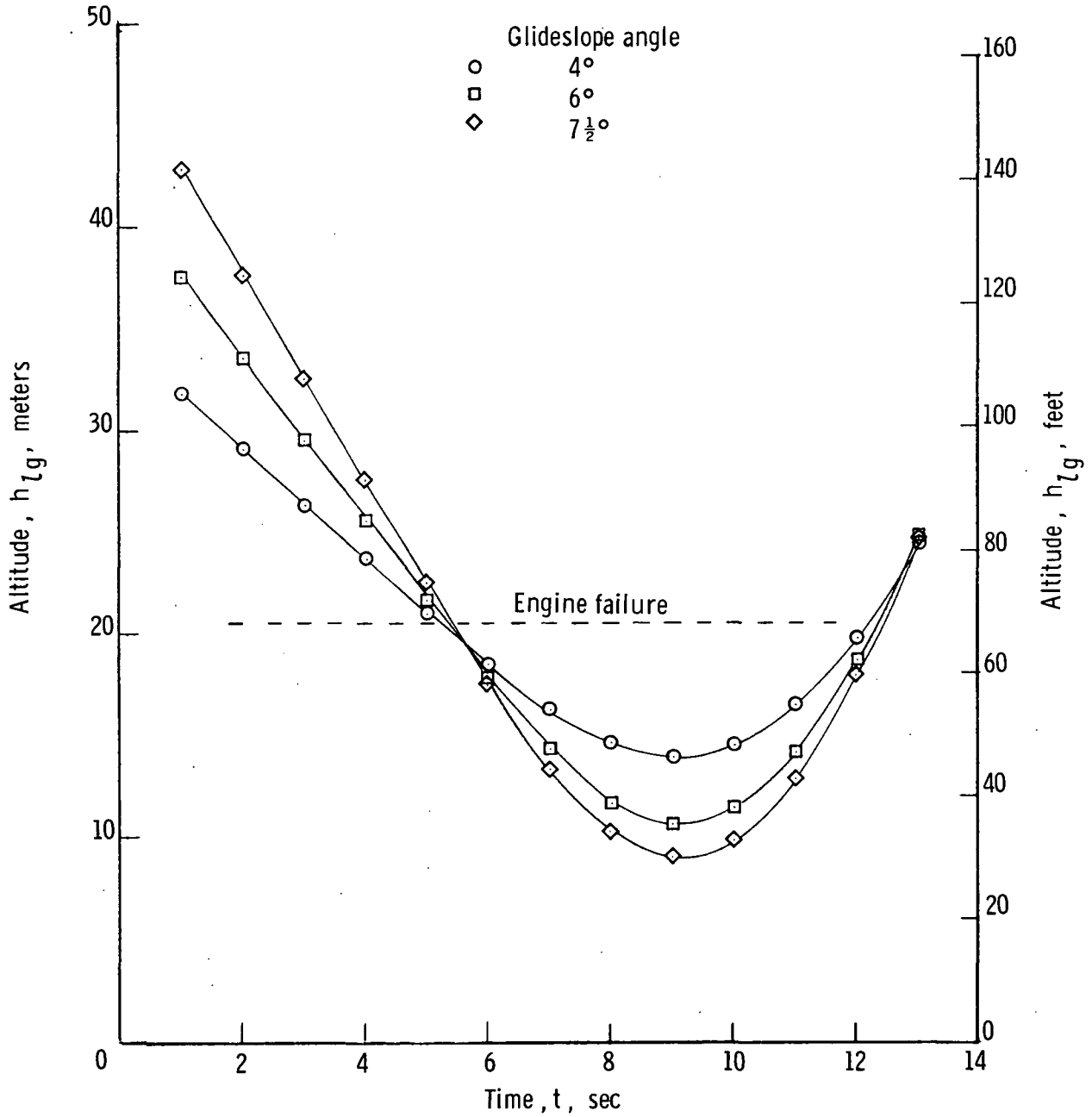

Figure 25.- Indication of minimum altitude from which a wave-off can be performed with only three engines operating from various glideslope angles.

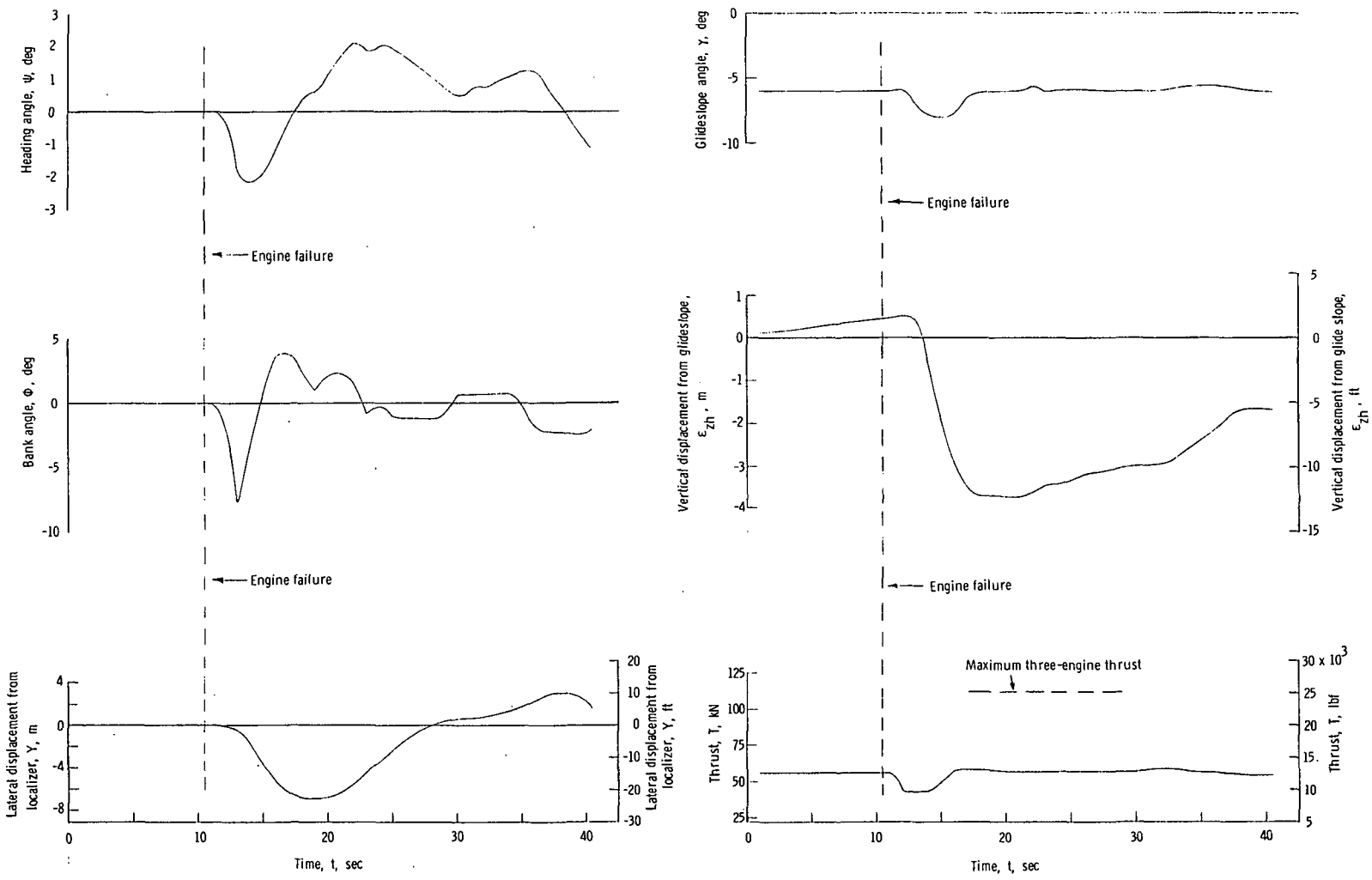

Figure 26.- Indication of lateral and vertical excursions experienced following failure of number one engine.

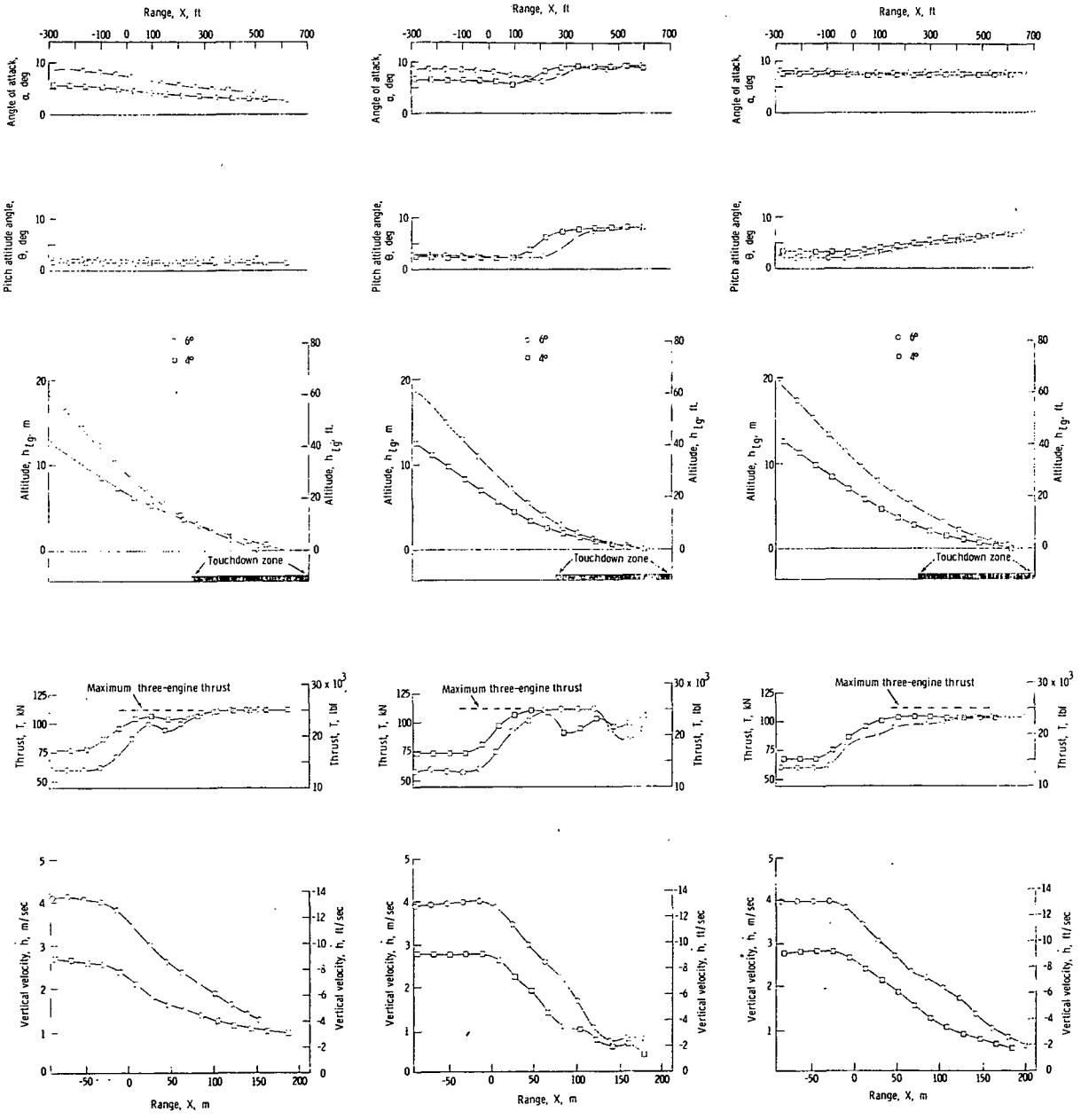

(a) Throttles for flare.

(b) Throttles and column for flare.

(c) Throttles (with α-command operative) for flare.

Figure 27.- Typical three-engine landings from glideslopes of 6^{o} and 4^{o} using various techniques to perform flare.

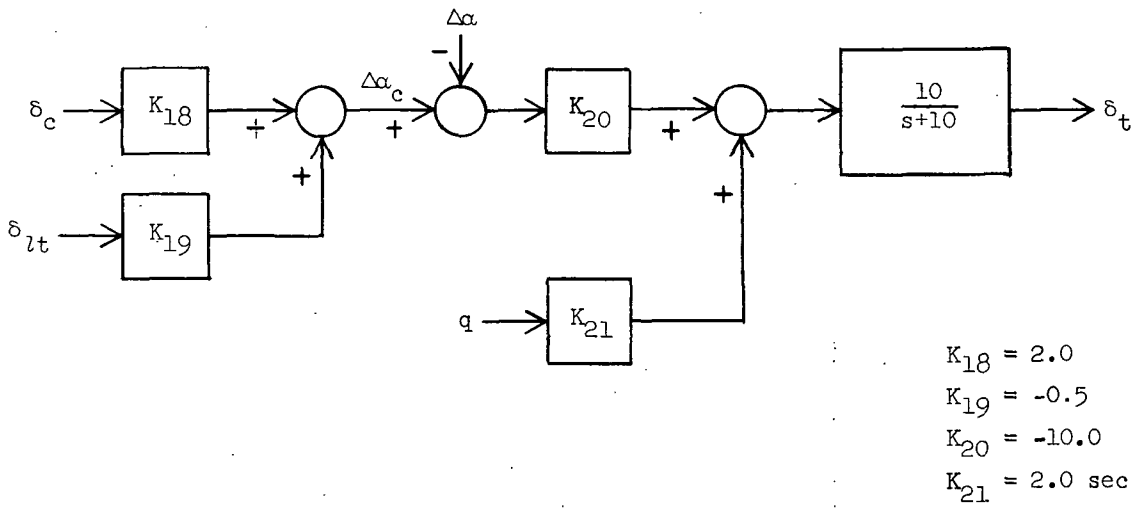

Figure 28.- Angle-of-attack command system.

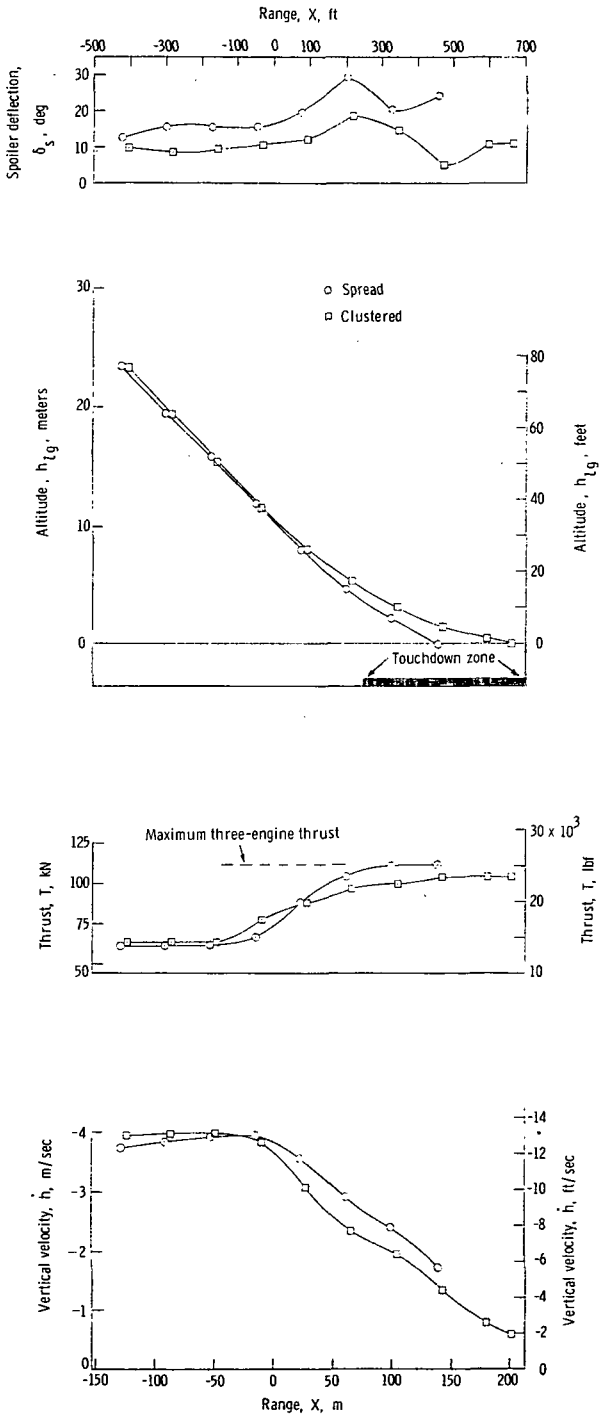

Figure 29.- Comparison of three-engine flare capability of clustered- and spread-engine configurations from 6° glideslope. (α-command system operative on both configurations.)

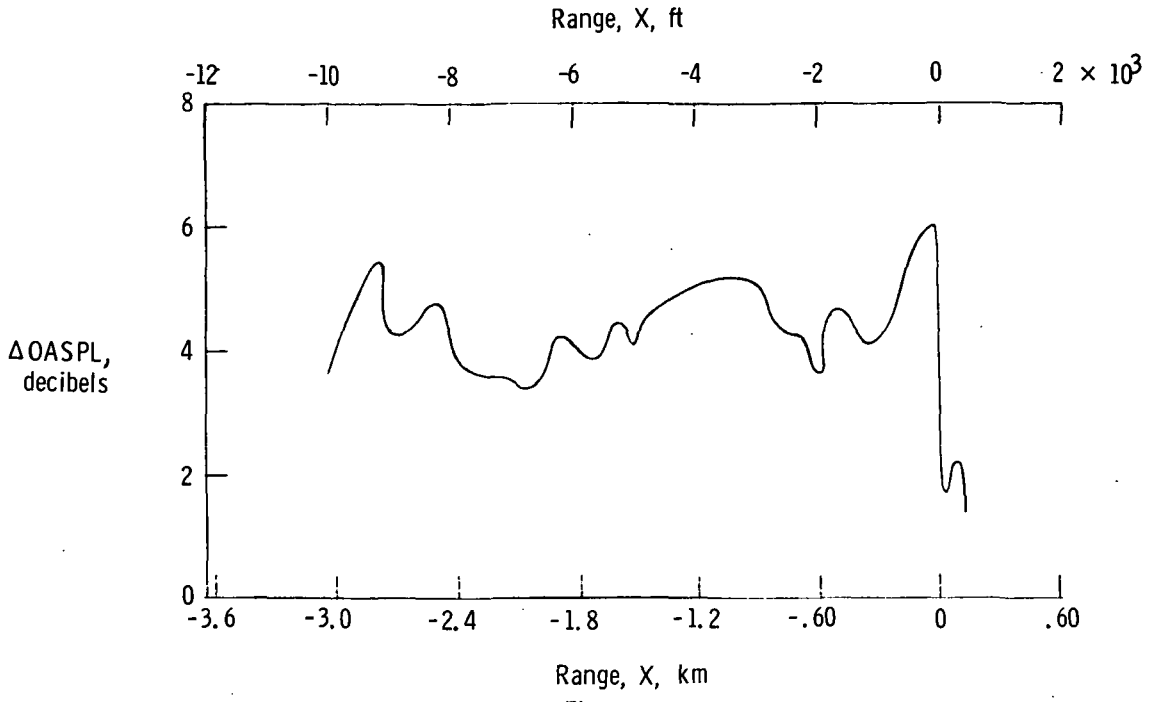

Figure 30.- Effect of speed (65 knots compared with 75 knots) on ground noise. (Reference V = 75 knots.)

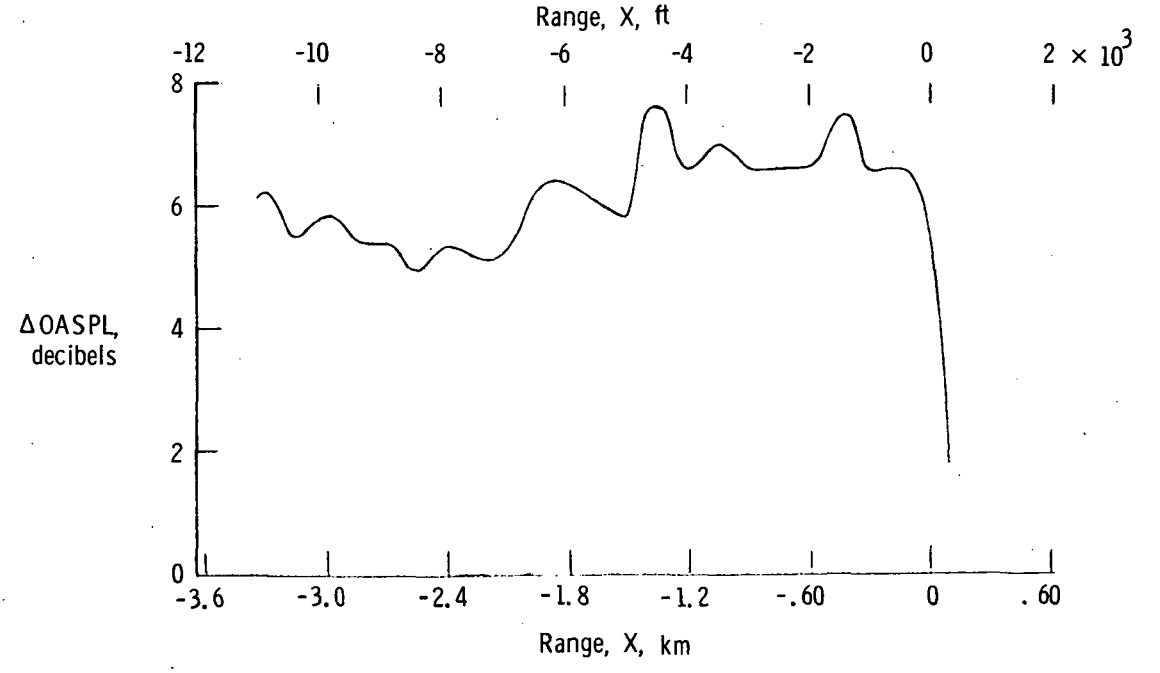

Figure 31.- Effect of pitch attitude ($\theta = -4.1^{o}$ compared with 4^{o}) on ground noise. (Reference $\theta = 4^{o}$.)

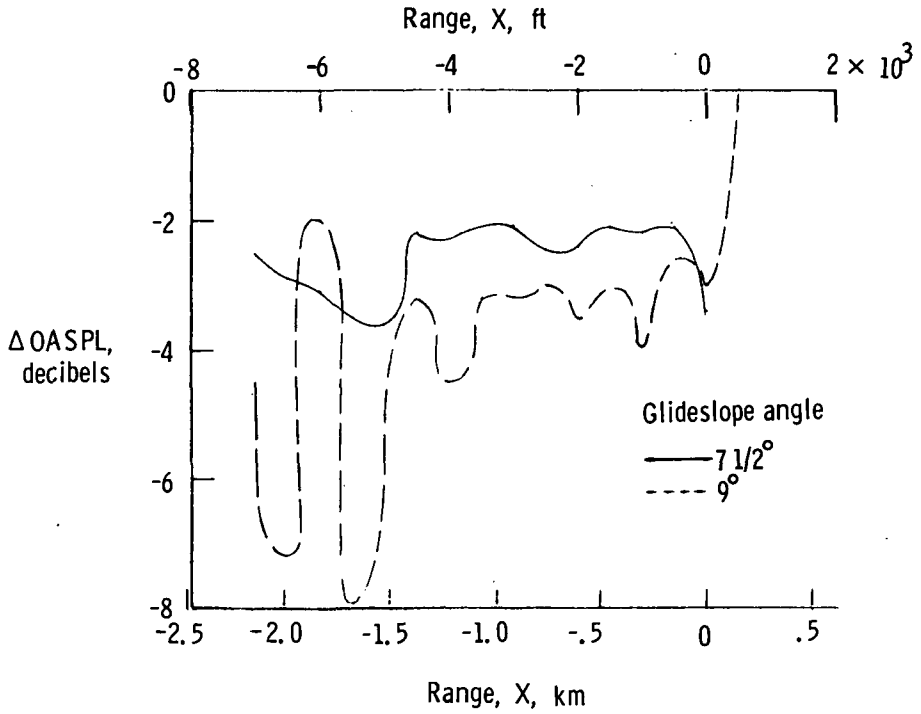

Figure 32.- Effect of steep glideslopes (>6°) on ground noise. (Reference glideslope is 6°.)

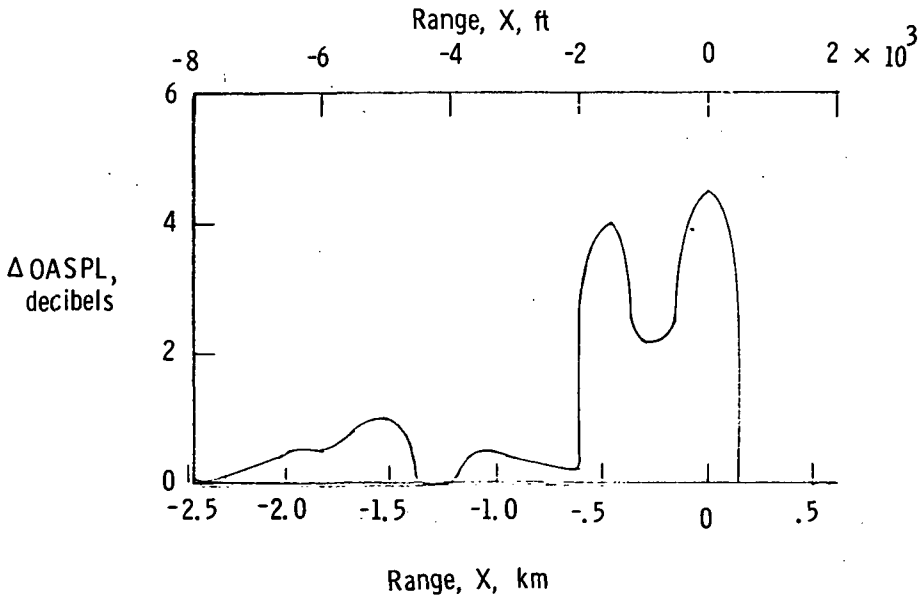

Figure 33.- Effect of two-segment approach (6°/4°) on ground noise. (Reference condition is 6° single segment.)

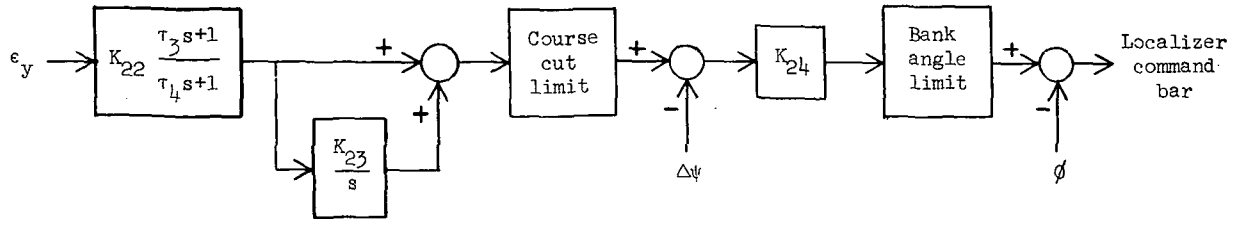

$K_{22} = 17.5$

$\tau_3 = 2.86$ sec

$\tau_4 = 0.2$ sec

$K_{24} = 1$

$$K_{23} = \begin{cases} 0.03 \text{ sec}^{-1}, & e_y \leq 0.3^\circ \\ 0, & e_y > 0.3^\circ \end{cases}$$

Figure 34.- Flight director localizer channel.

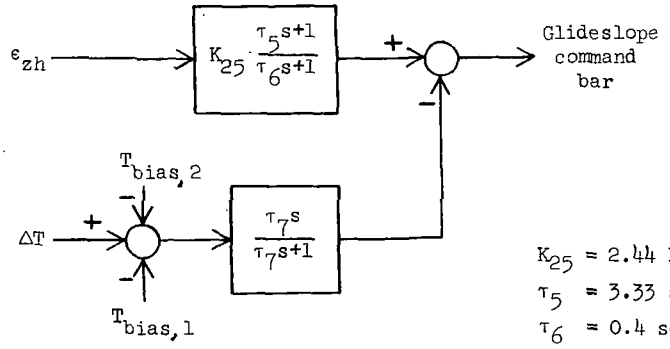

$K_{25} = 2.44$ kN/m (181 lbf/ft)

$\tau_5 = 3.33$ sec

$\tau_6 = 0.4$ sec

$\tau_7 = 10$ sec

Figure 35.- Flight director glideslope channel.

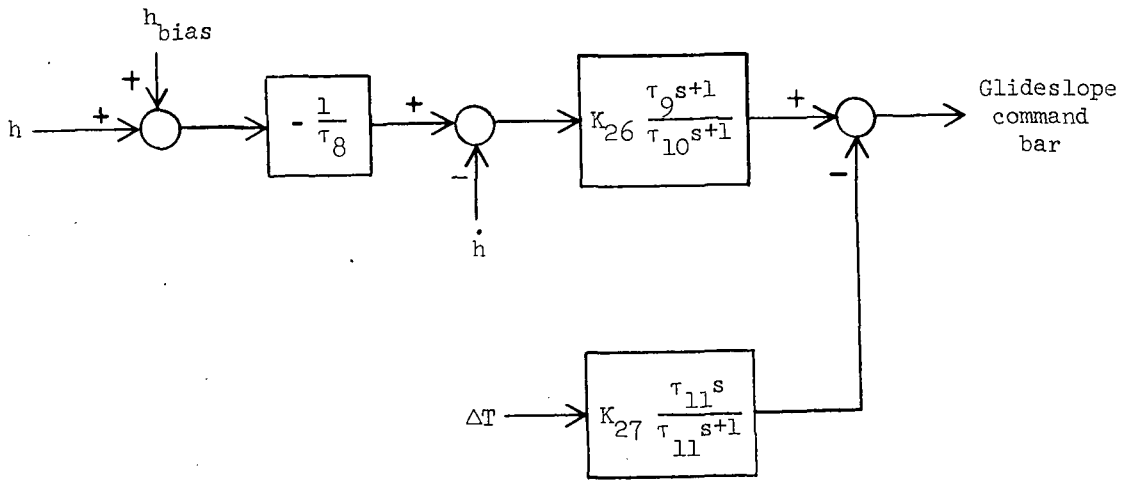

$\tau_8 = -\frac{h_{of}}{\dot{h}_{of}}$ where h_{of} = flare initiation altitude

K_{26} = 2.6 sec/m (0.8 sec/ft)

τ_9 = 2.5 sec

τ_{10} = 0.2 sec

K_{27} = 0.9×10^{-4} N^{-1} ($.4 \times 10^{-3}$ lbf^{-1})

τ_{11} = 2 sec

Figure 36.- Flight director flare mode.

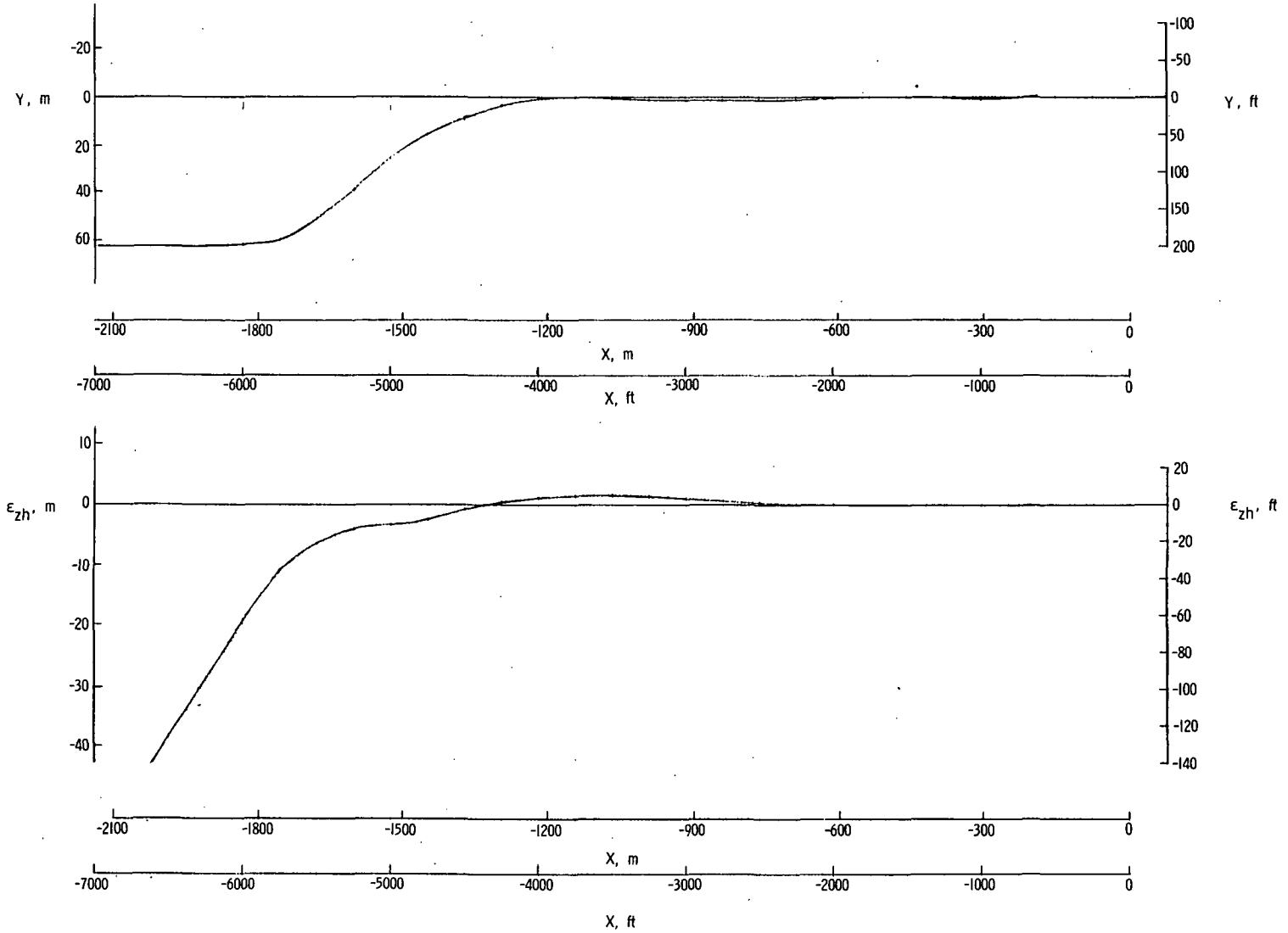

Figure 37.- Capture and tracking of ILS beams during a typical approach.

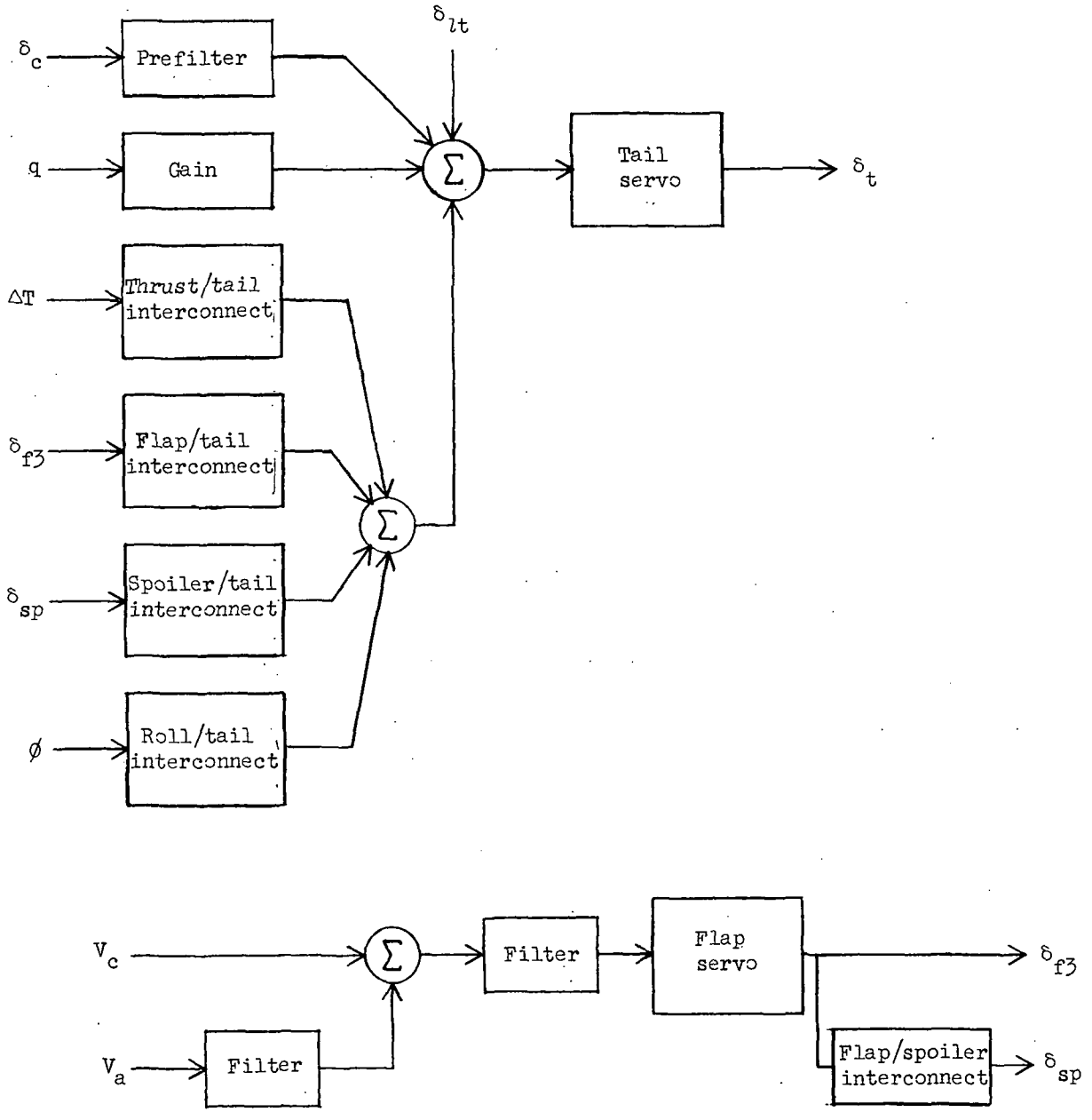

Figure 38.- Basic longitudinal augmentation.

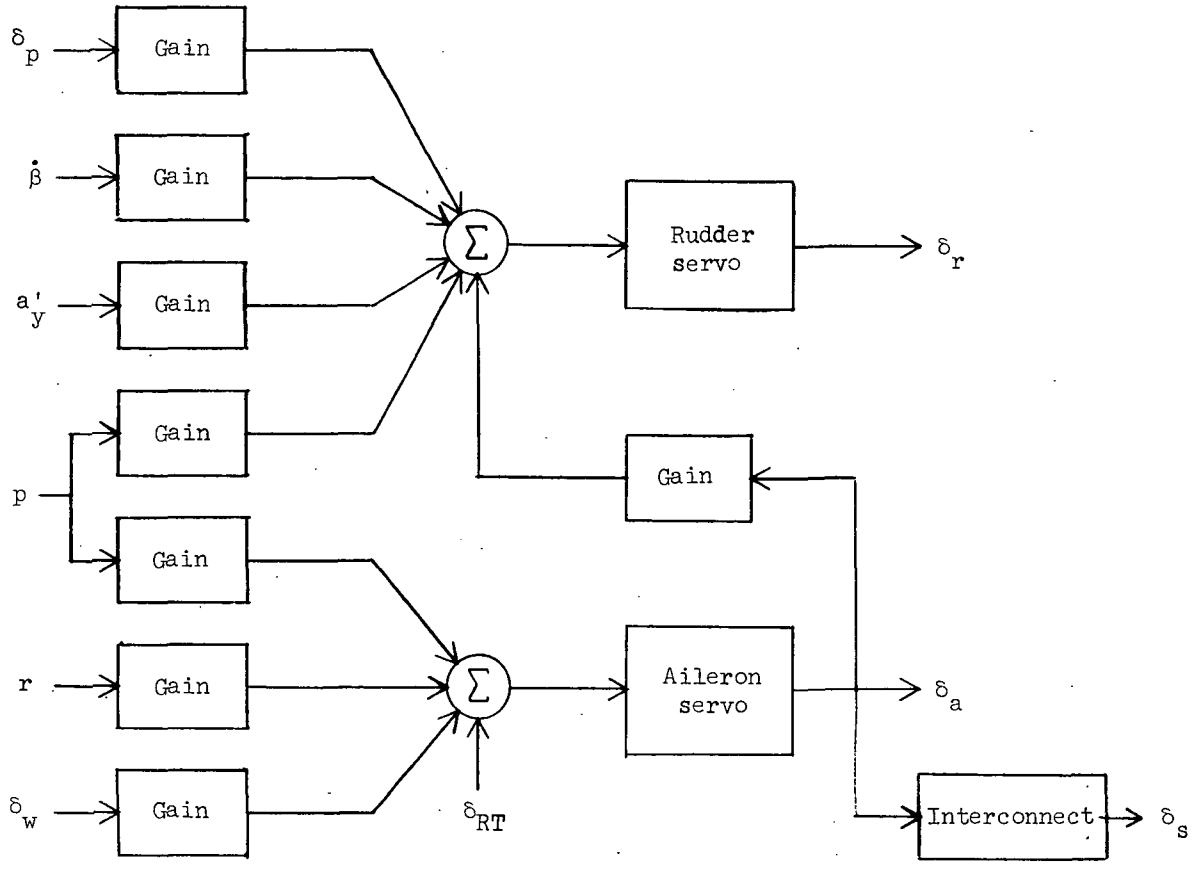

Figure 39.- Basic lateral-directional augmentation.

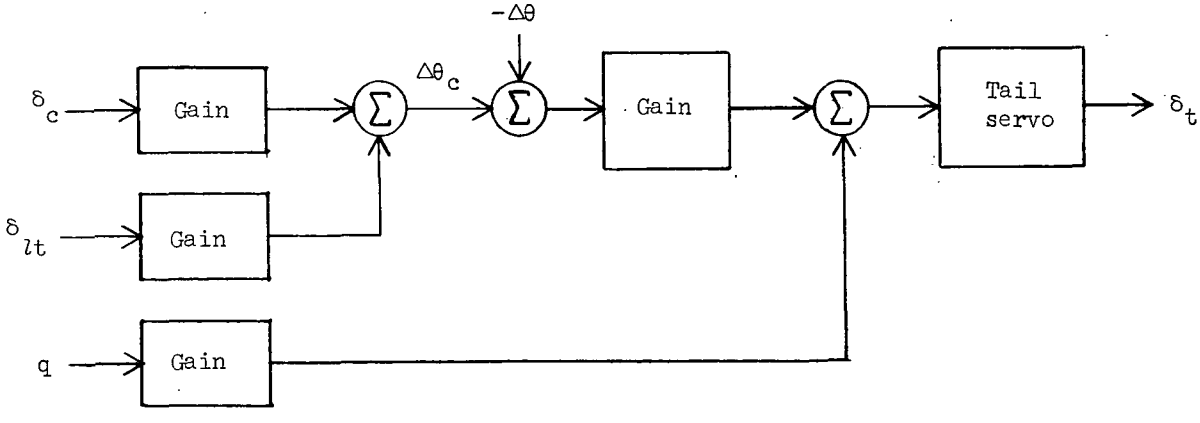

Figure 40.- Pitch-attitude command system.

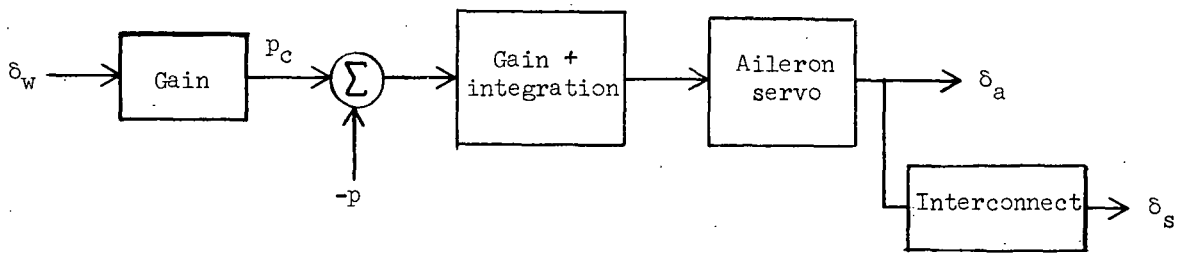

Figure 41.- Roll-rate command system.

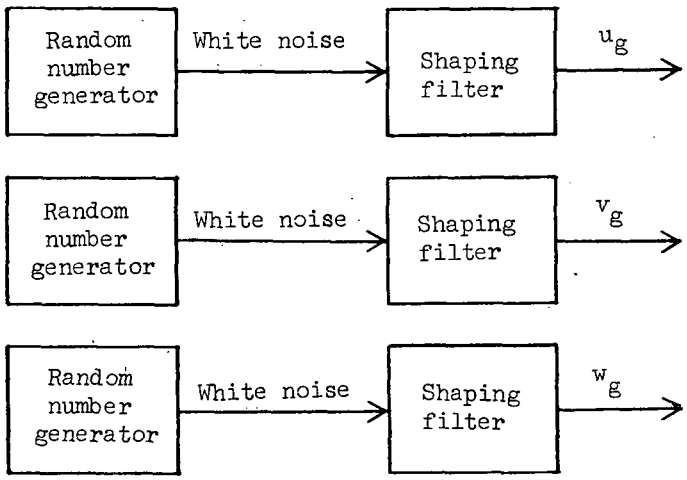

Figure 42.- Generation of simulated turbulence.

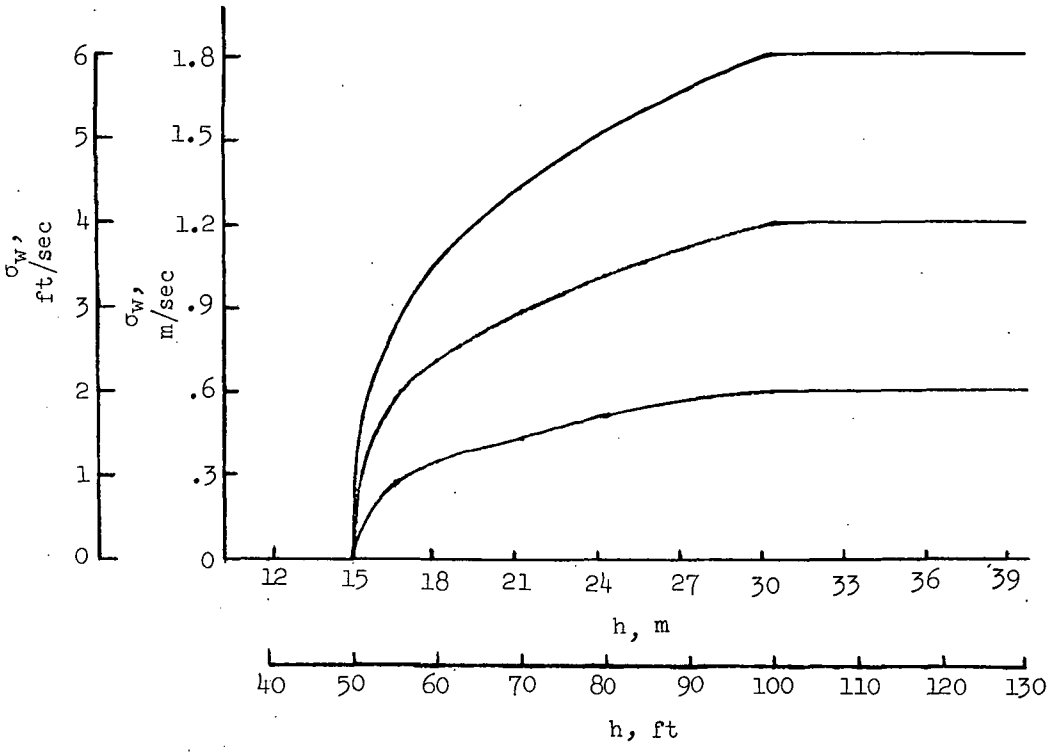

Figure 43.- Simulated decrease in vertical gust intensity below an altitude of 30.48 meters (100 ft).

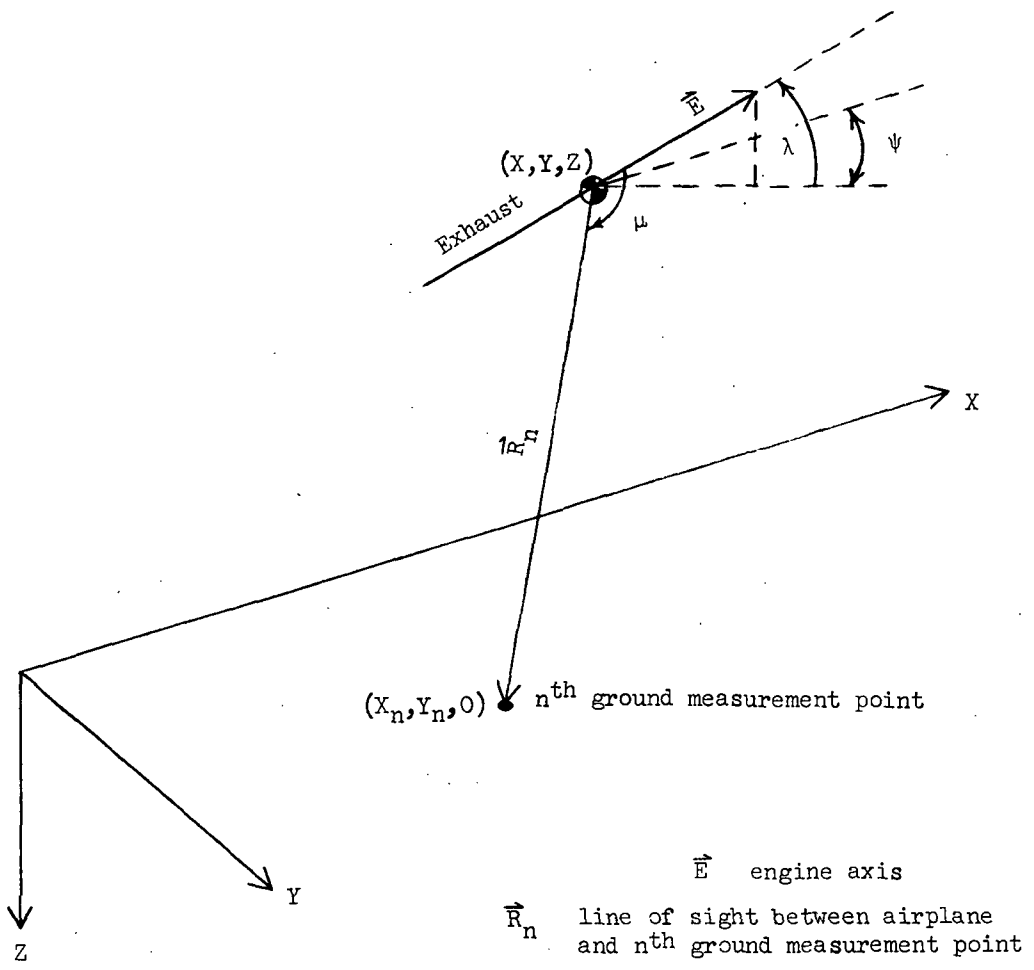

$$R_n = \sqrt{(X_n-X)^2 + (Y_n-Y)^2 + h^2}$$

$$\mu_n = \cos^{-1}\left[\frac{(X_n-X)\cos\psi\cos\lambda + (Y_n-Y)\sin\psi\cos\lambda - h\sin\lambda}{R_n}\right]$$

Figure 44.- Geometry of ground noise problem.

NATIONAL AERONAUTICS AND SPACE ADMINISTRATION
WASHINGTON, D.C. 20546

OFFICIAL BUSINESS
PENALTY FOR PRIVATE USE $300

SPECIAL FOURTH-CLASS RATE BOOK

POSTAGE AND FEES PAID
NATIONAL AERONAUTICS AND SPACE ADMINISTRATION
451

U.S.MAIL

POSTMASTER: If Undeliverable (Section 158 Postal Manual) Do Not Return

"The aeronautical and space activities of the United States shall be conducted so as to contribute . . . to the expansion of human knowledge of phenomena in the atmosphere and space. The Administration shall provide for the widest practicable and appropriate dissemination of information concerning its activities and the results thereof."

—NATIONAL AERONAUTICS AND SPACE ACT OF 1958

NASA SCIENTIFIC AND TECHNICAL PUBLICATIONS

TECHNICAL REPORTS: Scientific and technical information considered important, complete, and a lasting contribution to existing knowledge.

TECHNICAL NOTES: Information less broad in scope but nevertheless of importance as a contribution to existing knowledge.

TECHNICAL MEMORANDUMS: Information receiving limited distribution because of preliminary data, security classification, or other reasons. Also includes conference proceedings with either limited or unlimited distribution.

CONTRACTOR REPORTS: Scientific and technical information generated under a NASA contract or grant and considered an important contribution to existing knowledge.

TECHNICAL TRANSLATIONS: Information published in a foreign language considered to merit NASA distribution in English.

SPECIAL PUBLICATIONS: Information derived from or of value to NASA activities. Publications include final reports of major projects, monographs, data compilations, handbooks, sourcebooks, and special bibliographies.

TECHNOLOGY UTILIZATION PUBLICATIONS: Information on technology used by NASA that may be of particular interest in commercial and other non-aerospace applications. Publications include Tech Briefs, Technology Utilization Reports and Technology Surveys.

Details on the availability of these publications may be obtained from:

SCIENTIFIC AND TECHNICAL INFORMATION OFFICE

NATIONAL AERONAUTICS AND SPACE ADMINISTRATION

Washington, D.C. 20546